

# **Sustained drug delivery for local treatment of joint diseases**

Dissertation

zur Erlangung des Grades

des Doktors der Naturwissenschaften

der Naturwissenschaftlich-Technischen Fakultät

der Universität des Saarlandes

von

**Bernd Sterner**

München

2016

Tag des Kolloquiums: 14.06.2017

Dekan: Prof. Dr. Guido Kickelbick

Vorsitzender: Prof. Dr. Marc Schneider

Berichterstatter: Prof. Dr. Claus-Michael Lehr  
Prof. Dr. Thorsten Lehr

Akademische Mitarbeiterin: Dr. Sarah Barthold

Die vorliegende Arbeit wurde unter der Leitung von Herrn Prof. Dr. Claus-Michael Lehr und Frau Dr. Maike Windbergs am Institut für Pharmazeutische Technologie und Biopharmazie der Universität des Saarlandes und dem Helmholtz-Institut für pharmazeutische Forschung Saarland angefertigt.

Die vorliegende Arbeit entstand in Zusammenarbeit mit Herrn Dr. Markus Weigandt und Frau Dr. Meike Harms im Rahmen eines Forschungsprojektes bei der Merck KGaA in Darmstadt.

Für meine Frau, Angela

## Table of Contents

<b>Section A</b>	<b>Short Summary / Kurzzusammenfassung</b> .....	3
1	Short Summary.....	4
2	Kurzzusammenfassung.....	5
<b>Section B</b>	<b>General Introduction</b> .....	6
1	Synovial joints.....	7
1.1	The synovial membrane .....	8
1.2	Articular cartilage.....	9
1.3	The synovial fluid.....	11
2	Sustained release intra-articular drug delivery .....	12
2.1	Why do we need sustained release in synovial joints?.....	13
2.2	State of the art.....	13
3	Aim of the thesis.....	21
<b>Section C</b>	<b>Kinetic investigations on bovine joint tissues</b> .....	22
1	Introduction .....	23
1.1	Kinetic considerations .....	24
2	Materials and Methods .....	26
2.1	Materials.....	26
2.2	Methods.....	27
3	Results and discussion.....	31
3.1	Characterization of model polymers and small molecules .....	31
3.2	Permeation experiments .....	35
3.3	Penetration of cartilage tissue.....	41
4	Conclusion.....	57

---

## Table of Contents

---

<b>Section D</b>	<b><i>In vitro</i> release studies</b>	59
1	Introduction	60
1.1	Dissolution testing and <i>in vitro</i> release	60
1.2	The role of the release medium	65
1.3	<i>In vitro</i> release testing for intra-articular applied systems	65
2	Materials and methods	67
2.1	Materials	67
2.2	Methods	71
3	Results and discussion	78
3.1	Physico chemical characteristics	78
3.2	<i>In vitro</i> release studies	82
4	Conclusion	94
<b>Section E</b>	<b>Summary and outlook</b>	96
	List of Abbreviations	100
	Bibliography	102
	Scientific output	107
	Curriculum Vitae	108
	Danksagung	109

## **Section A**

### **Short Summary / Kurzzusammenfassung**

## 1 Short Summary

Synovial joints allow local treatment of joint diseases via intra-articular administration. In this context, it is of great value to understand the transport and retention mechanisms of intra-articular administered drugs. The present work picks up these challenges in two major sections:

The first part concerns the characterization of potential retention of compounds inside synovial joints. It was shown that increasing molecular weight of investigated compounds led to increased retention by the synovial membrane. In addition, a clear relation was observed between the positive charge of applied model compounds and the partition into cartilage tissue. Furthermore, fluorescence microscopy revealed that positively charged macromolecules (up to 233 kDa) penetrated deeply into the cartilage matrix.

The second part investigated a modified USP apparatus IV for the assessment of the *in vitro* release of intra-articular depot formulations. It was demonstrated that the applied setup was able to discriminate between different formulation options and that the release setup has the potential to be further modified with regards to more bio-relevance.

In summary, it was shown that positively charged macromolecules have the potential to enable prolonged drug exposure to synovial joints. Moreover, the modified USP apparatus IV was demonstrated to be a suitable and predictive tool for the characterization of the *in vitro* release of intra articular formulations.

## 2 Kurzzusammenfassung

Die Struktur synovialer Gelenke begünstigt die lokale Behandlung von Gelenkkrankheiten mittels intra-artikulärer Applikation. In diesem Zusammenhang spielt das Verständnis über relevante Transport und Retentionsmechanismen eine wichtige Rolle. Die vorliegende Arbeit greift diese Fragestellungen in zwei Abschnitten auf:

Der erste Abschnitt beschäftigt sich mit der Charakterisierung synovialer Gelenke hinsichtlich ihres Retentionspotenzials. Es wurde gezeigt, dass die Synovialmembran größere Moleküle verstärkt zurück hält. Zudem wurde ein klarer Zusammenhang zwischen der positiven Ladung eines Moleküls und dessen Verteilungsverhalten in Knorpelgewebe gezeigt. Außerdem konnte mittels Fluoreszenzmikroskopie herausgefunden werden, dass positiv geladene Makromoleküle (bis zu 233 kDa) tief in Knorpelgewebe vordringen.

Im zweiten Abschnitt wurde ein modifizierter USP Apparatus IV im Hinblick auf seine Eignung zur Bestimmung des Freisetzungsverhaltens intra-artikulärer Depot-Formulierungen untersucht. Es konnte gezeigt werden, dass das System zwischen unterschiedlichen Formulierungen zu diskriminieren vermag und zudem das Potenzial besitzt, im Hinblick auf höhere Biorelevanz angepasst zu werden.

Zusammen genommen konnte gezeigt werden, dass positiv geladene Makromoleküle das Potential besitzen, um verlängerte Wirkstoffexposition im Gelenk erreichen zu können und dass mit dem modifizierten USP IV Freisetzungssystem ein geeignetes Charakterisierungsinstrument zur Verfügung steht.

## **Section B**

### **General Introduction**

## 1 Synovial joints

The most common type of joints is the synovial joint like the knee, elbow and hip joint. Figure 1 gives a schematic illustration of these kinds of joints. They are defined by two or more bony ends, facing each other and being separated by the synovial cavity, which is filled with synovial fluid. The bones are covered by hyaline cartilage tissue and are embedded into a fibrous joint capsule, of which the innermost layer is the synovial membrane. The synovial membrane enables the constitution of the synovial fluid, which is a filtrate of blood, enriched by hyaluronic acid and lubricin. It fills the joint cavity and, due to its lubrication properties, allows almost frictionless gliding between the cartilage surfaces.

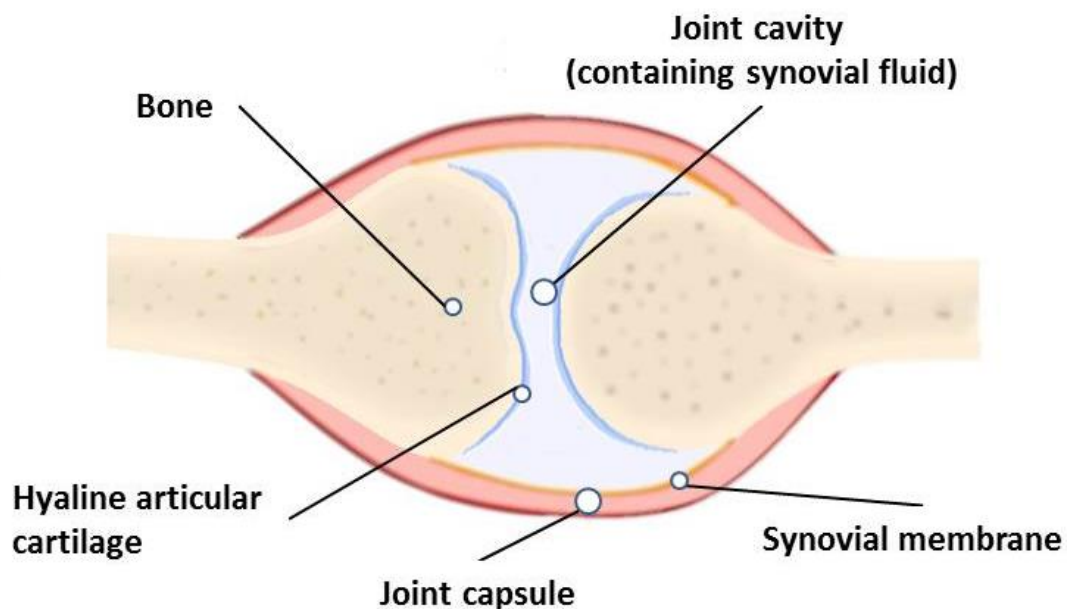


Figure 1: Schematic illustration of a synovial joint

Intra-articular administration is the injection of drug product through the skin, joint capsule and synovial membrane directly into the synovial cavity. Depending on the size of the joint, a suitable needle size has to be chosen in order to avoid irritations of the synovial membrane, often followed by an inflammatory response (synovitis). Furthermore, a contact between the needle and cartilage has to be prevented in order to avoid ruptures in the cartilage surface. Considering non-systemic joint diseases like osteoarthritis, intra-articular treatment seems to be an attractive opportunity: with a

minimum of administered API, the maximum pharmaceutical concentration at the site of action can be achieved. This approach minimizes systemic side effects. However, joint injections usually come along with pain and the risk of inducing infections or inflammation, which reduces patient compliance and therapeutic success.

### **1.1 The synovial membrane**

The synovial membrane lines the entire joint cavity of synovial joints and consists of two tissue layers: intima and sub-intima.

The intima, facing the joint cavity, consists of synoviocytes, embedded in an extracellular matrix. It usually is formed by 1-4 cell layers<sup>1</sup>, which can be distinguished in two types of cells:

- Type A synoviocytes are macrophage-like cells. They possess the ability to migrate from the synovia into the joint cavity and are responsible for the phagocytosis of foreign particles and cartilage debris. This immunogenicity has to be considered for the IA administration of drugs.
- Type B synoviocytes are fibroblast-like cells whose main function is the secretion of hyaluronic acid, an essential component of synovial fluid. Together with the extracellular matrix, type B synoviocytes form a compact but discontinuous diffusion barrier for molecules and particulate systems.

Associated to the intima, the sub-intima can consist of different types of tissue. Roughly, it can be distinguished between areole fibrous or adipose type tissues. Generally, the sub-intima of each tissue type can contain several different cell types: fibroblasts, macrophages, mast cells, and adipocytes. Furthermore, the sub-intima is traversed by blood- and lymph vessels. Depending on the tissue type, the distribution of the cells and the degree of vascularization is highly varying.

The character of the synovial membrane to act as a semi-permeable diffusion barrier between the synovial fluid and the blood- and lymph vessels located in the sub-intima, maintains an intact micro-environment within the joint cavity and is responsible for an optimal function of the joint.

## 1.2 Articular cartilage

The bony ends of synovial joints are covered by hyaline articular cartilage, which consists of an extracellular matrix (ECM) and the embedded chondrocytes. Even though, the weight percentage of the chondrocytes is only 2 – 5 %<sup>2,3</sup> of the whole cartilage tissue, these cells are responsible for the preservation of the ECM by secretion of essential matrix components. The ECM consists of a collagen network, cross-linked with glycosaminoglycans (GAG, e.g. hyaluronic acid) and proteoglycans (e.g. aggrecan). The main component of the ECM, however, is water (70 – 80 % of the overall weight), which binds to the hydrophilic, negatively charged GAGs and proteoglycans and leads to a swelling of the tissue. A classification of layers of the cartilage matrix can be done as illustrated in Figure 2.<sup>4</sup>

- The **superficial zone** (or surface or tangential zone) is characterized by smaller, oval formed chondrocytes. The cells, as well as the collagen fibrils are parallel aligned to the surface of the cartilage. This structure allows a smooth and gliding surface, inducing very little friction. Furthermore, the collagen network of the ECM within this zone is not as dense as in deeper layers. In addition, small fissures and inversions (so called clefts) make the cartilage surface accessible for active molecules.
- The chondrocytes in the **transitional zone** (or intermediate zone) are slightly bigger and are frequently aligned in cell clusters.
- Within the **radial zone** (or deep zone), amount and size of the cells further increases. The cells are vertically aligned in rod like cell clusters. Frequently, the radial zone and the intermediate zone are united as middle zone in literature. Both layers show an increased activity of chondrocytes regarding cell division and secretion. For this reason, the “middle zone” is an interesting target for so called “disease modifying osteoarthritis drugs” (DMOADs) for the treatment of osteoarthritis.
- The **calcified zone** is separated from the radial zone by the calcification line (or tidemark) and represents the connection to the subchondral bone. Aggregations of collagen fibrils (“Benninghoff arcades”) are anchored here, drifting apart tangentially towards the surface.

While the collagen network gives mechanical stability to the cartilage, the swollen gel of GAGs, aggrecan and water contributes elasticity to the tissue. Thereby, cartilage acts like a sponge: Under mechanical load, water is squeezed out and the impact force is absorbed and distributed. Under relaxation, the ECM aspirates synovial fluid. In this way, nutrient supply for the chondrocytes is provided, as the avascular cartilage cannot provide nutrients systemically. Besides, this mechanism bares the potential for the aspiration of dissolved active molecules. In particular, positively charged APIs may be absorbed and bound within the ECM through interaction with negatively charged GAGs and proteoglycans.

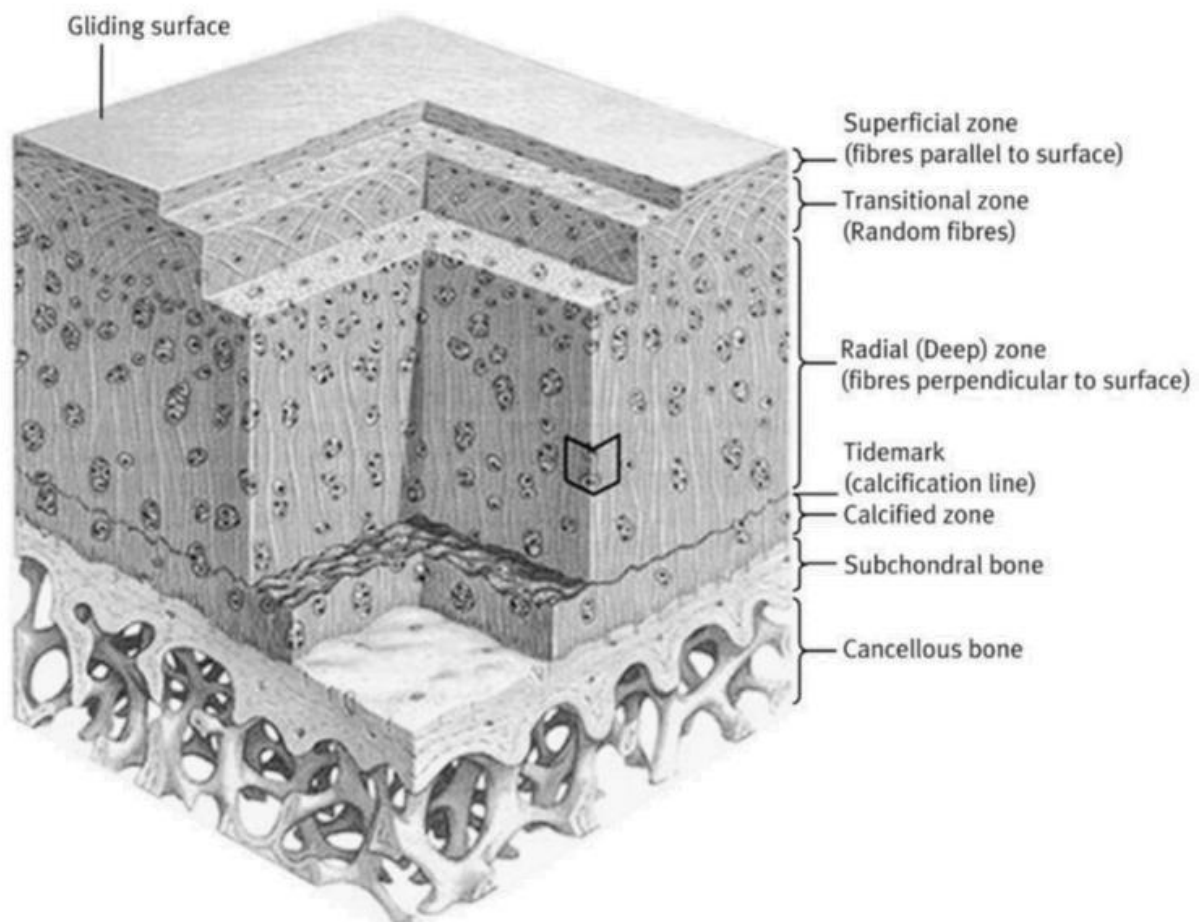


Figure 2: Schematic cross-section of hyaline articular cartilage (reprinted from <sup>4</sup> with permission)

### 1.3 The synovial fluid

The synovial cavity is filled with synovial fluid (SF). It is a filtrate of blood, enriched with lubricants like hyaluronic acid and lubricin. It mainly serves as a lubricant in order to reduce friction within the joint. Its composition is mainly controlled by the size selective and secreting properties of the synovial membrane. As Table 1 depicts, the volume of synovial fluid in a healthy human knee joint is up to 4 ml and its composition matches the composition of blood plasma in terms of small molecules content, osmolarity and pH. Larger molecules like plasma proteins, however, can be found in SF as well, but in reduced concentrations. Also blood cells occur in synovial fluid in significantly reduced amounts, which illustrates the size-selective filter function of the synovial membrane. In addition, the SF contains hyaluronic acid (HA), which is secreted by the synovial membrane. HA is an essential component of SF and serves as viscosity increasing agent and as lubricant. As shown in Table 1, the high concentration of HA in SF leads to distinctly increased viscosity. Compared to healthy joints, the SF undergoes specific alterations in osteoarthritic patients: the volume increases, the content of hyaluronic acid and thus viscosity decreases, and the appearance of SF becomes slightly turbid due to debris from cartilage degeneration processes. Furthermore, an increased amount of leukocytes can be observed, which is attributed to inflammatory processes.

Parameter	Healthy	Osteoarthritis	Plasma
Viscosity [mPas]	> 300	decreased	1.4
Osmolarity [mOsm]	~ 300	unchanged	~ 300
pH	7.4	unchanged	7.4
Appearance	Clear, slightly yellowish	Slight turbid, yellow	--
Hyaluronic content [g/L]	3 - 4	decreased	$4.2 \times 10^{-6}$
Leukocytes ( $\times 10^9$ )	< 0.2	< 3	7
Erythrocytes ( $\times 10^9$ )	< 2	n/a	4900
Total protein [g/L]	10 – 30	unchanged	60 - 80
Albumin [g/L]	8 – 13	unchanged	35 - 45
Lactate [mmol/L]	1.0 – 1.8	increased	1.0 – 1.8

Table 1: Composition of synovial fluid in healthy and osteoarthritic human knee joints compared to plasma<sup>5-8</sup>

## 2 Sustained release intra-articular drug delivery

As described, the unique structure of synovial joints comprises an enclosed synovial cavity, lined by the synovial membrane. This structure provides the potential for the local treatment of joint diseases like osteoarthritis or rheumatoid arthritis via direct injection of drugs into the joint cavity. However, as intra-articular (IA) injections usually come along with pain and the risk of infection or inducing an inflammation, intra-articular treatments require long injection intervals, which may prevent a successful therapy.

Hence, sustained release drug products are required, in order to provide effective concentrations of active pharmaceutical ingredients (API) inside the joint cavity over the whole duration of the therapy, without exceeding a maximum tolerable amount of joint injections. In general, the physiology of synovial joints offers three kinds of mechanisms to gain prolonged API exposure:

- (i) Physical retention of particulate systems by the synovia

As physical barrier between the joint cavity and surrounding blood- and lymph vessels, the synovial membrane has the potential to retain particulate systems inside the joint, so that API exposure within the synovial cavity over a longer period of time can be achieved. For instance, polymeric microparticles and nanoparticles have been investigated for this purpose before<sup>9-11</sup>. In addition, crystal suspensions of poorly water soluble actives can be considered in this context. Furthermore, at present, this type of formulation is the only option for sustained drug exposure upon intra-articular administration which can be purchased on the market. However, currently available crystal suspensions provide only relatively short half-lives inside the joint.

- (ii) Size-selective retention by the synovial membrane

The synovial membrane serves not only as a physical barrier, but also acts as a size-selective diffusion barrier. Accordingly, the retention of small molecules by the synovia is limited: The half-life for chemical entities inside the joint upon intra-articular administration is about 1 – 6 hours<sup>12-15</sup>. Larger molecules (like proteins or polymers), however, are retained by the synovial membrane<sup>16,17</sup> and have the potential to gain significantly prolonged residence times within the synovial cavity. Thus, prodrug formulations, coupling an active ingredient with a biocompatible polymer in a suitable size range, may prevent rapid clearance of the active substance and provide extended pharmaceutical action inside the joint. In addition, formulations may be considered containing the API, embedded in a polymeric gel matrix.

- (iii) Retention within the joint by distribution into the cartilage matrix

The cartilage matrix consists of about 3% chondrocytes, 15% extracellular matrix (ECM) and about 80% water. The ECM is highly porous and consists of a network of negatively charged proteoglycans and glycosaminoglycans. The negative charges bare the potential to attract and bind positively charged compounds and to form a drug depot. As a matter of course, this approach may also be combined in synergy with the effect of synovial retention (i and ii).

## 2.1 Why do we need sustained release in synovial joints?

Worldwide, osteoarthritis (OA) is the most common joint disorder, affecting about 33% of the adult population<sup>18</sup>. This disease is basically characterized by the loss of cartilage mass, coming along with intervallic inflammation of the joint. This leads to significant constriction of joint mobility, phases of strong pain perception and finally the entire loss of joint flexibility.

As in OA usually only one or a few joints are affected, a main focus in the pharmacological therapy is the local treatment via intra-articular administration into the joint cavity. This provides a maximum of API at the site of action, while minimizing the overall dose und thus systemic side effects.

However, for a continuous treatment, frequent injections have to be administered, as dissolved molecules are rapidly cleared through the synovial membrane into systemic circulation<sup>13</sup>. As each injection comprises pain, as well as the risk of inducing infection and inflammation, this often leads to bad patient compliance and the risk of even accelerating the progression of the disease.

Sustained release drug products have the potential to overcome this issue by increasing injection intervals and providing pharmacological active drug levels inside the joint over a longer period of time.

## 2.2 State of the art

The amount of currently marketed drug products for sustained intra-articular drug delivery is still quite limited. With one exception, these drug products are consistently composed of crystal suspensions of poorly water soluble glucocorticoids, in some cases combined with a partition of a second, dissolved API, for an immediate effect. The exception among these preparations is Lipotalon<sup>®</sup>, which is a liposomal formulation. Besides, Supertendin<sup>®</sup> combines the crystal suspension of a glucocorticoid with a dissolved local anesthetic. Table 2 gives an overview on currently available drug products for sustained intra-articular drug delivery.

As mentioned before, the amount of currently available drug products for sustained intra-articular drug delivery is quite limited. Furthermore, the residence times inside the joint are relatively short. However, the duration of pharmacological action (or biological half-life) of these glucocorticoid drugs can achieve several weeks, which is attributed to their pharmacological mode of action.

Besides marketed drug products, research on improved solutions for the challenges of intra-articular drug delivery can be found in literature, with several new formulation options. Table 3 gives a literature overview:

- Particulate systems

As mentioned before, the synovial membrane acts as a physical barrier for particulate systems. Thus, micro- and nanoparticles of biodegradable polymers seem to be a particularly attractive approach for intra-articular drug delivery. For the function of such release systems, however, several structural conditions have to be considered. In particular, the particle size is a major parameter. It affects particle retention, as well as the intensity of a potential inflammatory response upon intra-articular administration. Howie et al., for instance, showed that particles smaller than 5µm provoke a mononuclear macrophage response inside the joint<sup>27</sup> and that phagocytosed particles are transported into the sub-intima. Within the sub-intima, particles are no longer available for drug release into the synovial cavity. Particles in a larger size range (~ 26 µm), however, do not undergo phagocytosis<sup>10</sup> and are either dispersed within the synovial fluid or attached to the synovial membrane and cartilage surface<sup>9</sup>. Hence, on the one hand, a size range > 5 µm seems to be preferred for particulate systems in the context of intra-articular drug delivery. On the other hand, functionalized nano-scaled formulations may lead to prolonged API exposure within the joint as well. Morgen et al., for example, investigated polymeric nanoparticles, covered with a positively charged shell. It was demonstrated, that 73 % of the administered API load was still present inside the joint after 7 days (in contrast to 23 % upon administration of unformulated API)<sup>19</sup>. In this case, this can be explained by electrostatic interaction between the positively charged nanoparticles and the negatively charged cartilage surface. Furthermore, nano-scaled formulations bare the potential for direct tissue targeting within the joint. In the case of an acute synovitis, for instance, the phagocytosis and transport of the particles into the Synovia may be quite advantageous. Similar to a “Trojan horse”, anti-inflammatory drugs, for example, can be transported directly into the affected tissue<sup>20,28,29</sup>. In addition, Hua-Ding et al. showed that hyaluronic acid / chitosan nanogels effectively targeted and transfected cartilage cells (chondrocytes)<sup>30</sup>.

In contrast, Rothenfluh et al. investigated specialized binder-peptides and demonstrated active targeting and retention inside the cartilage extracellular matrix. Besides particle size, also the shape of the particles has an influence on their performance, in particular their tolerability inside the joint. For instance it was shown that round shaped particles lead to inflammatory reactions to a less extent than needle or rod-shaped particles do<sup>31,32</sup>.

- *In situ* forming systems

Besides particular systems, literature also discusses *in situ* forming gels as type of formulation, being formed after injection into the joint. The amount of publications in this field, however, is quite limited. To the author's best knowledge, basically only two approaches for *in situ* forming systems for IA drug delivery were published: (i) thermosensitive, *in situ* forming gels and (ii) *in situ* forming crystal suspensions. Sandker et al., for instance, investigated acyl-masked PCLA-PEG-PCLA triblock co-polymers, which form a gel matrix at body temperature, entrapping the API and forming a drug depot. Besides good biocompatibility, a residence time inside the joint of 3 - 4 weeks was demonstrated<sup>21</sup>. A similar approach was followed by Miao et al., applying a PCL-PEG-PCL triblock co-polymer, loaded with Methotrexate<sup>23</sup>. In contrast, Betre et al. utilize so called "elastin-like polypeptides" (ELP) as gel matrix. In a placebo-trial, this approach also showed significant retention inside the joint<sup>22</sup>. An entirely different approach is followed by Larsen et al. with *in situ* forming crystal suspensions<sup>24</sup>. In this work, the poorly water soluble active celecoxib was dissolved in high concentration in PEG 400. Upon injection into the joint, the solvent (PEG 400) is eliminated through the synovial membrane and celecoxib precipitated inside the joint cavity, forming a crystalline depot. An *in vivo* trial with 4 healthy horses showed detectable amounts of celecoxib in the horse plasma after 10 days, suggesting the formation of a drug depot. However, a significant immune reaction (synovitis) on the crystals was observed as well. In addition, uncontrolled crystallization process may bare the risk of developing different polymorphs, differing from the original form.

- Liposomal systems

Besides glucocorticoid crystal suspensions, a liposomal formulation (Lipotalon<sup>®</sup>) is the only formulation option for sustained intra-articular drug delivery, which is available on the market. Additionally, several investigations on liposomal formulations can be found in literature, mostly concentrating on anti-inflammatory aspects by applying antiphlogistic drugs

(glucocorticoids, methotrexate, diclofenac). On the one hand, the liposomal formulation of these drugs serves for the retention of drugs inside the joint cavity. Williams et al., for instance, investigated liposomes in 2 size ranges (100 nm and 1.2  $\mu\text{m}$ ). They demonstrated that the larger liposomes were still present in the synovial cavity after 21 days, in contrast to the smaller liposomes<sup>33</sup>. As already mentioned before, Bonanomi et al. showed a size dependency of the retention of liposomal formulations in the joint as well<sup>25</sup>. On the other hand, this kind of formulation also bares the potential for drug targeting. As described for the nano-scaled formulations, liposomes in a specific size range (0.75 – 5  $\mu\text{m}$ ) are preferably phagocytosed and transported to the sub-intimal tissue of the synovial membrane<sup>26</sup>. Thus, anti-inflammatory drugs are directly transported to the affected tissue, as inflammatory processes within synovial joints are usually triggered by the synovial membrane.

In summary, the choice of a suitable drug delivery approach strongly depends on the desired indication, as different formulations allow different ranges of release duration or different targets inside the joint. For the treatment of osteoarthritis, for instance, one approach is the inhibition of catabolic enzymes (matrix metalloproteinases, hyaluronidases), which leads to deceleration of cartilage degradation<sup>34,35</sup>. In order to provide an appropriate treatment, constant levels of pharmacological active drug within the joint are required. To avoid weekly re-administration of drug, a drug delivery system (DDS) would be desirable, which releases the API over a period of several months. Liposomal formulations and non-functionalized polymeric nanoparticles demonstrated to be suitable for drug release over several days. Thus, these formulation options do not seem to be suitable for intra-articular drug delivery in the range of months, as active clearance via phagocytosis occurs. However, polymeric microparticles in a certain size range showed not to undergo phagocytosis by synovial macrophages. Furthermore, several *in vitro* release studies on microparticulate formulations indicate the suitability for this kind of formulation to provide drug delivery over several weeks<sup>36-40</sup>.

Generally, the choice of polymer matrix plays an important role in this context. For polymeric microparticles, most approaches concentrate on the application of PLGA. However, it has been shown that functionalized, nano-scaled formulations have the potential to gain significantly prolonged residence times inside the joint as well. For instance positive charges on the particle surface or specialized binder peptides are considered to achieve interactions of the formulation with the cartilage matrix. This additionally bares the potential for targeting the cartilage matrix or the chondrocytes.

<b>Drug</b>	<b>API(s)</b>	<b>Technology</b>	<b>Kinetic data</b>
<i>Celestan<sup>®</sup> Depot</i>	Betamethasone acetate Betamethasone dihydrogen phosphate	crystal suspension solution	Detectable in plasma for > 2 weeks
<i>Delphicort<sup>®</sup> 40 mg</i>	Triamcinolone-16 $\alpha$ , 21-diacetate	crystal suspension	Mean residence time in joint: 1.4 days
<i>Diprosone<sup>®</sup> Depot</i>	Betamethasone dipropionate Betamethasone dihydrogen phosphate	crystal suspension solution	Duration of action: 4-6 week (biological half-life)
<i>Lederlon 20 mg<sup>®</sup></i>	Triamcinolone hexacetonide	crystal suspension	n/a
<i>Lipotalon<sup>®</sup></i>	Dexamethasone-21-palmitate	emulsion	Mean residence time in joint: 8 days
<i>Supertendin<sup>®</sup></i>	Dexamethasone acetate Lidocaine hydrochloride	crystal suspension solution	Duration of action: 2-4 weeks (biological half-life)
<i>Prednigalen<sup>®</sup></i>	Prednisolone acetate	crystal suspension	n/a
<i>Volon<sup>®</sup> A 40</i>	Triamcinolone acetonide	crystal suspension	Mean residence time in joint: 3 days

Table 2: Prolonged release glucocorticoid formulations on the German market (2016)

Matrix / Polymer	API / Marker	Animal model	Comments	Reference
<b><u>Particulate systems</u></b>				
<i>Microparticles</i>				
PLGA	Placebo	Rat (healthy)	Investigation of the influence of particle size on synovial phagocytosis Median diameters: 265nm and 26,5µm	10
PEG	Placebo	Sheep (healthy)	Particle size: 40 - 100 µm Location inside the synovial cavity and inflammatory response was investigated	9
<i>Nanoparticles / Nanogels</i>				
Modified Dextran Eudragit RL 100	RFK-FITC	Rat (healthy)	Median diameter: ~ 100nm neutral core (Dextran), positive charged shell (Eudragit) In situ gelation with endogenous hyaluronic acid Investigation of retention vs. uncharged particles	19
Chitosan / Hyaluronic acid	Photosens. TPPS4, TPCC4 and Ce6	Mice (induced arthritis)	Nanogel formulation was shown to promote synovial macrophage uptake and synovial retention Particle size < 1µm	20

Matrix / Polymer	API / Marker	Animal model	Comments	Reference
<b><u>In-situ forming systems</u></b>				
PCLA-PEG-PCLA	Triiodobenzoyl (TIB)	Rat (healthy)	After IA administration, signal intensity of the visualized gel gradually declined over 4 weeks.	21
Elastin-like polypeptides (ELPs)	Placebo	Rat (healthy)	A 25-fold increase in joint half-life of thermally aggregating ELPs was demonstrated in comparison to soluble proteins of similar molecular weight	22
PCL-PEG-PCL	Methotrexate (MTX)	Rat (healthy)	3 times lower values of maximum plasma concentration of MTX were observed for the MTX loaded thermosensitive in situ formed gels than for MTX solutions.	23
PEG 400	Celecoxib	Horses (healthy)	Crystalline depots of precipitated celecoxib lead to detection of celecoxib in plasma over a period of 10 days.	24

Matrix / Polymer	API / Marker	Animal model	Comments	Reference
<b>Liposomes</b>				
Egg-lecithin, cholesterol, phosphatidic acid (7:2:1)	Methotrexate (MTX- $\gamma$ -DMPE)	Rat (induced arthritis)	Anti-inflammatory effects were still observed after 21 days for the multilamellar vesicles (in contrast to unilamellar liposomes)	25
Egg-phosphatidylcholine, octyl-glucoside phosphatidic acid	Dexamethasone palmitate (DMP)	Rat (healthy and induced arthritis)	Size-dependent retention inside the joint was observed (for larger liposomes). Macrophage uptake between 0.75 and 5 $\mu$ m was demonstrated.	26

Table 3: Examples for sustained release intra-articular formulation options

### 3 Aim of the thesis

As mentioned, mainly three retention mechanisms are considered to enable sustained drug delivery in synovial joints:

- Physical retention of particulate systems by the synovia
- Size-selective retention of solutes by the synovial membrane
- Retention by distribution of solutes into the cartilage matrix

This work follows these approaches in two major sections:

Section C investigates the potential for sustained drug delivery by (ii) synovial retention and (iii) cartilage distribution. For a deeper understanding, the relevant influence parameters molecular size, positive charge and charge density are evaluated with the help of different model polymers.

Section D discusses the intra-articular treatment with sustained release particular systems. In particular, crystal suspensions of poorly soluble peptides are characterized, focusing on their *in vitro* release behavior. For this purpose a novel *in vitro* release setup is introduced and investigated for its potential to mimic physiological relevant conditions.

## Section C

# Kinetic investigations on bovine joint tissues

*Parts of this work were published in the European Journal of Pharmaceutics and Biopharmaceutics:*

*Sterner, B., Wöll, S., Harms, M., Weigandt, M., Windbergs, M. & Lehr, C. M.:*

*“The effect of polymer size and charge of molecules on permeation through synovial membrane and accumulation in hyaline articular cartilage.”*

*European Journal of Pharmaceutics and Biopharmaceutics 101, 126-136 (2016)*

## 1 Introduction

As described above, retention of intra-articular injected drugs can be obtained via retention of particulate systems by the synovial membrane. In addition, the synovial membrane also bares the potential to retain intra-articular injected dissolved compounds:

On the one hand, in literature, the synovial membrane is described as size selective barrier for the entry of molecules (> 10 kDa) into the joint cavity<sup>41-44</sup>. Discussing the retention of intra-articular administered drug solutions, this size-selectivity also applies for clearance of substances from the joint cavity into systemic circulation: While small molecules undergo rapid clearance upon intra-articular injection, showing half-lives of about 1-6 hours, macromolecules like albumin and hyaluronic acid were observed to show distinctly prolonged dwell times inside the joint (13-26 hours)<sup>12,16,45,46</sup>. Thus, macromolecular actives (e.g. proteins and antibodies) as well as small molecules, linked to biocompatible polymeric carriers, are considered to exhibit distinctly decelerated clearance and therefore provide prolonged pharmacological activity within the joint<sup>47</sup>.

On the other hand, the observed half-lives for macromolecules inside the joint (13-26 hours) are not considered to be adequate to provide sufficiently prolonged injection intervals. However, not only the synovial membrane is an interesting structure to be investigated in this context. The extracellular cartilage matrix (ECM) essentially consists of glycosaminoglycans (GAGs), like hyaluronic acid, and proteoglycans like aggrecan. These strong negatively charged components have been shown to be able to attract and bind positively charged compounds through electrostatic interaction. Van Lent et al., for example, demonstrated that cationic bovine serum albumin (cBSA) showed significant absorption in cartilage tissue<sup>48</sup>, in contrast to uncharged bovine serum albumin (BSA). Independently from this, the size dependency for the penetration of cartilage tissue was investigated before as well. A significant decline of cartilage penetration capability for increasing size of the solute was shown by Maroudas et al.<sup>49</sup>. This potential for positively charged, macromolecular compounds to penetrate cartilage tissue may be a reasonable approach to consider cartilage tissue as a deep compartment, enabling prolonged exposure with API inside the joint.

The idea of section C is that the combination of synovial retention and a depot-effect of the cartilage matrix may enable joint dwell times in the range of weeks.

In order to be able to evaluate the influence of molecular parameters on synovial retention and cartilage accumulation, essentially two major questions had to be answered:

- To which extent influences the molecular size of a compound the retention by the synovial membrane?
- To which extent influences positive charge and size the ability of a compound to accumulate inside cartilage tissue?

For this purpose, PEG polymers of different molecular size were investigated for their retention by the synovial membrane. In addition, different model polymers (PEG, chitosan, HEMA-Co-TMAP) with different size and charge were investigated for their ability to penetrate and accumulate inside the cartilage matrix.

The results demonstrate the influence of size and charge of a molecule on synovial retention as well as on distribution into cartilage tissue. Thus, relevant information for the rational development of novel intra-articular sustained release therapeutics is gained.

### 1.1 Kinetic considerations

The critical parameter for sustained intra-articular drug delivery is the joint residence time or the half-life of injected compounds inside the joint. In order to describe the connection between synovial retention, cartilage accumulation and the joint residence time, a reflection of the kinetic situation is crucial.

As Figure 3 depicts, the kinetic situation of an IA administered solution can be described as an open two-compartment model according to <sup>51</sup>:

$$c_{SF}(t) = \frac{D \cdot [(k_r - \beta) \cdot e^{-\beta t} + (\alpha - k_r) \cdot e^{-\alpha t}]}{V_i \cdot (\alpha - \beta)} \quad (1)$$

where  $c_{SF}$  is the concentration in synovial fluid,  $D$  is the administered dose,  $V_i$  is the initial distribution volume and

$$\alpha, \beta = \frac{1}{2} \cdot [(k_a + k_r + k_e) \pm \sqrt{(k_a + k_r + k_e)^2 - 4 \cdot k_r \cdot k_e}] \quad (2)$$

As equations (1) and (2) present, the concentration of an injected compound in the synovial fluid ( $c_{SF}$ ) is mainly controlled by “ $k_e$ ”,  $k_a$  and  $k_r$ . The retention by the synovial membrane determines “ $k_e$ ”. The ratio between  $k_a$  and  $k_r$  can be expressed as the partition coefficient ( $P_{coeff}$ ):

$$P_{coeff} = \frac{k_a}{k_r} = \frac{c_{analyte}(cartilage)}{c_{analyte}(donor)} \quad (3)$$

Consequently, the residence time of potential new drug candidates inside the joint after IA administration is defined by the retention through the synovial membrane and by the partition into cartilage tissue. These parameters are essentially influenced by the size and positive charge of a compound. Section C of this work is intended to quantify and to give estimation about the influence of these parameters.

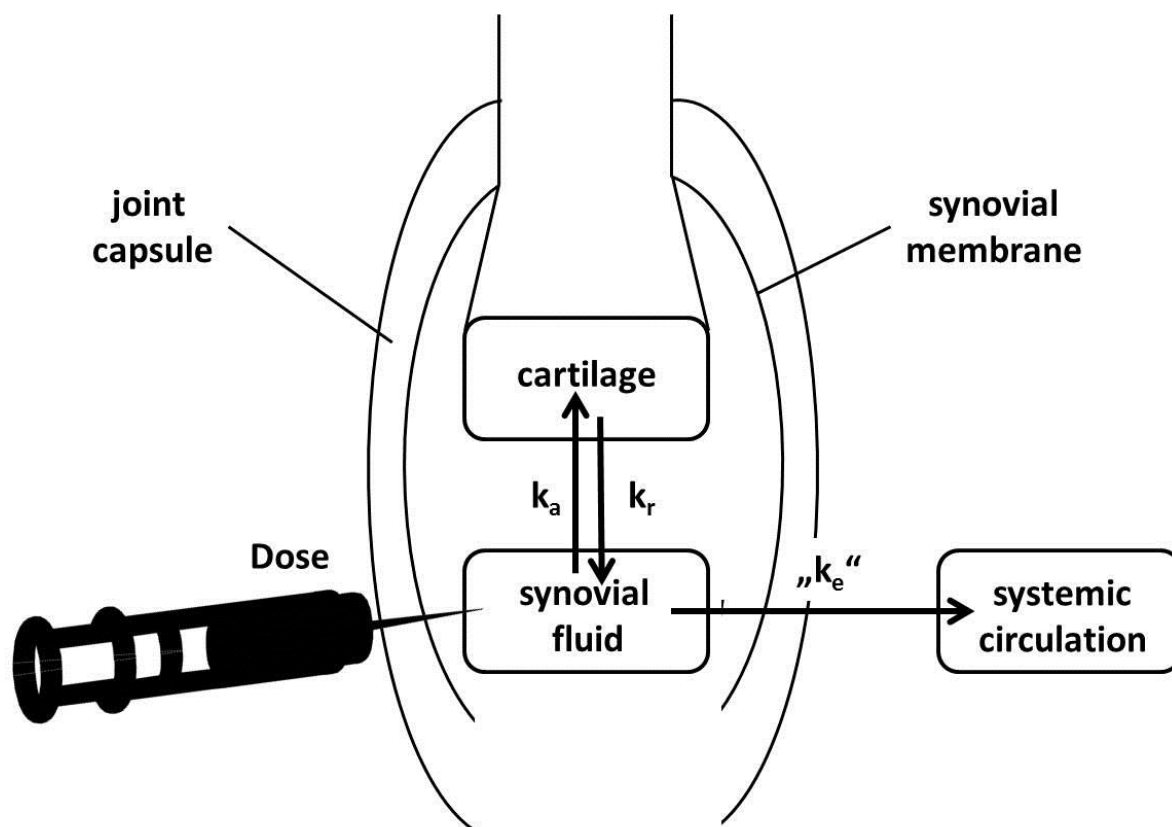


Figure 3: Schematic illustration of distribution upon intra-articular injection.  $k_a$  and  $k_r$  describe distribution into cartilage tissue. The elimination through the synovial membrane is described by  $„k_e“$  (reprinted from <sup>50</sup> with permission)

## 2 Materials and Methods

### 2.1 Materials

Polymers and small molecules of different molecular weight and positive charge were applied in the following experiments. Polyethylene glycol with 6, 10, 35 and 200 kDa (PEG 6 – PEG 200) was purchased from Sigma-Aldrich (St. Louis, USA). Chitosan 95/5, Chitosan 70/5 as well as Chitosan oligomer were purchased from Hepe Medical (Halle, Germany). Five different hydroxyethylmethacrylate-Co-trimethylammoniumpropylacrylamid polymers (HEMA-Co-TMAP, HCT A1 – A3 and HCT B2 and B3) were synthesized at Merck (Darmstadt, Germany) with different molecular weights and different degrees of substitution by positive charged TMAP.

For fluorescence microscopic evaluation of the cartilage experiments, chitosans and HCT polymers were derivatized with fluorescein isothiocyanate (FITC). For this purpose, the polymers were dissolved in 0.1M acetic acid. Fluorescein isothiocyanate isomer I (Sigma-Aldrich, St. Louis, USA), dissolved in Methanol was added. The mixture was shaken at room temperature and light exclusion for 1h. Purification was performed by alkalic precipitation for the chitosan polymers, by size exclusion chromatography for the chitosan oligomers and by tangential flow filtration for the HCT polymers. The degree of FITC labeling is given in Table 5, Table 6, Table 7 and Table 8.

Methylene blue (MB) was obtained from Merck (Darmstadt, Germany).

D1408 Dulbecco's phosphate buffered saline (PBS) and Dulbecco's modified eagle medium (DMEM), as well as P4333 Penicillin-Streptomycin solution (Pen/Strep) and A2942 Amphotericin B solution (AmphoB) were purchased from Sigma-Aldrich (St. Louis, USA). Sodium acetate was purchased from Merck (Darmstadt, Germany).

Bovine synovial membrane and cartilage explants were prepared from knee joints of healthy cows, purchased from a local slaughterhouse.

## 2.2 Methods

### 2.2.1 Characterization of model polymers

Model polymers were characterized for their molecular weight, charge and size. Gel permeation chromatography was applied for the determination of molecular weight and hydrodynamic radius. A Malvern Viscotek® TDMax triple detector device (Worcestershire, UK) with a refractive index detector, a light scattering detector and a viscometer detector was utilized for this purpose. For the detector calibration, PEG standards (for PEG polymers) and pullulan standards (for chitosans) (Sigma-Aldrich, St. Louis, USA) were applied. Data assessment was done with Malvern OmniSEC® GPC software (Worcestershire, UK). Characterization of the HEMA-Co-TMAPs was done by means of <sup>1</sup>H-NMR.

The pKa values, degree of deacetylation (DD) and finally the number of positive charges per molecule of the chitosans were determined via titration of the compounds (dissolved in HCl) against NaOH. The charge density was calculated according to equation (4):

$$D_{ch} = \frac{\# \text{ pos.charges / molecule}}{MW} \cdot 1000 \quad (4)$$

### 2.2.2 Preparation of tissue explants

Tissue explants were prepared from knee joints of healthy cows, delivered by a local slaughterhouse. Upon removal of muscles and connective tissue, the joint capsule was carefully dissected in order to avoid cutting the synovial membrane. A scalpel was used to remove the synovial membrane from the joint. The bare synovial membrane was preserved in Dulbecco's Modified Eagle Medium (DMEM) containing a mixture of Penicilline, Streptomycine and Amphotericine B (Pen/Strep and AmphoB).

The cartilage explants were obtained by perforation and separation of round pieces of cartilage tissue with a die-cutter (round, ø 10 mm) from the condylar surface of bovine knee joints. The explants were weighed and preserved in DMEM containing Pen/Strep and AmphoB.

### 2.2.3 Diffusion experiments with bovine synovial membrane

The synovial membrane explants were cropped in appropriate slices of approximately 20 mm diameter and fixed in customized diffusion chambers (Figure 4).

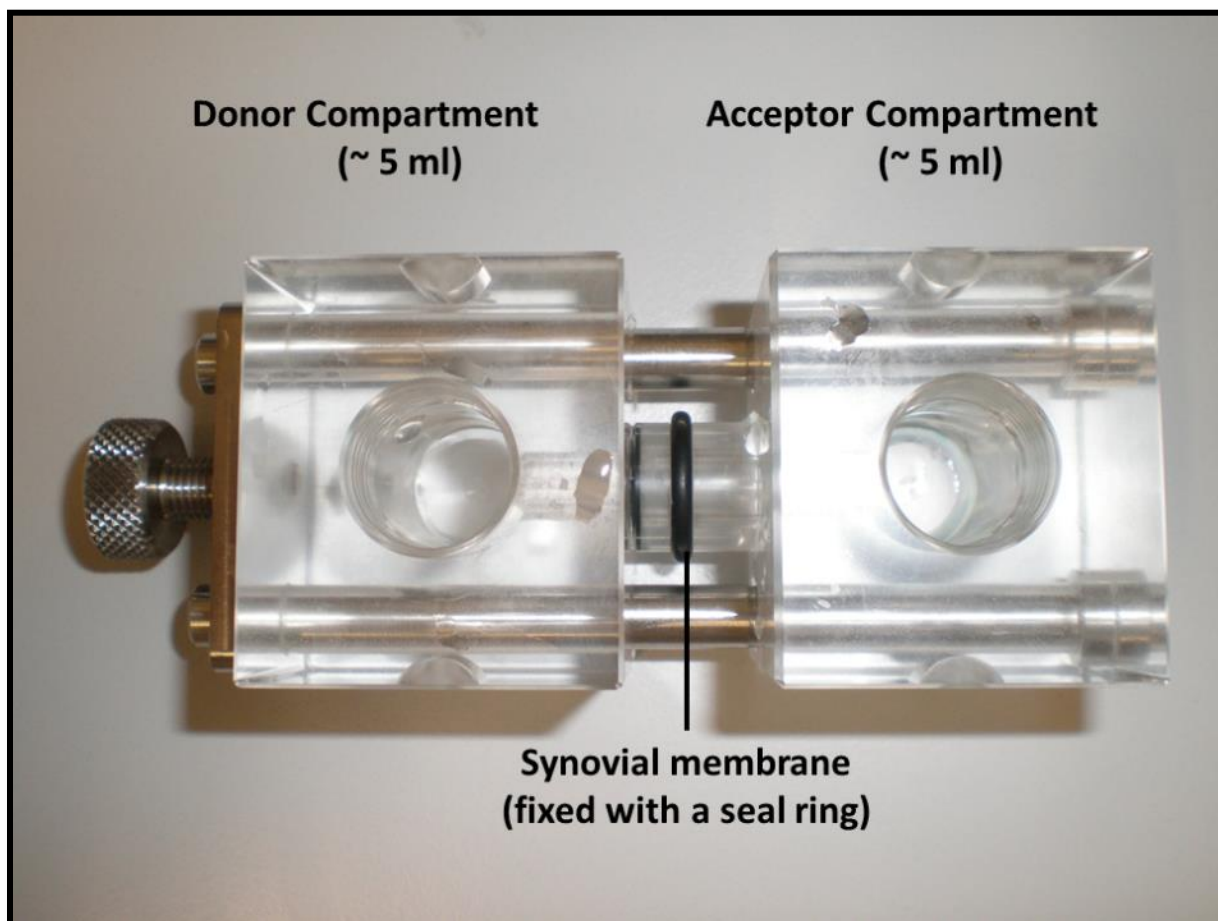


Figure 4: Illustration of the diffusion chamber for synovial membrane explants (reprinted from <sup>50</sup> with permission)

5 ml of a solution containing PEG 6, 10, 35 and 200 kDa (5 mg/ml each) and methylene blue (0.1 mg/ml) in PBS (with Pen/Strep and AmphoB) were added to the donor compartment. The acceptor compartment was filled with 5ml PBS (+ Pen/Strep and AmphoB). The chambers were incubated under magnetic stirring at 37 °C. 200µl samples were taken from both, the donor and the acceptor compartment at predetermined time intervals.

For reference experiments, a 0.2 µm regenerated cellulose filter membrane (Whatman, Maidstone, UK) instead of synovial membrane was fixed between the compartments. This membrane enabled free diffusion for all analytes and thus a chamber-specific reference for each analyte. The PEG samples

were quantified by gel permeation chromatography (GPC), with a refractive index detector. Methylene blue was quantified by a UV plate reader (Tecan®, Männedorf, Switzerland).

#### 2.2.4 Penetration experiments with bovine cartilage tissue

The cartilage explants were washed with PBS and placed inside 10 ml snap-cap vials. The explants were covered with analyte solution (2 ml). Subsequently, the vials were stored in a shaker at 37 °C or room temperature for up to 6 days. 200 µl samples were taken at predetermined time intervals. Samples containing chitosan solution were analyzed by GPC, using a refractive index detector. HEMA-Co-TMAPs were quantified with a UV detector. Reference samples (methylene blue solutions) were analyzed by a UV plate reader. From the decline of analyte concentration in the donor solution and from the corresponding cartilage mass, a partition coefficient was determined according to equation (5):

$$P_{coeff} = \frac{c_{analyte}(cartilage)}{c_{analyte}(donor)} \quad (5)$$

*Preparation of histologic slices:* In an additional set of experiments, cartilage explants were treated accordingly with solutions of FITC labeled derivatives of the model polymers. After 4 hours, 8 hours, 1 day and 2 days of incubation, the cartilage was washed with 1 ml of buffer and fixed in a solution of 1% paraformaldehyde (PFA) in PBS. Cross sections were prepared with a microtome and fluorescence microscopic pictures were taken with a Leica DM6000B (Wetzlar, Germany).

### 2.2.5 Quantification of the model polymers:

All analytes (PEG, chitosan, HEMA-Co-TMAP) were quantified via gel permeation chromatography as follows:

Parameter	PEG	Chitosan	HEMA-Co-TMAP
Device	Malvern Viscotek <sup>®</sup> TDAmx	Malvern Viscotek <sup>®</sup> TDAmx	Agilent <sup>®</sup> 1100 HPLC
Column	Tosoh <sup>®</sup> TSKgel G3000 PWXL	Tosoh <sup>®</sup> TSKgel G3000 PWXL	Tosoh <sup>®</sup> TSKgel G3000 PWXL-CP
Eluent	0.1M NaNO <sub>3</sub>	0.5M ammonium acetate (pH 4.8)	0.1M (NH <sub>4</sub> )HCO <sub>3</sub> / ethanol (80/20)
Flow rate	0.5 ml/min	0.5 ml/min	0.5 ml/min
Temp.	30°C	30°C	40°C
Detector	Refractive Index (RA)	Refractive Index (RA)	Agilent <sup>®</sup> Diode Array Detector (230 nm)

Table 4: Analytical parameters for quantification of model polymers

### 3 Results and discussion

#### 3.1 Characterization of model polymers and small molecules

The influence of molecular weight and charge of different model compounds should be investigated. Thus, PEG-polymers, chitosan polymer and oligomers, HEMA-Co-TMAP polymers and different small molecules were chosen and characterized.

Table 5, Table 6, Table 7 and Table 8 give an overview on the properties of the applied model compounds, regarding molecular weight, hydrodynamic radius and positive charge.

Summarized, four different types of model compounds were applied:

- PEG-polymers

These compounds served as uncharged specimen with molecular weights between 6.8 and 204 kDa. They were applied both for permeation experiments through synovial membrane and penetration experiments with cartilage tissue in order to evaluate the impact of molecular weight.

- Chitosan polysaccharides

Chitosans were applied in two size ranges (polymeric: 58 kDa; oligomeric: 2.1 kDa). As can be seen in the structure, chitosan possesses primary amino-groups, leading to pH-dependent positive charge. This enables the adjustment of the amount of positive charge per molecule by variation of the buffer system and pH value of the applied medium. Consequently, the chitosans were used for cartilage penetration experiments. Under variation of the positive charge (adjusted by the pH of applied buffer media), the impact of positive charge (and thus the charge density) on the ability to penetrate and accumulate inside cartilage tissue was investigated. In addition, FITC-labelled derivatives were synthesized for corresponding experiments and fluorescence microscopic evaluation of cartilage tissue.

- HEMA-Co-TMAP (HCT)

HCT polymers were applied in two different size ranges (A1-A3: 13-14 kDa; B1 and B2: 98 and 233 kDa). As the molecular structure depicts, the quaternary amino-groups possess fixed (pH independent) positive charges and were synthesized with a range of different amounts of positive charge. This allowed the evaluation of the dependency of cartilage penetration from the

charge density at a fixed pH value. FITC-labelled derivatives were synthesized and applied for penetration experiments and fluorescence-microscopic evaluation.

- Small molecules

Methylene blue (permeation through synovial membrane and cartilage penetration), MSC-C1 and MSC-D1 (only cartilage penetration) were applied as well. While methylene blue and MSC-D1 possessed positive charge, MSC-C1 represented an uncharged small molecule.

In summary, **molecular weights** between 0.32 and 204.2 kDa and **positive charge densities** between zero and  $5.1 \text{ kDa}^{-1}$  were covered by the presented compounds. This enabled the investigation of the impact of these two parameters on permeation through synovial membrane and penetration of cartilage tissue in a wide range and across different molecules.

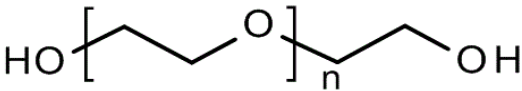
Parameter	PEGs			
Molecular formula				
Type	6	10	35	200
MW [kDa]	$6.8 \pm 0.4$ (n=3)	$13.0 \pm 0.1$ (n=3)	$37.9 \pm 0.8$ (n=3)	$204.2 \pm 1.6$ (n=3)
PDI ( $M_w/M_n$ )	1.04	1.05	1.11	1.48
$R_h$ [nm]	$2.6 \pm 0.1$	$3.8 \pm 0.0$	$7.1 \pm 0.1$	$20.6 \pm 0.2$

Table 5: Properties of PEG polymers. 4 different PEGs with molecular weight between 6.8 and 204 kDa were applied (reprinted from <sup>50</sup> with permission)

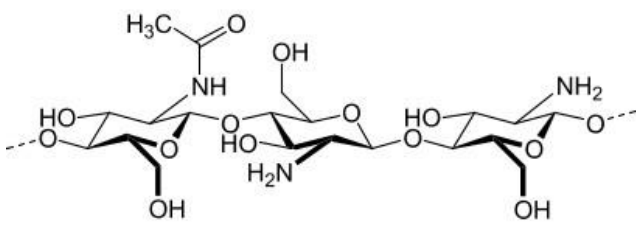
Parameter	Chitosans			
Molecular formula				
Type	95/5	70/5	Oligomer	
MW [kDa]	58.4 ± 6.5 (n=5)	57.5 ± 5.1 (n=5)	2.1 ± 0.2 (n=3)	
PDI ( $M_w/M_n$ )	3.0	3.1	2.1	
$R_h$ [nm]	9.9 ± 0.7	7.5 ± 0.5	1.1 ± 0.0	
pK <sub>a</sub>	6.4	6.4	6.7	
DD [%]	94	73	39	
Degree of FITC labeling	2.3%	3.1%	0.5%	
# positive charges / molecule	301 (pH 5.5)	206 (pH 5.5)	pH 5.5	4.3
			pH 6.0	3.8
			pH 6.5	2.8
			pH 7.0	1.5
			pH 7.4	0.8
Charge density [kDa <sup>-1</sup> ]	5.1 (pH 5.5)	3.6 (pH 5.5)	pH 5.5	2.0
			pH 6.0	1.8
			pH 6.5	1.3
			pH 7.0	0.7
			pH 7.4	0.4

Table 6: Properties of applied Chitosans (reprinted from <sup>50</sup> with permission)

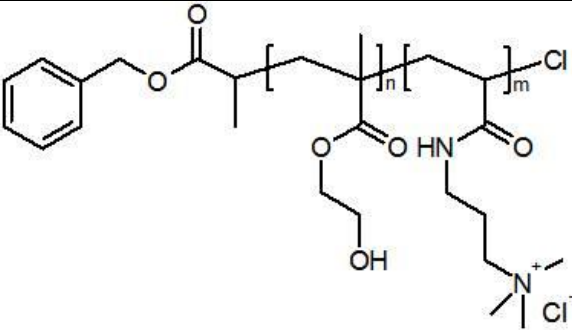
Parameter	HEMA-Co-TMAPs				
Molecular formula					
Type	A1	A2	A3	B2	B3
MW [kDa]	14 (n=1)	14 (n=1)	13 (n=1)	98 (n=1)	233 (n=1)
PDI ( $M_w/M_n$ )	N/A	N/A	N/A	N/A	N/A
$R_h$ [nm]	N/A	N/A	N/A	N/A	N/A
Degree of FITC labeling	1.0%	1.0%	1.0%	1.0%	1.0%
# positive charges / molecule	7	25	39	230	1000
Charge density [ $\text{kDa}^{-1}$ ]	0.5	1.8	3.1	2.3	4.3

Table 7: Properties of applied HEMA-Co-TMAP polymers (reprinted from <sup>50</sup> with permission)

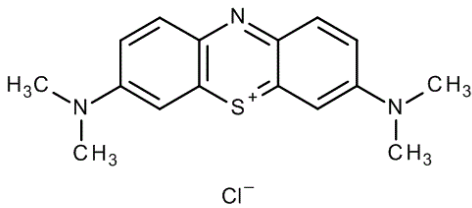
Parameter	Small molecules		
Type	Methylene blue	MSC-C1	MSC-D1
Molecular formula		Confidential	Confidential
MW [kDa]	0.32	0.69	0.54
# positive charges / molecule	1	0	1 (pH 7.4)
Charge density [ $\text{kDa}^{-1}$ ]	3.1	0	1.9

Table 8: Properties of the applied small molecules (reprinted from <sup>50</sup> with permission)

## 3.2 Permeation experiments

### 3.2.1 Characterization of the diffusion chambers

For quantification of the permeation, the Flux (J) of the analytes from the donor into the acceptor compartment was determined according to equation (6):

$$J = \frac{dm_{acceptor}}{dt} \quad (6)$$

However, according to Fick's law of diffusion, the Flux (J) is dependent on the size (respective the molecular weight) of the model compounds. Thus, the different model PEGs would be subject to different diffusion velocity due to their differing molecular size and would falsify the permeation / retention results. In order to determine a chamber-specific "diffusion-benchmark" for each PEG analyte, initial diffusion experiments were performed, applying a 0.2 µm filter membrane instead of synovial membrane. The 0.2 µm membrane provided free diffusion for all analytes and allowed the calculation of a "benchmark-Flux" for each PEG polymer and methylene blue.

As expected, the "benchmark" experiment showed higher Flux values for lower molecular weights of the PEGs (Figure 5). Regarding methylene blue, significantly lower initial amounts were applied to the donor compartment. Thus, a direct comparison to the PEG results is not applicable. However, as these values serve as benchmark parameters, this is not critical.

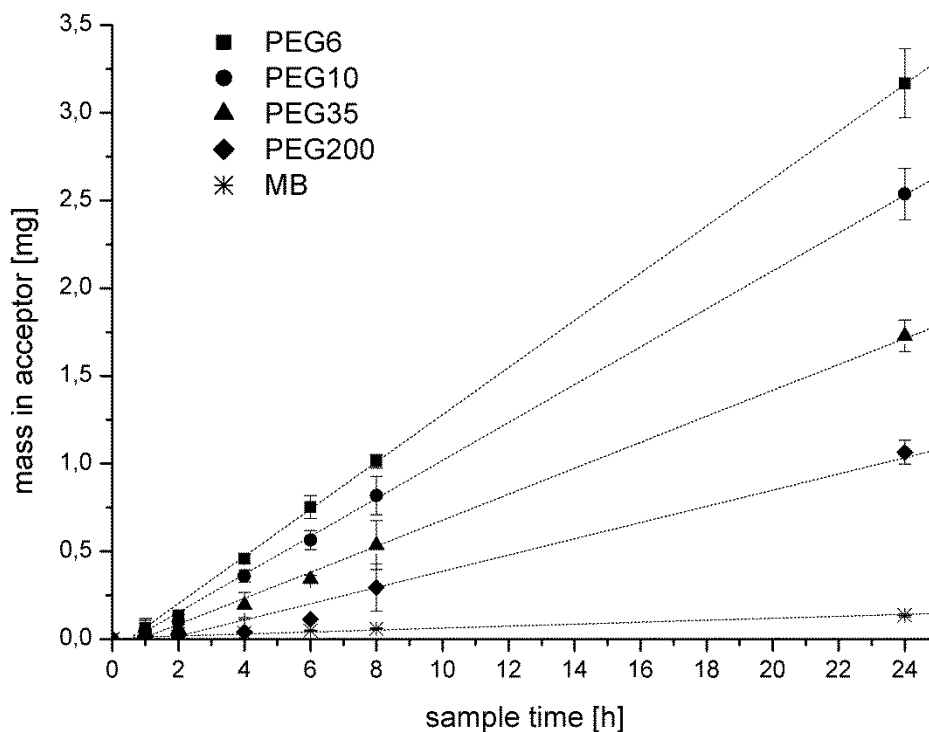


Figure 5: Diffusion into the acceptor compartment of PEG and methylene blue (MB) through a 0.2  $\mu\text{m}$  filter (“benchmark” experiment) (reprinted from <sup>50</sup> with permission)

In summary, size dependent and chamber specific diffusion differences between the analytes were evaluated with this experiment. The results can be expressed in a “benchmark”-Flux ( $J_{\text{benchmark}}$ ), which were used to normalize the values for the following permeation experiments with synovial membrane in the same setup.

### 3.2.2 Permeation of bovine synovial membrane

Permeation experiments with bovine synovial membrane were performed under the same experimental conditions as in the “benchmark” experiment. The diffusion chambers were prepared as described above. Accordingly, the Flux through synovial membrane ( $J_{\text{synovia}}$ ) was determined for each analyte.  $J_{\text{synovia}}$  was related to the benchmark ( $J_{\text{benchmark}}$ ) expressing the synovial retention ( $R_{\text{syn}}$ ) according to:

$$R_{\text{syn}} = \frac{J_{\text{benchmark}}}{J_{\text{synovia}}} \quad (7)$$

Figure 6 illustrates the size-selective retention of methylene blue and the PEG polymers. As depicted, a synovial retention between 11 (methylene blue) and 132 (PEG 35) was observed. As no detectable amounts of PEG 200 were found in the acceptor compartment after 24 hours, no retention values for PEG 200 were obtained.

The high standard deviations can be explained by variations in thickness and constitution of the bovine synovial membrane explants. However, due to the fact that for each single experiment a mixture of all analytes was applied and consistently high or low retention values were obtained respectively, normalization against PEG 6 was performed in order to decline standard deviations (Figure 7). The normalized retention ( $R_{\text{syn}}'$ ) was calculated according to:

$$R_{\text{syn}}' = \frac{R_{\text{Syn}(PEG)}}{R_{\text{Syn}(PEG 6)}} \quad (8)$$

Figure 6 and Figure 7 distinctly demonstrate the relation between molecular weight and retention by synovial membrane, showing the potential to gain extended residence times of large molecules inside synovial joints after intra-articular administration.

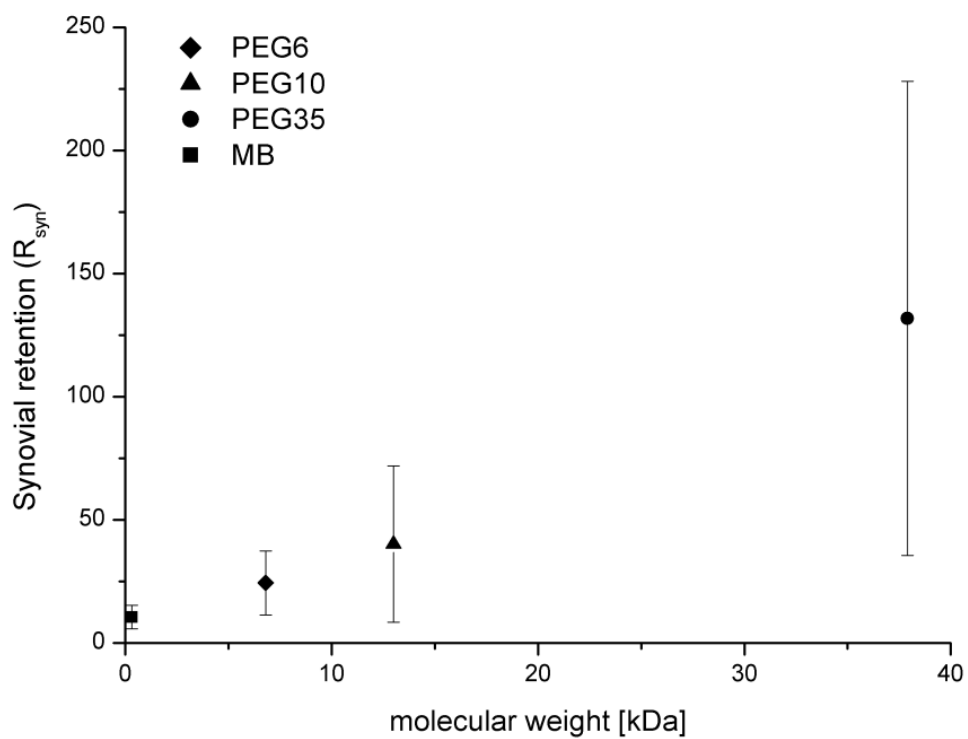


Figure 6: Illustration of synovial retention ( $R_{syn}$ ) vs. molecular weight of applied model compounds (reprinted from <sup>50</sup> with permission)

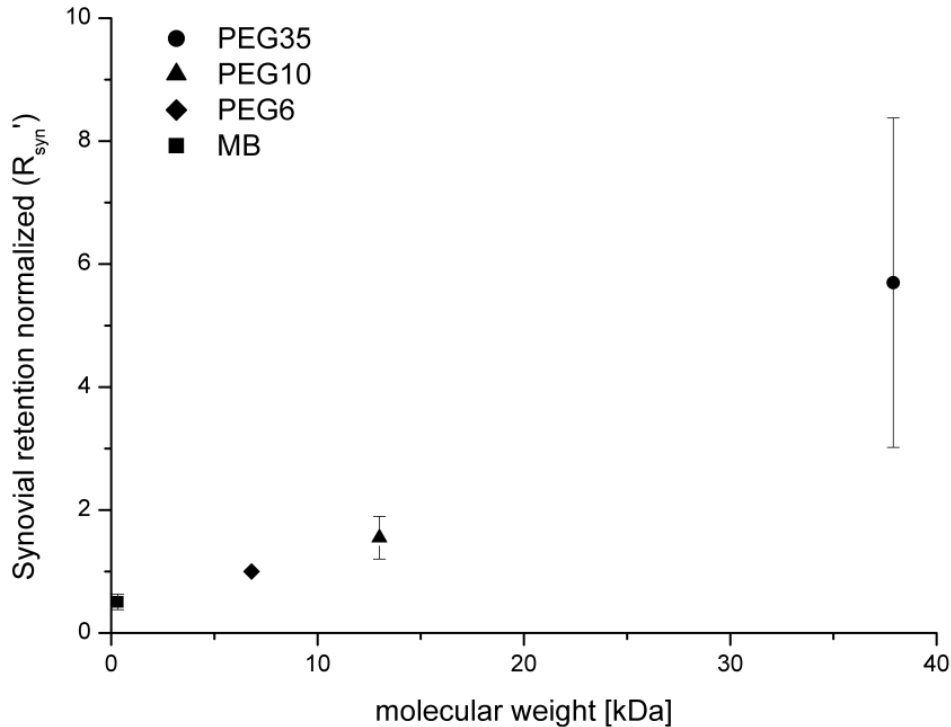


Figure 7: Synovial retention, normalized against PEG6 ( $R_{syn'}$ ) vs. molecular weight (reprinted from <sup>50</sup> with permission)

Based on the synovial retention ( $R_{syn}$ ), another parameter, the retention factor ( $F_{ret}$ ), was determined according to equation (9):

$$F_{ret} = \frac{R_{Syn(PEG)}}{R_{Syn(methyleneblue)}} \quad (9)$$

The retention factor reflects the retention of the PEG polymers against the small molecule, methylene blue. As literature data reports half-lives of about 1-6 hours for intra-articular administered small molecules <sup>12-15</sup>, the retention factor provides an approximation of actual half-lives inside the joint cavity that can be reached by synovial retention of large molecules (see Table 9). However, it has to be considered, that all presented data was gained in *in vitro* experiments which do not consider additional effects (like active membrane transport).

<b>Molecule</b>	<b>J<sub>benchmark</sub></b> <b>[μg/h]</b>	<b>J<sub>syn</sub></b> <b>[μg/h]</b>	<b>R<sub>syn</sub></b>	<b>R<sub>syn</sub>'</b>	<b>F<sub>ret</sub></b>
<b>PEG 6</b>	136 ± 10	7.6 ± 5.2	24 ± 13	1 ± 0	2.1 ± 0.6
<b>PEG 10</b>	109 ± 8	4.2 ± 3.1	40 ± 32	1.6 ± 0.4	3.2 ± 1.2
<b>PEG 35</b>	75 ± 6	1.0 ± 0.9	132 ± 96	5.7 ± 2.7	13 ± 8
<b>PEG 200</b>	48 ± 5	n/a	n/a	n/a	n/a
<b>MB</b>	8.2 ± 0.4	0.9 ± 0.4	11 ± 5	0.5 ± 0.1	1 ± 0

Table 9: Determined parameters for permeation through bovine synovial membrane

Nevertheless, a clear correlation between the determined retention factors and the molecular weight of corresponding analytes was observed (Figure 8). In addition, a maximum retention of factor of 13 (related to methylene blue) was found for PEG 35. As mentioned, PEG 200 was not detected in the acceptor compartment and thus no retention values were obtained. However, considering the analytical limit of detection, a minimum retention factor of 20 can be assumed for PEG 200. These results indicate that intra-articular administered macromolecular drugs or drug-conjugates may be subject to significant retention by the synovial membrane and thus exhibit distinctly prolonged residence times in synovial joints. However, this *in vitro* study only examined the pure physical retention by bovine synovial membrane. In addition, factors like active membrane transport or protein binding still have to be considered and investigated. Finally, the presented *in vitro* data have to be confirmed by further *in vivo* experiments. Nevertheless, the understanding of the dimension in which synovial retention correlates with molecular weight may be of great value in the development of intra-articular applied sustained release pharmaceutical products. For example, macromolecular drugs as well as polymeric carriers for small molecules could be designed with customized molecular weights in order to target for specific residence times inside the joint upon intra-articular administration.

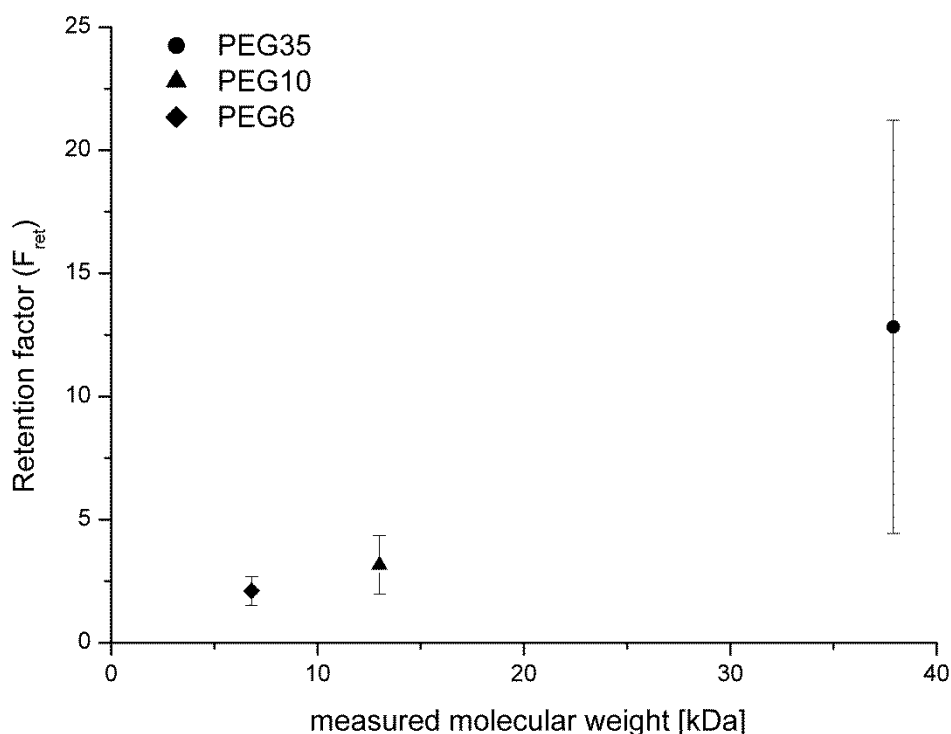


Figure 8: Retention of PEG polymers related to the small molecule methylene blue (reprinted from <sup>50</sup> with permission)

### 3.3 Penetration of cartilage tissue

As shown in the permeation experiment with bovine synovial membrane, size dependent retention may promote prolonged joint residence times upon intra articular administration. In addition to that, penetration into and accumulation inside cartilage tissue has to be considered in this context as well. As described above, the cartilage matrix is negatively charged. Thus, cartilage penetration may be enhanced by electrostatic interaction with positively charged drugs or drug conjugates. In this context, the influence of positive charge and size of a compound on cartilage penetration (and accumulation), was investigated with a series of model compounds, differing in size and positive charge (see Table 5, Table 6, Table 7 and Table 8).

### 3.3.1 Chitosan-Oligomer

Chitosan oligomer is an oligosaccharide, composed of  $\beta$ -(1,4)-linked D-glucosamine and N-acetylglucosamine. The amount of de-acetylated D-glucosamine within a molecule determines the “degree of deacetylation (DD)”, the number of primary amino-groups and thus determining the alkaline properties of the compound. As Table 6 depicts, the applied chitosan oligomer (~2.1 kDa) has a DD of 39%, resulting in a  $pK_a$  of 6.7. The basicity of the primary amino-groups enables the adjustment of positive charge within a chitosan oligomer molecule by variation of the pH of the donor medium. Thus, cartilage penetration experiments were performed in different donor media at pH 5.5, pH 6.0, pH 6.5, pH 7.0 and pH 7.4, resulting in charge densities of the chitosan oligomer between 0.4 and 2.0  $kDa^{-1}$ . However, the molecular weight remained constant for all analytes (refer to Table 6).

It was observed that increasing acidity of the donor medium (which is correlated to increasing positive charge) results in increasing partition of the chitosan oligomer into cartilage tissue (see figure 9). Over a period of 24 hours, the highest partition into cartilage tissue was observed at pH 5.5 after 8 hours of incubation. At pH 7.4, no partition into cartilage was observed. This was rather expected, as chitosan oligomer is nearly un-charged at pH 7.4. The observed results support the hypothesis that electrostatic interaction between positively charged compounds and the negatively charged cartilage matrix promotes the accumulation of these compounds inside the cartilage tissue.

Despite the observed correlation between the partition coefficient and the positive charge density, it has to be considered that the experiments were carried out under varying acidic conditions (in order to gain varying positive charge of the analytes). Thus, it cannot be excluded, that the varying acidity altered the performance of the cartilage tissue itself and led to falsification of the results. For this purpose, additional control experiments with methylene blue (pH independent charge) were performed at different pH levels.

As Figure 9 depicts, increasing acidity declined the partition of positively charged methylene blue into cartilage tissue. This is the opposite observation as demonstrated for the chitosan oligomers and can be explained by protons, neutralizing the GAGs and thus partly eliminating negative charge within the cartilage matrix. These results further underline the observation from the experiments with chitosan oligomer and support the hypothesis that partition into cartilage tissue is increased with increasing positive charge. Nevertheless, the pH seems to exert distinct influence on the cartilage performance. This is shown in the penetration experiment under pH 5.5, where the partition coefficient declines between 8 and 24 hours, which deviates from the observations at pH 7.4 – 6.0. This re-distribution of

analyte into the donor solution can be explained by starting cartilage degradation at pH 5.5 due to activation of cartilage degrading enzymes, like Cathepsin D (which is known to be activated below pH 6).

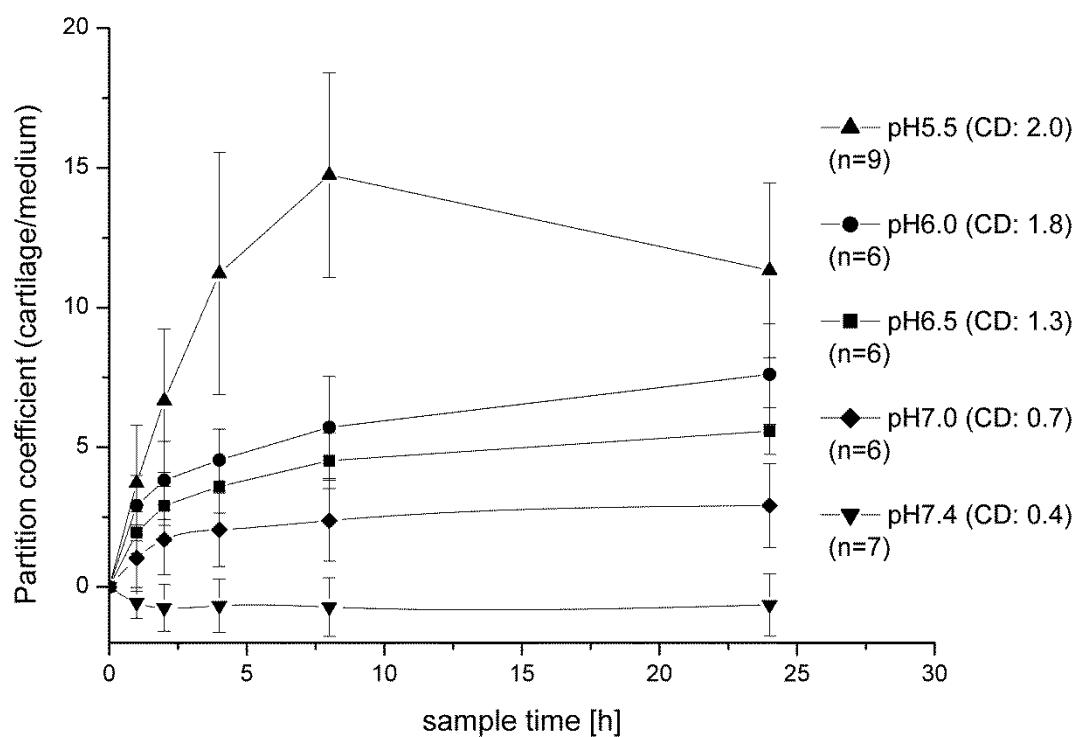


Figure 9: Partition coefficient (cartilage / medium) vs. time of chitosan oligomers at different pH values of the incubation medium. The pH of the incubation medium determines the positive charge density of the chitosan oligomers (decreasing positive charge with increasing pH) (reprinted from <sup>50</sup> with permission)

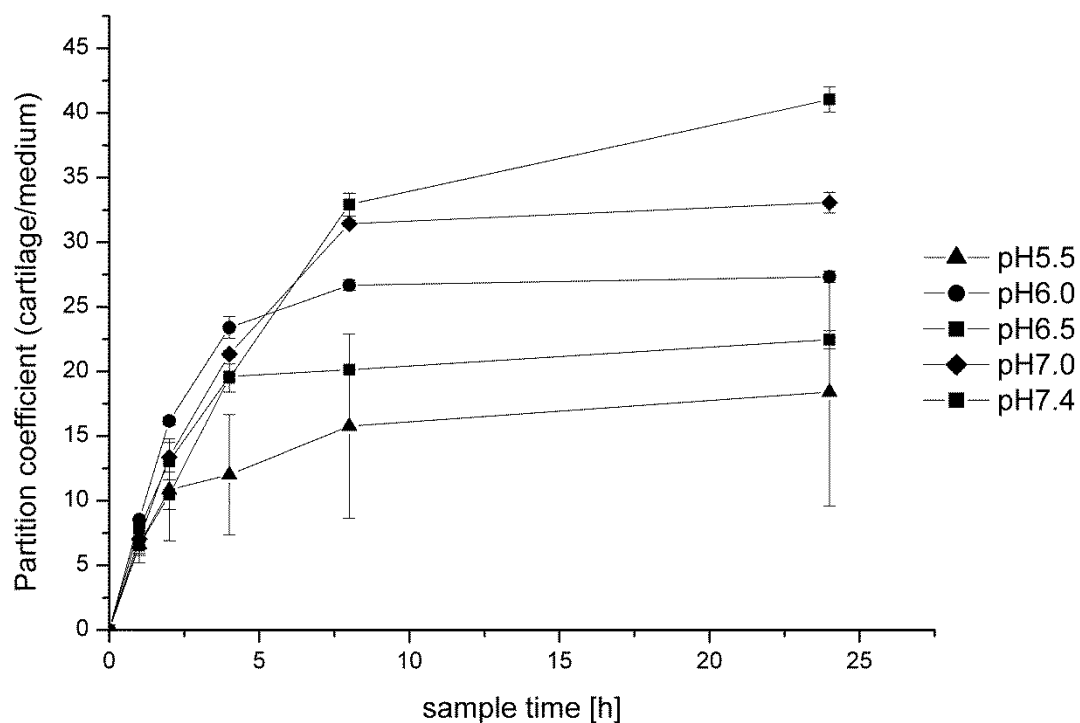


Figure 10: Partition coefficient of methylene blue in cartilage tissue at pH 5.5 – 7.4 vs. sample time (reprinted from <sup>50</sup> with permission)

As can be seen in Figure 10, a maximum partition coefficient of the oligomers was reached at 8 (pH 5.5) or 24 hours (below pH 5.5). For a comparison of the experiments, the 8h values were applied. Plotting these values against the calculated charge density of the analytes and adding the value for methylene blue, a linear trend between charge density and the partition into the cartilage matrix was observed (Figure 11).

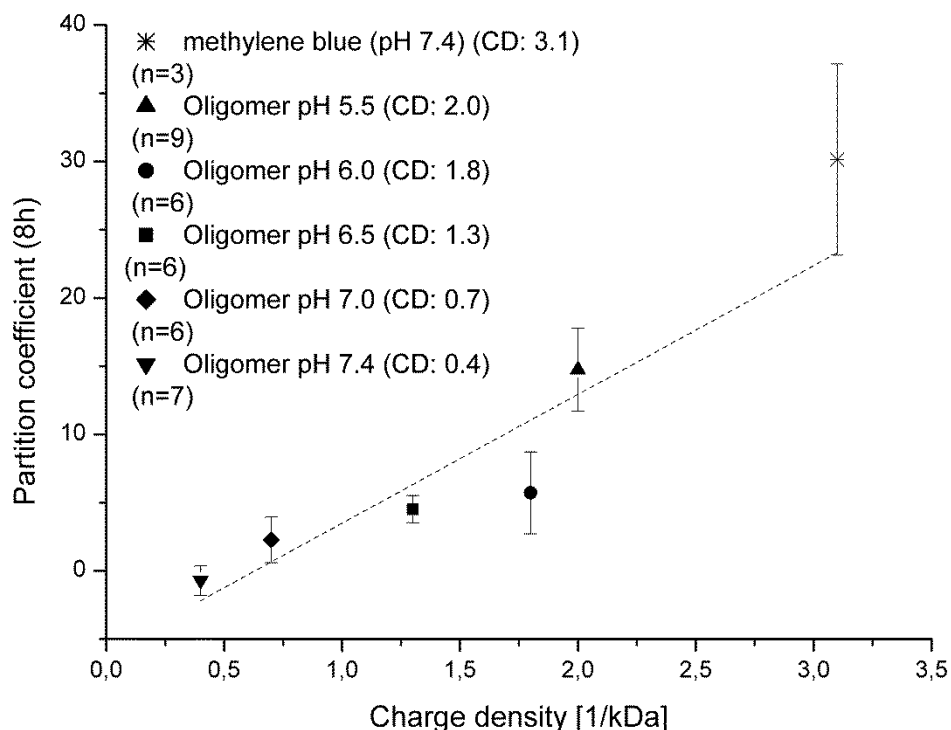


Figure 11: Partition coefficients of methylene blue and Chitosan oligomers at 8 hours, plotted against their positive charge density (reprinted from <sup>50</sup> with permission)

### 3.3.2 Chitosan and PEG polymers

The presented data with chitosan oligomers revealed a clear relation between the extent of cartilage accumulation and the positive charge density of compounds with a molecular weight of 2.1 kDa. In a next step, this relation was envisaged to be confirmed also for macromolecular entities. For this purpose, corresponding penetration experiments were carried out with uncharged PEG polymers and positively charged chitosan polymers.

Due to the poor solubility of polymeric chitosans in neutral environment, these experiments were carried out in acidic buffer at pH 5.5. This has to be considered with respect to the discussed influence of medium acidity (cartilage degradation, refer to figure 10).

The results for the experiments are illustrated in Figure 12. Obviously, the uncharged PEG polymers do not penetrate or accumulate inside the cartilage matrix in detectable amounts. This applies for

PEGs in a wide size range between 6 and 200 kDa. In contrast, the positively charged chitosan polymers showed strong affinity and distinctly accumulated inside the cartilage matrix. After 24 hours of incubation, no detectable amounts of chitosans were found in the acceptor solution samples, resulting in partition coefficients ( $P_{\text{coeff}}$ ) of  $>120$  for chitosan 95/5 and  $>220$  for chitosan 70/5. Thus, despite their relatively high molecular weight of approximately 60 kDa, the positive charge enabled massive accumulation of the analytes inside the cartilage matrix.

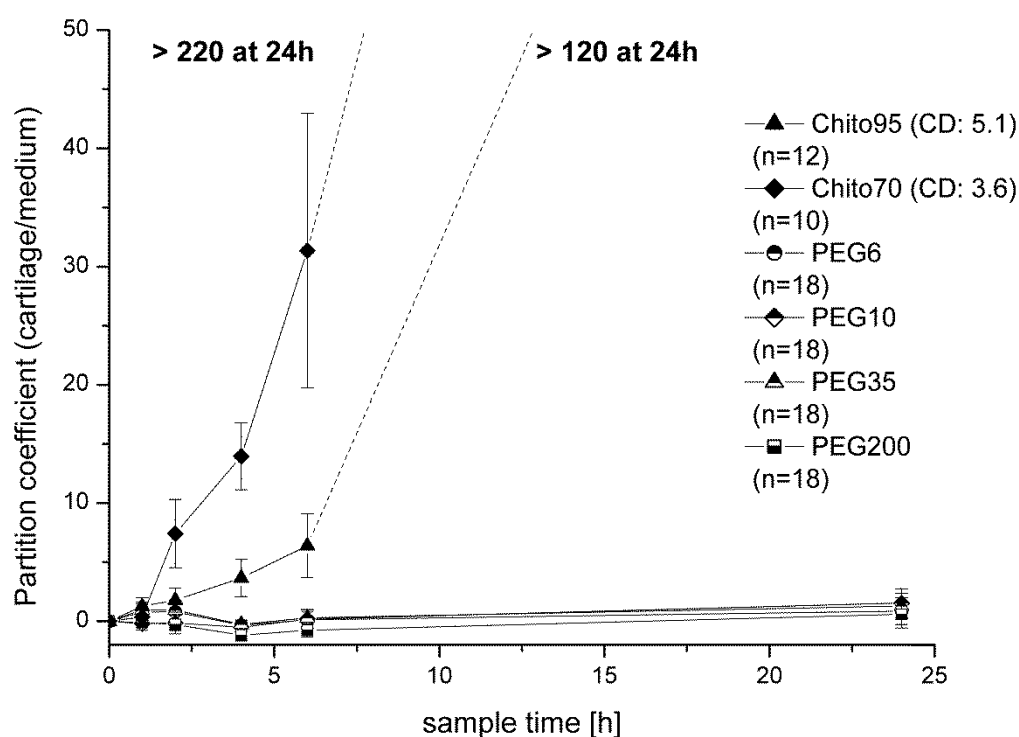


Figure 12: Partition into cartilage vs. sample time of polymeric chitosans and uncharged PEG polymers

Despite the distinctly higher molecular weight compared to the relatively small chitosan oligomer (60 kDa vs 2.1 kDa), the chitosan polymer exhibited an approximately 10 times higher affinity to the cartilage tissue ( $P_{\text{coeff}} \sim 15$  vs  $P_{\text{coeff}} \sim 120-220$  at pH 5.5), which was rather unexpected. This was further investigated by an additional experiment, adding (i) 100  $\mu\text{l}$  of bovine synovial fluid as well as (ii) 100  $\mu\text{l}$  of 1% solutions of hyaluronic acid to 10 ml of chitosan solutions. As a result, immediate precipitation was observed for solutions with chitosan polymer, while solutions containing chitosan oligomers remained clear (Figure 13). These results indicate the presence of an interaction between the

chitosan polymer and hyaluronic acid, leading to co-precipitation of these components. Most likely this mechanism also occurs inside the cartilage matrix, creating a “pull-effect” and leading to the observed high accumulation of chitosan polymers inside the cartilage matrix.

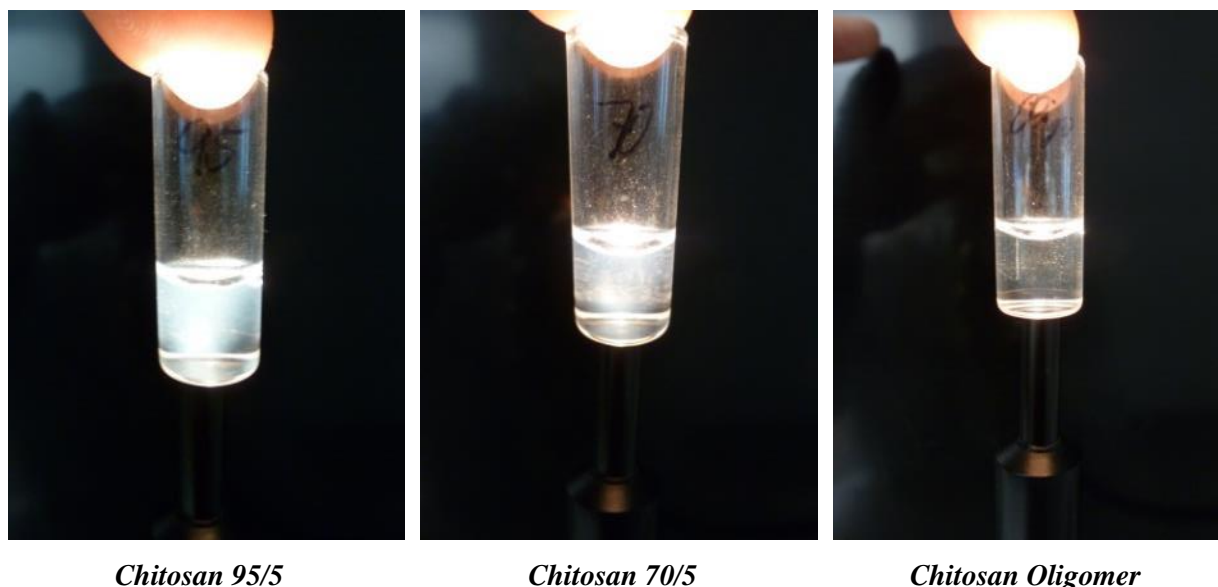


Figure 13: Solutions of different chitosans (10 ml each) upon addition of 100  $\mu$ l of a 1% solution of hyaluronic acid. Immediate precipitation was observed for the polymeric chitosans (95/5 and 70/5), while the chitosan oligomer remained clear.

Due to the deviating behavior and the lack of a plateau or maximum of the partition coefficient of the chitosan polymers, a direct comparison with the oligomers cannot be performed. Nevertheless, it was demonstrated, that also high molecular weight compounds (up to 60 kDa) have the ability to penetrate the cartilage matrix and to accumulate inside cartilage tissue, when they possess positive charge. In addition, the effect of charge seems to exceed the influence of size in this context. Besides, the interaction between chitosan and hyaluronic acid/cartilage has already been subject to various investigations, aiming for different applications (e.g. tissue engineering)<sup>52-54</sup>.

### 3.3.3 HEMA-Co-TMAP (HCT)

The experiments with polymeric chitosans and PEG polymers revealed that positive charge distinctly promotes accumulation of high molecular weight compounds ( $\sim$  60 kDa) inside cartilage tissue. Additionally, a correlation between cartilage partitioning and the charge density was demonstrated for the chitosan oligomers. In order to be able to confirm cartilage penetration and charge dependency for high molecular weight compounds in a more physiological environment (pH 7.4 buffer) and without

falsification through co-precipitation with hyaluronic acid, another polymer type, exhibiting pH-independent charge, was introduced (HEMA-Co-TMAP, HCT). According to Table 7, five different polymers in two size ranges (14 kDa and ~100-200 kDa) and with a wide range of charge densities ( $0.5 - 4.3 \text{ kDa}^{-1}$ ) were applied for further penetration experiments in a corresponding setup.

The partition kinetics (Figure 14) revealed that the nearly uncharged representative, HCT A1 (charge density  $0.5 \text{ kDa}^{-1}$ ), does not show any distribution into the cartilage. In turn, increasing charge density led to increasing affinity to the cartilage matrix. In contrast to the chitosan polymers, the partition coefficients (cartilage / medium) of the HEMA-Co-TMAPs exhibit a plateau or maximum after 48 h of incubation. This indicates the absence of the co-precipitation which was observed for the chitosan polymers. Furthermore, the observed partition coefficients were in a similar range as shown for the chitosan oligomers (between 5 and 20). However, the observed plateau or maximum was reached at later time-points. The slower distribution into cartilage tissue may be attributed to distinctly higher molecular weight of the HCTs compared to the chitosan oligomers.

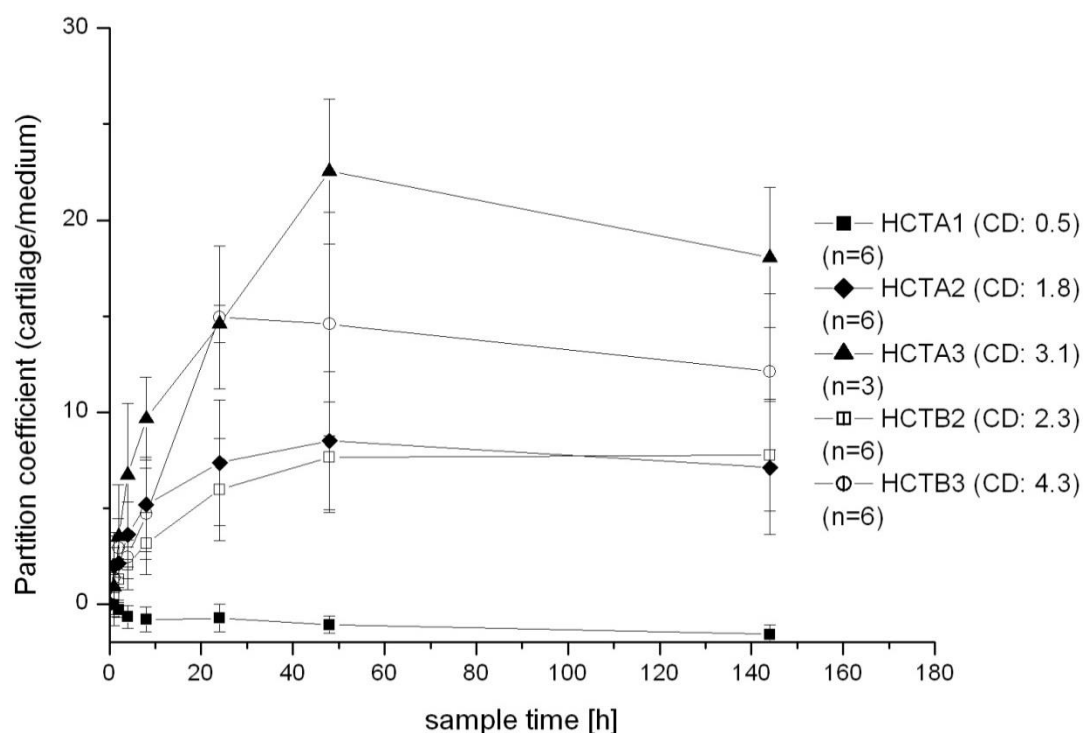


Figure 14: Cartilage penetration of HEMA-Co-TMAPs: Partition coefficient vs. sample time (reprinted from <sup>50</sup> with permission)

The observed maximum partition coefficients were plotted against the respective charge density. Despite a limited amount of data points and relatively high standard deviations, a linear trend between charge density and partition coefficient was observed for the smaller polymers (HCT A1 - A3). The larger polymers, HCT B1 and B2, deviate from this relation, which can be attributed to the very high molecular weight of these analytes (98 and 233 kDa). Taken together, the experiments with the HCTs confirmed the observations from the two previous experiments:

- A relation between the positive charge density and the distribution into cartilage tissue.
- Positive charge promotes the accumulation of high molecular weight compounds inside the cartilage matrix and enables penetration of compounds up to 233 kDa.

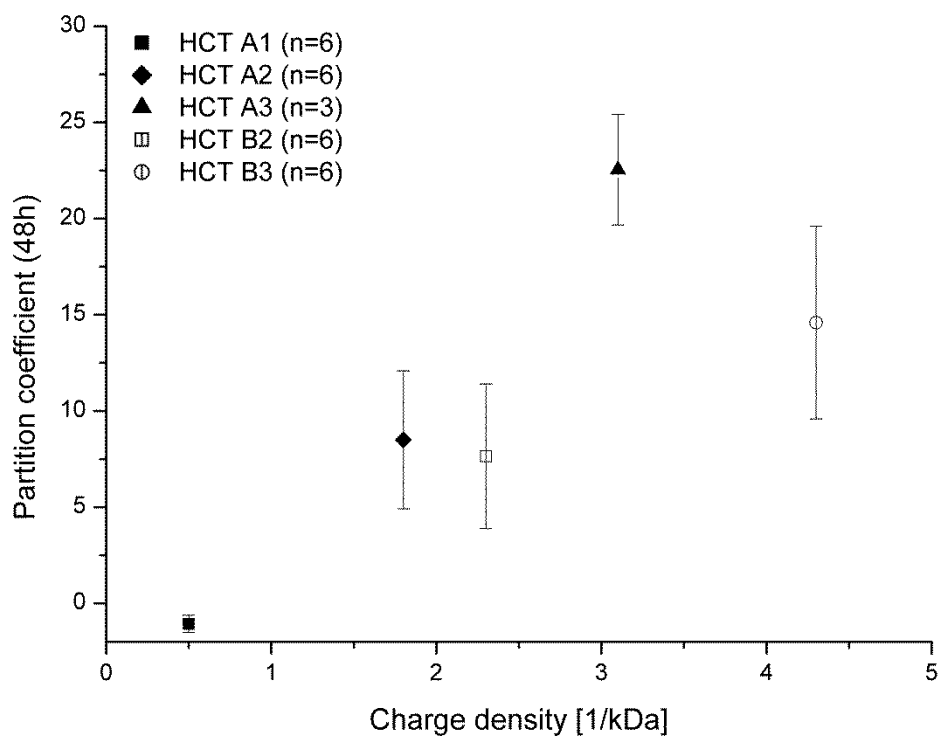


Figure 15: Partition coefficients of HCT polymers vs. their charge density (reprinted from <sup>50</sup> with permission)

### 3.3.4 Combined evaluation

Figure 11 and Figure 15 indicate a linear relation between the partition coefficient and the positive charge density of chitosan oligomers and HCTs. In a comprehensive summary of the data of both experiments (Figure 16), including additional data from the small molecules methylene blue, MSC-C1 and MSC-D1, the graph underlines the indication for a linear relation between the partition coefficient and positive charge density for compounds in a size range between 0.3 and 14 kDa. As discussed before, the very high MW polymers HCT B1 and B2 deviate from this relation.

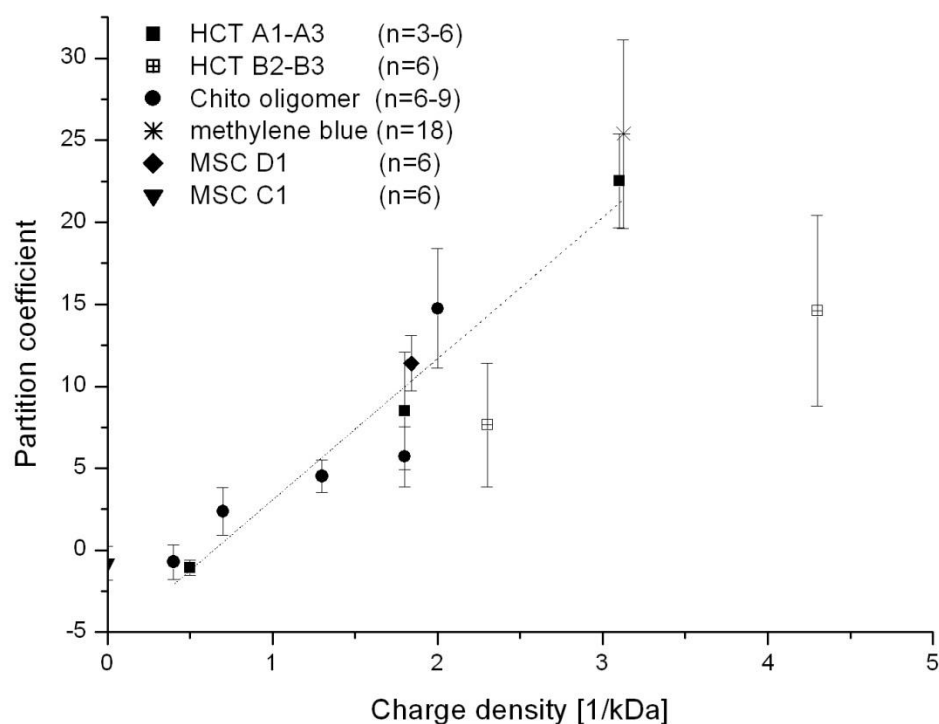


Figure 16: Illustration of cartilage penetration data of HEMA-Co-TMAP (HCT), Chitosan oligomer, methylene blue and MSC D1 and C1 (reprinted from<sup>50</sup> with permission)

### 3.3.5 Histologic evaluation

The discussed experiments provided quantitative data for the relationship between positive charge of a substance and its ability to distribute within cartilage tissue. For confirmation of this data and for a deeper understanding of how different compounds distribute within the cartilage matrix, further experiments were performed correspondingly with FITC-labelled derivatives of the applied model compounds (Chitosan-FITC and HCT-FITC).

#### Chitosans:

In order to investigate, if the FITC label has an altering effect on cartilage penetration of the respective compounds, additional control experiments were performed comparing native and FITC labeled chitosans (Figure 17, Figure 18 and Figure 19). A slight decrease of cartilage partition was observed for the FITC labeled derivatives. This is most likely attributed to the declined amount of positive charge within the FITC-labeled representatives. However, still there was the same trend observed as for the native compounds. Thus with regards to the fact that data assessment for the fluorescence microscopic experiments was carried out without any quantitative statement, the altering influence of the FITC-label was not regarded as critical.

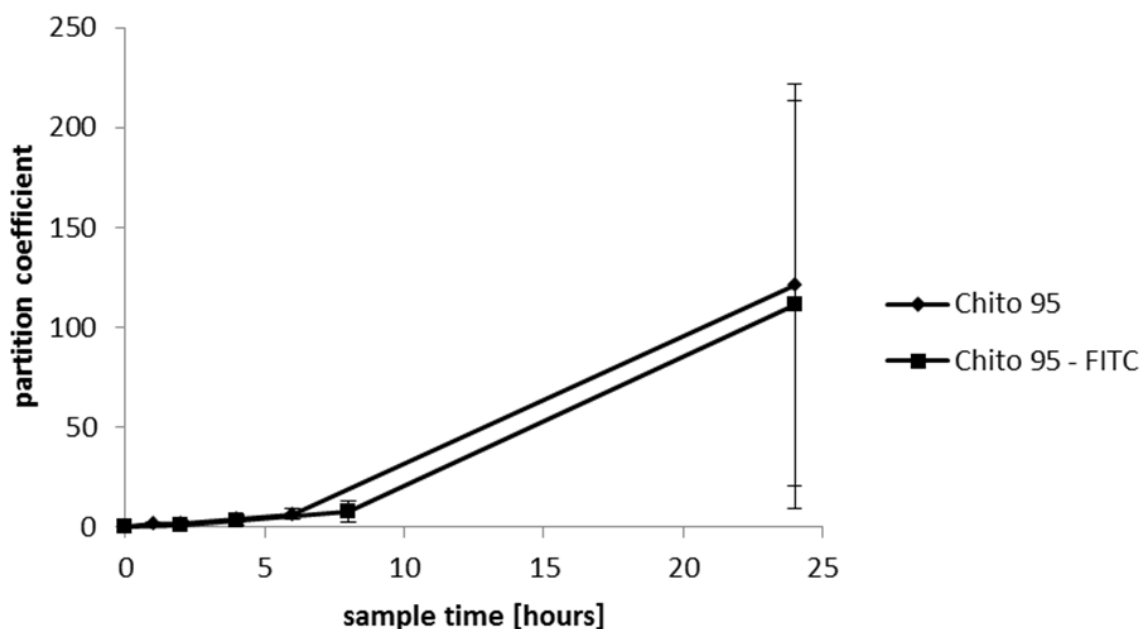


Figure 17: Comparison of partition into cartilage tissue of labeled and non-labeled chitosan 95/5 (reprinted from <sup>50</sup> with permission)

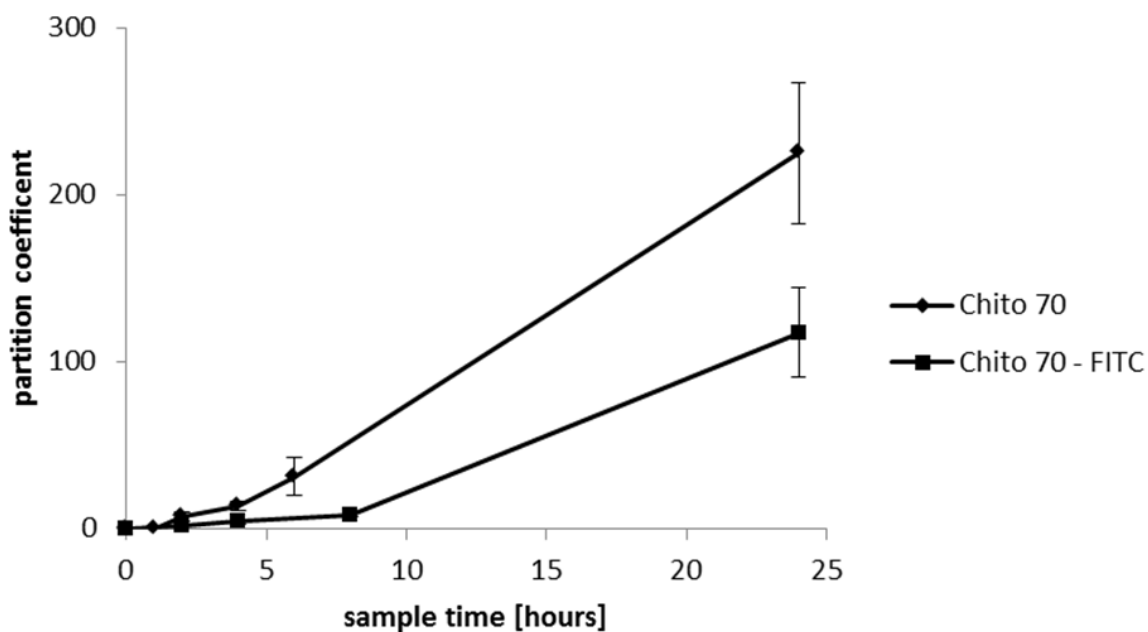


Figure 18: Comparison of partition into cartilage tissue of labeled and non-labeled chitosan 70/5 (reprinted from <sup>50</sup> with permission)

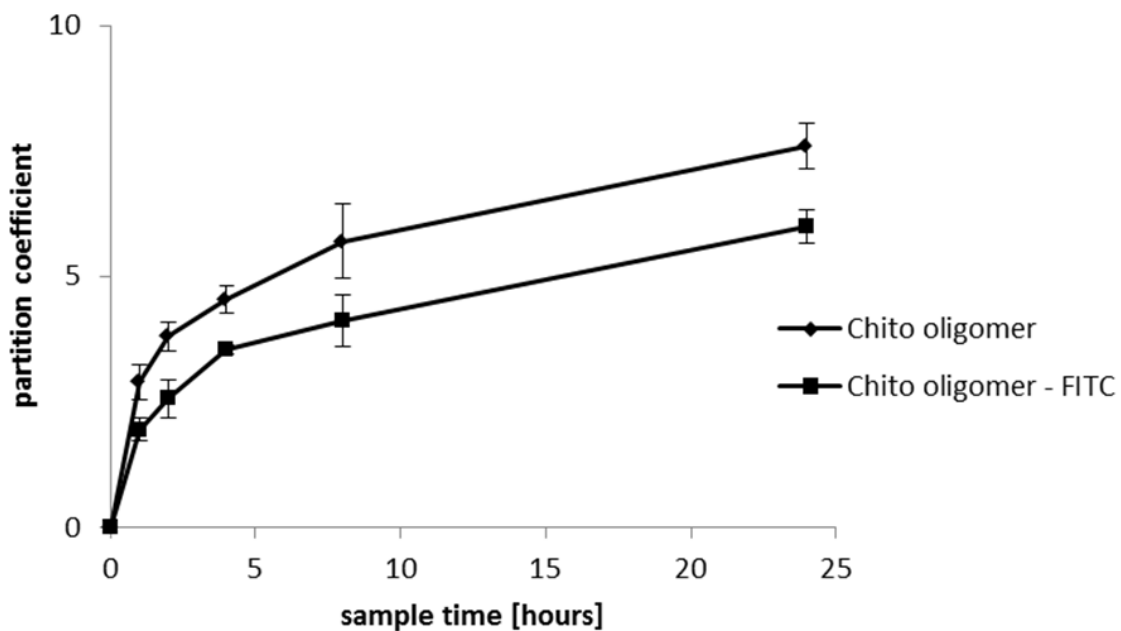


Figure 19: Comparison of partition into cartilage tissue of labeled and non-labeled chitosan oligomer (reprinted from <sup>50</sup> with permission)

Figure 20 shows cross sections of cartilage explants, incubated with FITC-labelled chitosan oligomer (A) and chitosan 95/5 (B). For the chitosan oligomer (A), penetration of the cartilage matrix preferably seems to take place from the deep zone of the tissue. However, also in the surface zone, fluorescence activity was observed. In contrast, the chitosan polymer (B) showed distinct penetration from both sides, the surface zone as well as from the deep zone. However, a defined penetration barrier was observed with a penetration depth of approximately 0.05 – 0.1 mm. This penetration barrier may be explained by co-precipitation of the Chitosans with matrix components (e.g. hyaluronic acid) as described before. Thus, the partition coefficient data for the chitosan polymers is supported with regards to their deviating accumulation behavior. The formation of this barrier is further illustrated in the time-dependent samples (Figure 21 and Figure 22):

- For the chitosan oligomers, penetration of the cartilage matrix seems to start from the deep zone (4 hours), followed by more or less equal distribution and also penetration from the surface zone (8 hours and 1 day).
- For the chitosan polymers, the formation of the penetration barrier can be observed from the first samples (4 hours) and intensifies over the following samples at 8 and 24 hours.

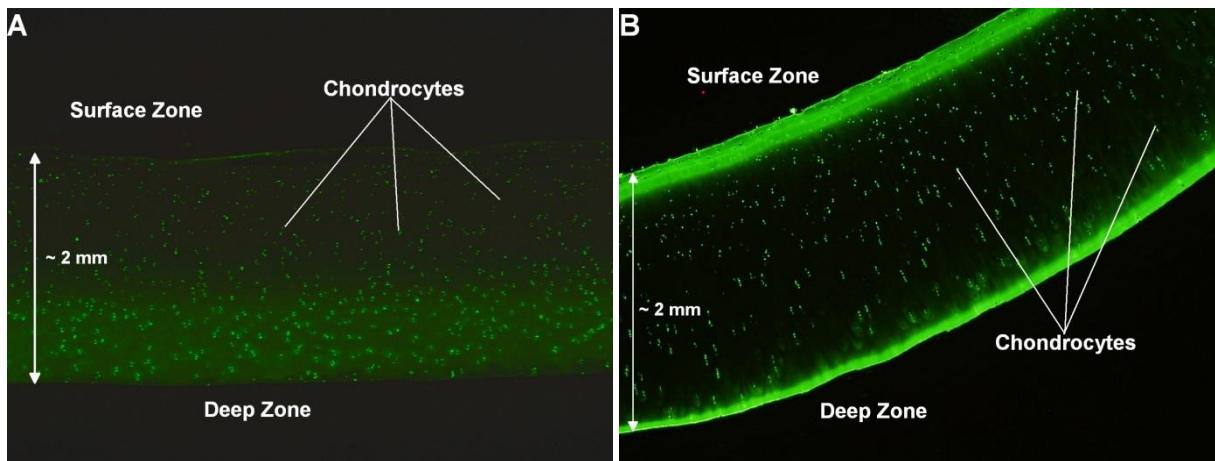


Figure 20: Cross sections of cartilage explants, after incubation with FITC-labelled (A) chitosan oligomer (at pH 5.5) and (B) chitosan 95/5 (at pH 5.5) (reprinted from <sup>50</sup> with permission)

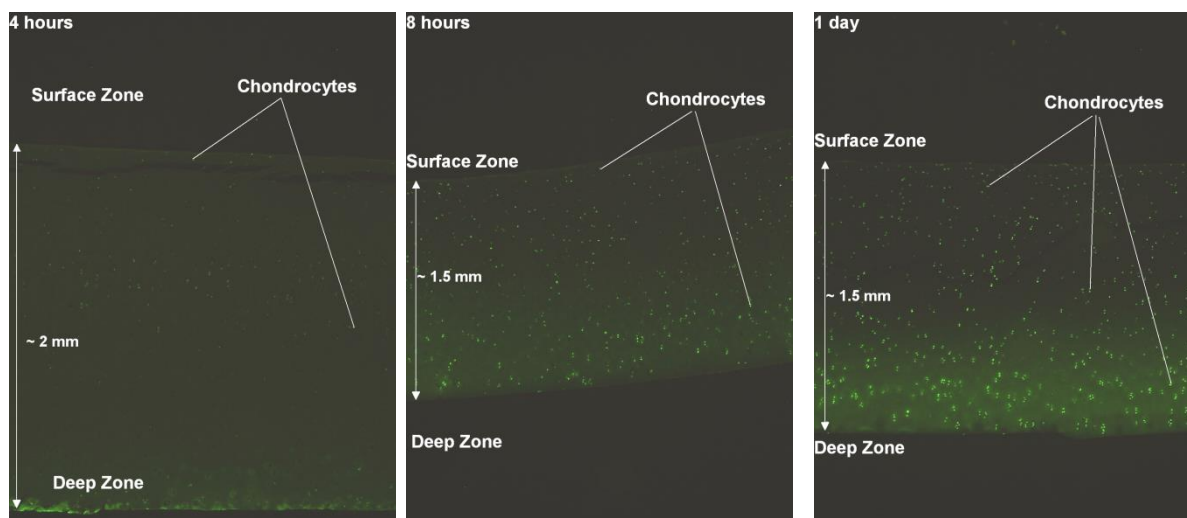


Figure 21: Time-dependent samples of cartilage explants, incubated with chitosan oligomer at 4 hours, 8 hours and 1 day (reprinted from <sup>50</sup> with permission)

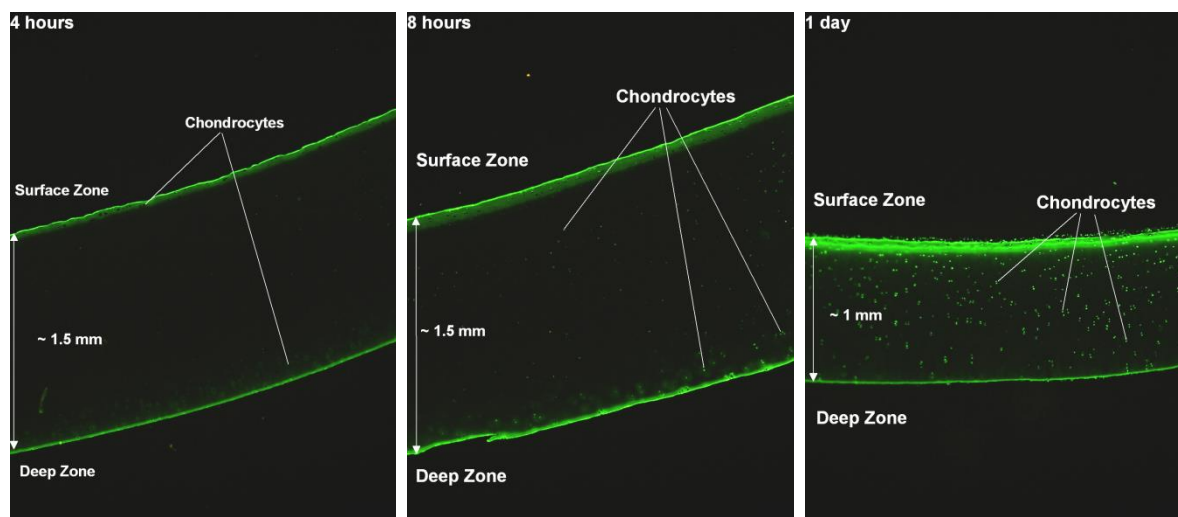


Figure 22: Time-dependent samples of cartilage explants, incubated with chitosan 95/5 at 4 hours, 8 hour and 1 day (reprinted from <sup>50</sup> with permission)

In addition to these observations, punctual fluorescence was detected for both, the chitosan oligomers and the chitosan polymers throughout the entire cartilage matrix, with increasing intensity over time (Figure 20, Figure 21, Figure 22 and Figure 23). These fluorescent dots are aligned vertically (as rod-like clusters) in the deep zone and horizontally in the surface zone. This alignment suggests that the punctual fluorescence is associated with the presence of chondrocytes, which are known to exhibit such formations in cartilage tissue. Thus, accumulation of the chitosans around or inside the cells has taken place. This behavior may be explained by:

- High concentrations of negatively charged cartilage components in the proximity of the cells. For instance, the GAGs (glycosaminoglycans) are secreted by the chondrocytes.
- Accumulation of fluorescent chitosan inside the chondrocytes. This hypothesis is supported by previous studies, which described the potential of chitosan for cell transfection<sup>55-57</sup>. In addition, higher magnification photographs from the deep zone of a cartilage sample incubated with chitosan 95/5 (Figure 23) suggest the presence of fluorescence activity inside the cells as well.

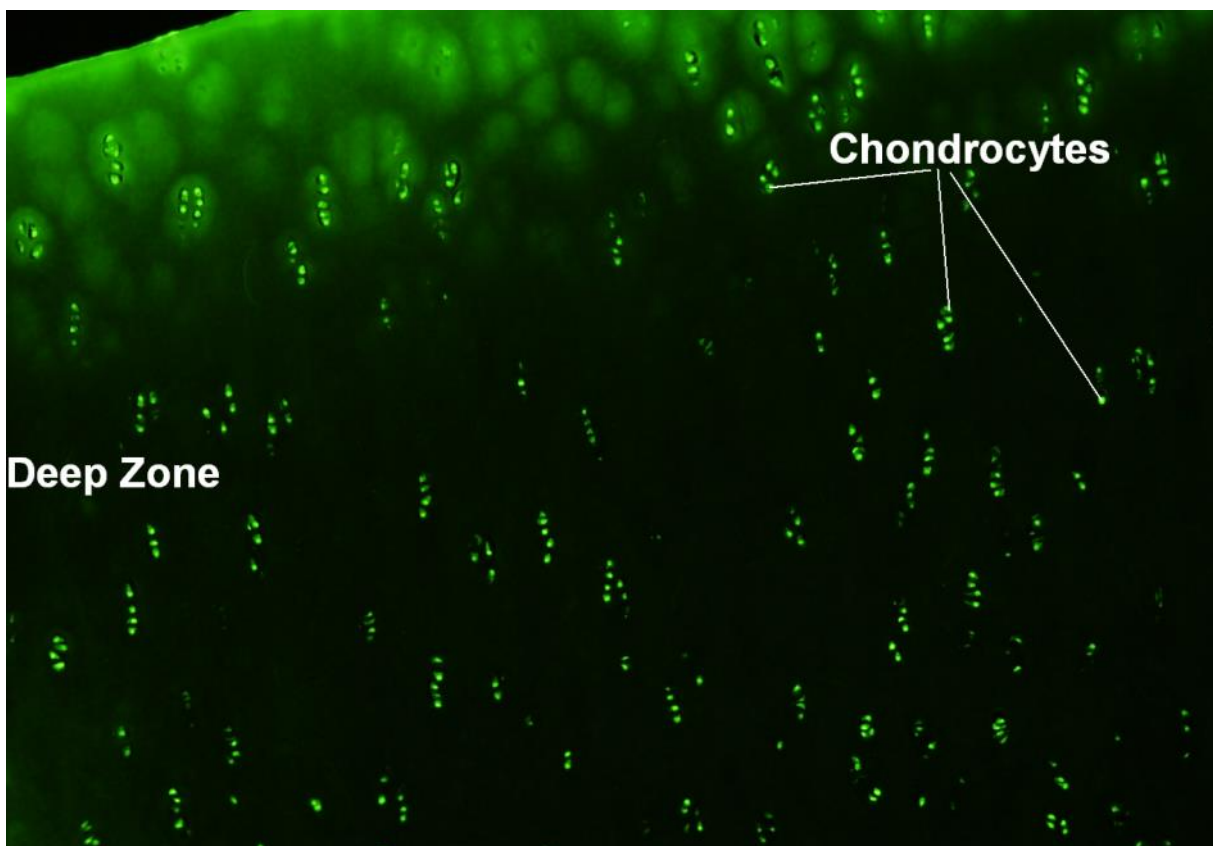


Figure 23: Fluorescent microscopic picture of the deep zone of a cartilage sample upon 1d of incubation with chitosan 95/5 (reprinted from<sup>50</sup> with permission)

#### **HEMA-Co-TMAP:**

As illustrated in Figure 24, the HCT polymers show a uniform distribution within the cartilage matrix without forming a penetration barrier (as observed for the chitosan polymers). The penetration behavior was rather comparable to the chitosan oligomer, as penetration was observed to take place preferably from the deep zone of the matrix.

In contrast to the chitosans, however, the chondrocytes do not appear as fluorescent dots but rather as dark spots inside the matrix. This observation further supports the hypothesis, that chitosan promotes accumulation inside the cells.

Nevertheless, the main conclusion from the fluorescent pictures of the HCTs is that positively charged macromolecules up to 233 kDa (HCT B2) accumulate inside cartilage tissue (as already shown in the analytical data above) and also even penetrates the entire cartilage matrix.

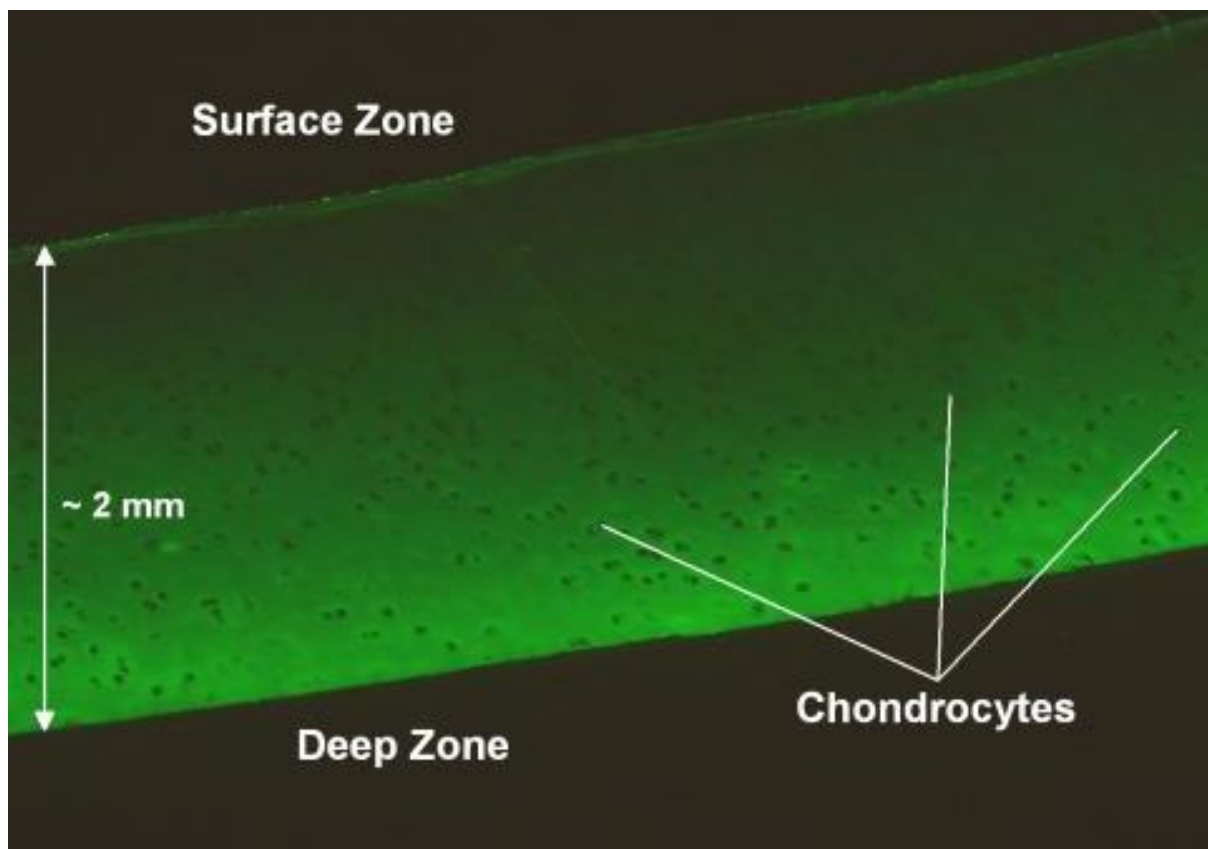


Figure 24: Cross section of a cartilage explant, after incubation with FITC-labelled HCT B2

## 4 Conclusion

Section C of this work can be separated in two different experiments:

### Permeation of synovial membrane:

For polyethylene glycol, 2-fold (PEG 6 kDa), 3-fold (PEG 10 kDa) and 13-fold (PEG 35 kDa) retention by the synovial membrane in reference to the small molecule, methylene blue, was demonstrated. In addition, an almost linear relation between the synovial retention and the molecular weight was observed. As PEG 200 kDa was not found in the acceptor in detectable amounts, a minimum retention factor of 20 can be assumed, considering the limit of detection for this polymer. These results show the potential for a distinct extension of joint residence times by increasing molecular weights. However, PEG was assumed to pass the synovial membrane via pure passive diffusion. Thus, active membrane transport has to be considered as well with respect to potential active substances. Nevertheless, distinct size-dependent retention of macromolecular drugs by the synovial membrane was demonstrated.

### Penetration of cartilage tissue:

With regards to the fact that very short half-lives of small molecules upon intra articular administration were reported in literature (~1-6 hours), even a 20-fold increase would not lead to satisfactory residence times and injection intervals. Though, the combination with a depot effect by synovial cartilage, promoted by positive charge of the drug, may have the potential to achieve this goal. Concerning cartilage penetration, the ability for positively charged, high molecular weight polymers (up to 233 kDa) to accumulate inside and distribute throughout the entire cartilage matrix was demonstrated. In contrast, a distribution into the cartilage matrix was not observed for neutral PEG polymers (6 – 200 kDa). Furthermore, a linear correlation was demonstrated between the charge density of a polymer and the partition into bovine cartilage tissue for small molecules and macromolecules in a size range between 0.3 and 14 kDa.

Summary:

The data obtained from the permeation and penetration experiments provide in-depth understanding of the impact of molecular size and positive charge of molecules on their retention by synovial membrane and accumulation inside cartilage tissue and thus on the potential retention inside the joint upon intra-articular injection. From this perspective, the sustained intra-articular drug delivery seems to be a feasible development goal, which may be achieved by modification of molecular size and positive charge of particular drugs. Furthermore, the presented data may support the screening of new drugs or drug conjugates with regards to suitable enabling sustained pharmacological activity in synovial joints.

## **Section D**

### ***In vitro* release studies**

*Parts of this work were published in the International Journal of Pharmaceutics:*

*Sterner, B., Harms, M., Weigandt, M., Windbergs, M. & Lehr, C. M.:*

*“Crystal suspensions of poorly soluble peptides for intra-articular application: A novel approach for bio-relevant assessment of their in vitro release.”*

*International Journal of Pharmaceutics 461, 46-53 (2014)*

## 1 Introduction

### 1.1 Dissolution testing and *in vitro* release

Dissolution testing and *in vitro* release testing are important tools for the characterization of new pharmaceutical products in drug development, as well as for quality control in pharmaceutical industry.

Generally, a method for dissolution or IVR testing should provide discriminatory capability, robustness, stability of the API and relevance for the *in vivo* performance.

For this purpose, a variety of test methods and apparatus for the assessment of dissolution or IVR performance is recommended in the common pharmacopeias<sup>58,59</sup>. Apparatus I – VII offer standardized methods for dissolution and *in vitro* release testing of immediate release, extended release and delayed release oral dosage forms as well as of suppositories and transdermal patches. However, the suitability for more complex dosage forms has to be carefully evaluated for each newly developed drug product. This might be one reason why still today there are no regulatory standards available for IVR testing of sustained release parenterals, for instance. However, most of the *in vitro* release techniques for innovative dosage forms in literature refer to the mentioned standard test methods<sup>36,60-63</sup>.

Especially in the case of sustained release parenterals, the lack of regulatory standards and suitable methods for IVR testing induced the need for modification of existing or development of new systems in order to gain reproducible, discriminating and predictive methods for the characterization of release kinetics. In this context, basically three kinds of IVR methods can be distinguished in literature<sup>64-68</sup>:

**Sample-and-separate methods:** Figure 25 gives a schematic illustration of the principle of sample-and-separate methods.

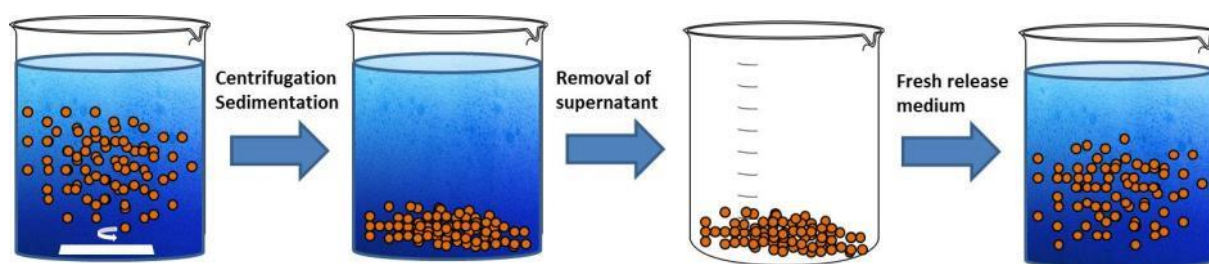


Figure 25: Schematic illustration of the principle of sample-and-separate methods

Generally, these methods comprise a suitable vessel containing the release medium, typically combined with a shaking or stirring device in order to provide agitation. Accordingly, the formulation is introduced into the release medium and incubated under temperature controlled conditions (usually 37 °C). For sampling, an aliquot is withdrawn at suitable time points and replaced by fresh release medium. In order to avoid withdrawal of formulation components, a separation step has to be performed either before or after sampling, in the latter case by re-introducing separated formulation components into the release medium. Separation can be either achieved by sedimentation, centrifugation or filtration. Volume of release medium as well as the sampling volume is adjusted by taking into account the expected release rate of the API, as well as the limit of quantification, in order to ensure and maintain sink conditions without losing sensitivity of the method. The sample-and-separate method is the most widely used technique in the field of drug release testing of parenteral sustained release dosage forms<sup>69-72</sup>, as there is a number of apparent advantages: It is easy to perform, provides high flexibility in terms of the applied volume of release medium and sample volume what makes it applicable also for very small scaled processes. In addition, the potential need for a pH exchange during drug release can easily be met. However, a major issue with the sample-and-separate methods is the problem of missing standardization. The extent of agitation may vary between differently shaped vessels, leading to limited scalability of the method. Furthermore, sampling is an important issue as well. In case of filtration, particulate systems tend to cause filter clogging. Centrifugation potentially leads to insufficient separation of the formulation and re-dispersion is difficult. In both cases, loss of volume might occur and distort release rates. In addition, sample-and-separate methods generally lack in the potential to simulate complex physiological applications like subcutaneous or intra-articular administration. In summary, the sample-and-separate method is a reasonable approach to gain first impressions about and to compare the release behavior of new formulation options in a small scale situation. However, for more standardization, bio-relevance and predictability, more sophisticated setups have to be considered.

**Flow-through methods:** Based on USP apparatus IV, a number of publications show the suitability of flow-through methods for drug release testing of a variety of different formulations. Figure 26 illustrates the principle of a flow-through setup:

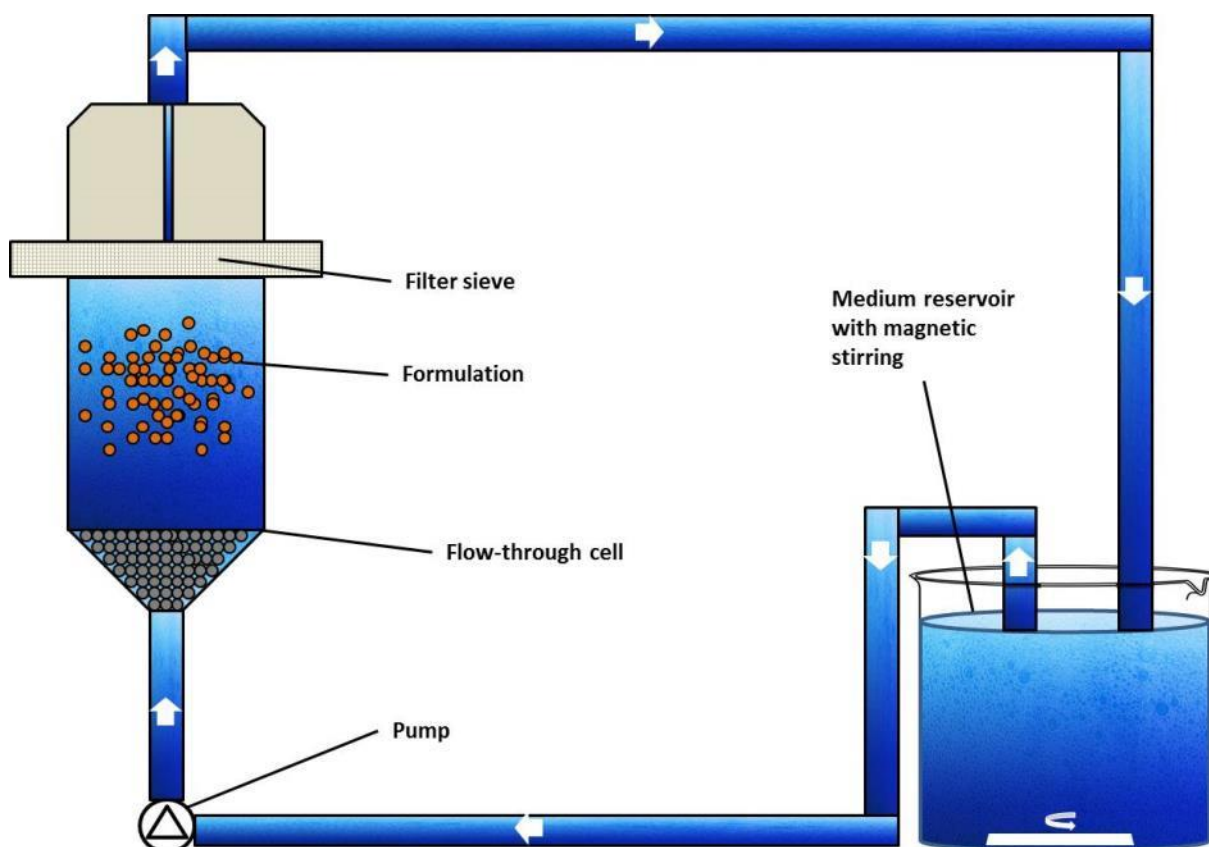


Figure 26: Schematic illustration of a flow-through cell

In general, the formulation is placed in a suitable container and the temperature controlled release medium is pumped through this container at a specific flow-rate. The immobilization of the formulation is usually achieved by a suitable inlet filter, preventing formulation components to be carried away with the media flow. The system can be operated as an open setup, while sampling is performed by collecting the fractions of the media flow, gaining fractional release data. Alternatively, the system can be operated in a closed loop setup, recycling the release medium back into a well stirred media reservoir. In the latter case, sampling is performed from the media reservoir, gaining cumulative release data. In both cases, an automated sampling system and online UV analytics can be

introduced. The container, the formulation is placed inside, can be a filtration cell, the base of which is a large area filter<sup>64,73</sup>. Jacketed columns have also been reported as formulation holding containers, with the release medium being pumped through by a syringe pump<sup>74</sup> or an HPLC pump<sup>75</sup>. Besides these in-house developed techniques, approaches utilizing standardized USP IV equipment are reported as well. For instance, USP IV flow-through cells for tablets can be used by placing the formulation (e.g. microparticles) on top of the introduced glass beads<sup>76</sup> with a filter sieve at the medium outlet in order to prevent clearance of formulation components from the cell. Especially in the application of particulate systems, this method often bares the difficulty of agglomeration of particles, leading to decreased release rates. Clogging of the outlet filter might be a problem as well, especially in the case of nanoparticulate systems to be tested. In order to avoid these issues, the flow-through cell can be completely packed with glass beads and the formulation can be embedded evenly distributed<sup>77,78</sup>. This enables immobilization and prevents agglomeration of the particles. Major advantages of the flow-through methods are the potential for automated operation of the setup and the well-defined standardized apparatus, described in the USP. This guarantees a highly controlled experimental setup, providing the best conditions for reproducible results. In addition, sampling is easy to perform and loss of formulation components can be excluded. However, the execution of the system is more complex and has to be performed by a well-trained operator. The major weak point of this setup, though, is the risk of filter clogging and resulting variations of the flow-rate, in particular when dispersed systems are applied.

**Dialysis methods:** Immobilization, respective separation of the formulation from the release medium is a major issue for IVR testing for sustained release parenterals, in particular for dispersed systems. As commented above, this affects sample-and –separate methods as well as flow-through techniques. An approach to handle this difficulty is the application of dialysis membranes. Figure 27 illustrates the principle:

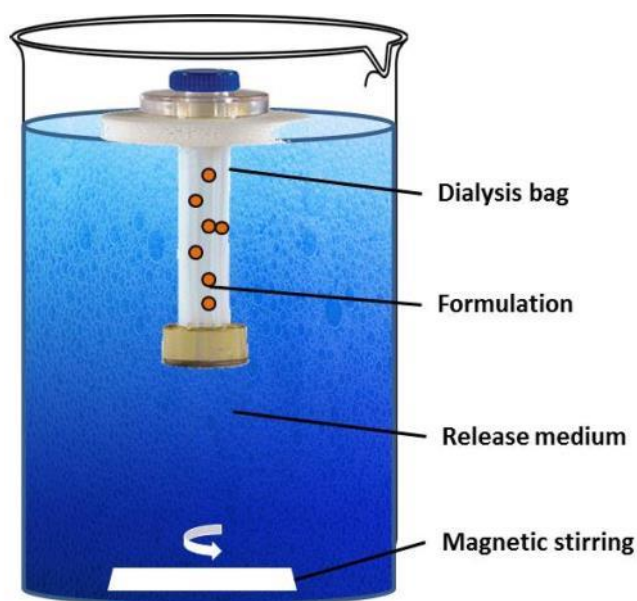


Figure 27: Schematic illustration of a dialysis method

Generally, the formulation is placed inside a dialysis bag and introduced into a suitable vessel, containing the stirred and temperature controlled release medium. Basically, this method can be applied for a number of different dosage forms: microspheres<sup>36</sup>, nanoparticles<sup>79</sup>, liposomes<sup>80</sup> and suppositories<sup>81</sup>, for instance. Apart from the type of formulation, the choice of the membrane is an important issue for this method. The membrane essentially acts as a physical barrier to separate the formulation from the release medium and is generally not supposed to be a diffusion barrier for the respective analyte. Thus, MWCO of the membrane has to be chosen in order to allow free passage of the analyte and can be found in literature in a broad range between 3.5 and 300 kDa<sup>38,82</sup>. In addition, instead of simple dialysis bags, dialysis tubes are frequently applied in order to be able to control the area of the membrane<sup>36,80</sup>. As already mentioned, an advantage of dialysis methods is the separation of the formulation from the release medium. This facilitates the sampling procedure and provides the

potential to separate dissolved high molecular weight formulation components (like phospholipids or albumin) from the release medium, as these might cause interference with API analytics. However, a major issue with these methods is the lack of standardization capability. Even if the outer media reservoir is subjected to agitation, the rate of agitation which is transferred to the dialysis bag is more or less coincidental.

## 1.2 The role of the release medium

Besides the selection of the type of setup, the identification of a suitable release medium is an important step in the development of an IVR method. Basically, release media for IVR testing should meet some fundamental criteria <sup>83</sup>:

- a) Since it may affect solubility and stability of the API, the pH and ionic strength of the medium is supposed to be stabilized at controlled values over the duration of the release experiment. For this purpose, the use of buffers can be helpful.
- b) The medium is supposed to provide “sink conditions”, which is defined as the volume of medium required to maintain concentrations of API below 10% - 30% of saturation solubility. For poorly soluble compounds, the addition of surfactants (polysorbate 80, sodium lauryl sulfate, bile salts) can be helpful in order to increase solubility of the API.
- c) In order to mimic *in vivo* conditions, the use of bio-relevant media can be considered (like simulated gastric or intestinal fluid). In this context, also the addition of enzymes is tolerable.

Finally, the selection of the most appropriate composition of the release medium has to be evaluated for each new API or dosage form in order to meet the basic criteria for IVR testing: discriminatory capability, robustness, stability of the analyte and relevance for *in vivo* performance.

## 1.3 IVR testing for intra-articular applied systems

As mentioned above, synovial joints provide a unique environment for the administration of sustained release dosage forms. These physiological characteristics have to be taken into account in the selection of a suitable IVR method. Figure 28 illustrates the kinetic situation of an intra-articular administered drug product, where  $D_s$  is the total dose of API injected into the joint,  $k_a$  (absorption constant) describes the rate of API release from the depot into the synovial fluid and  $k_e$  (elimination constant) describes the rate of elimination through the synovial membrane into systemic circulation.

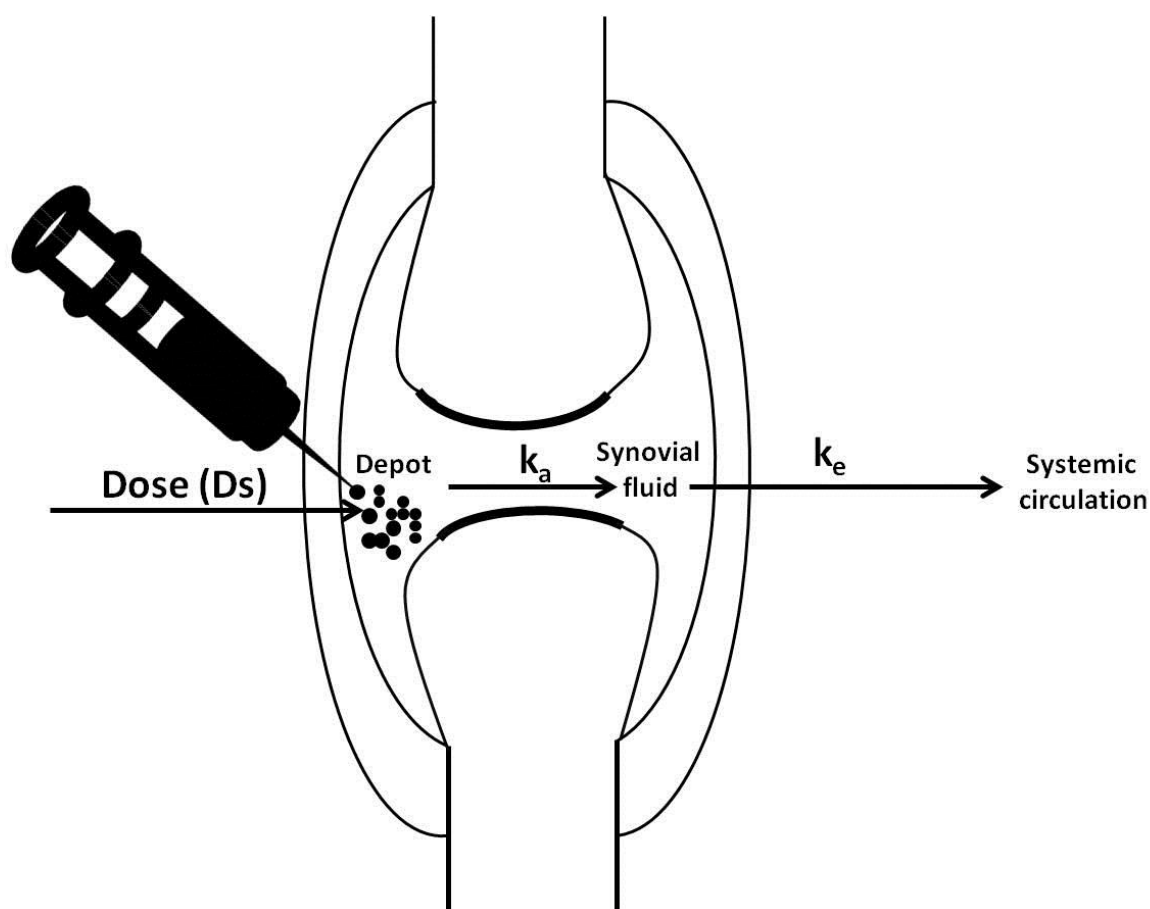


Figure 28: The fate of a substance upon intra-articular administration

Thus, concerning IVR testing, a dialysis method might be the method of choice, as the kinetic situation can potentially be displayed by the dialysis membrane simulating the synovial membrane. Accordingly, Blewis et al. demonstrated semi-permeable membranes to be suitable to mimic the synovial membrane as a diffusion barrier<sup>84</sup>. Furthermore, Larsen et al. already introduced the rotating dialysis cell as a helpful tool for IVR testing in the field of IA drug delivery<sup>63,85,86</sup>. Thus, concerning standardization of the setup, it seems to be a reasonable approach to combine a dialysis method with the advantages of the well-established USP IV flow-through cell, as introduced by Bhardwaj et al.<sup>87</sup>. That work demonstrated that this setup bears the potential to serve as a useful tool to elucidate *in vitro* release of crystal suspensions and liposomes. Furthermore, Gao et al. performed release experiments with solutions and suspensions of Acetaminophen on this setup. In that work, it was stated, that release kinetics of a suspension are mainly driven by three kinds of processes: dissolution of the API, migration to the membrane and permeation through the membrane, while all of these processes could

be rate-limiting steps<sup>62</sup>. As this most likely also applies for the *in vivo* kinetics in synovial joints, this setup, combining a dialysis method with the advantages of the well-established USP IV apparatus, is considered to be a useful tool to mimic the release of intra-articular administered drugs.

## **2 Materials and methods**

### **2.1 Materials**

#### **2.1.1 Compounds**

##### **Merck Serono development compounds (MSC1, MSC2 and MSC3)**

These compounds were provided in the context of a research project at Merck KGaA (Darmstadt, Germany). MSC1, MSC2 and MSC3 are hexapeptides, intended to inhibit CathepsinD, which is known to be an important enzyme in the degradation of cartilage matrix in osteoarthritis (OA). They were chosen as representatives of this anti-catabolic group of compounds in the progression of OA to be administered in form of a crystal suspension or formulated in a sustained release formulation.

##### **Methylene blue**

Methylene blue (purchased by Merck, Darmstadt) belongs to the group of phenothiazines and finds application in many fields of biology and medicine. In the context of the following work, it was chosen as slightly water soluble, positively charged and easy to detect small molecule. It was applied for the characterization of the *in vitro* release setup, introduced below.

##### **Diclofenac-sodium**

Diclofenac-sodium (purchased from Sigma-Aldrich, St. Louis) is the water soluble sodium salt of the analgesic and antiphlogistic non-steroidal-anti-inflammatory-drug (NSAID) Diclofenac. It is applied for the treatment of slight and medium pain, also in the therapy of osteoarthritis. In the context of the following work, it was applied as model compound for the characterization of the mentioned *in vitro* release setup. It was chosen due to available literature data on its *in vivo* pharmacokinetics after intra-articular administration<sup>13</sup>.

##### **Sodium-salicylate**

As well as Diclofenac, Sodium-salicylate (purchased from Sigma-Aldrich, St. Louis) belongs to the group of NSAIDs and also finds application in the treatment of osteoarthritis. For the following

experiments it was chosen as another model compound with available *in vivo* data were chosen due to available literature data on their *in vivo* pharmacokinetics after intra-articular administration<sup>13</sup>.

### **Paracetamol**

Due to its superior properties concerning gastro-intestinal side effects, paracetamol is used for the treatment of osteoarthritis as well, in particular with elderly patients. Corresponding to diclofenac and salicylate, paracetamol was applied for the characterization of the IVR setup.

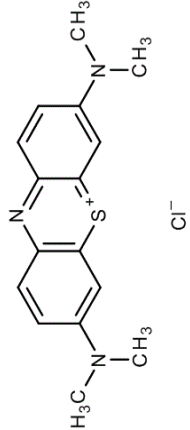
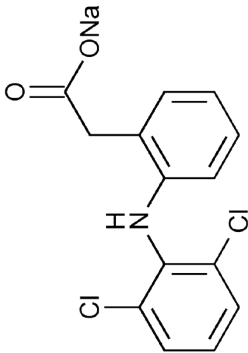
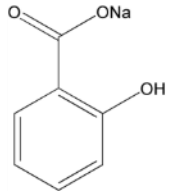
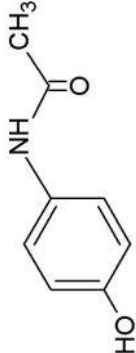
Substance	MSC1	MSC2	MSC3	Methylene blue	Diclofenac sodium	Sodium salicylate	Paracetamol
<b>Chemical structure</b>	Confidential	Confidential	Confidential				
<b>Group</b>	Hexapeptide	Hexapeptide	Hexapeptide	Chemical entity	Chemical entity	Chemical entity	Chemical entity
<b>Molecular weight</b>	690 Da	717 Da	718 Da	320 Da	318 Da	160 Da	151 Da
<b>CAS number</b>	--	--	--	61-73-4	15307-79-6	54-21-7	103-90-2
<b>Indication</b>	Enzyme-inhibitor	Enzyme-inhibitor	Enzyme-inhibitor	Antidote / dye	Analgesic / Antiphlogistic	Analgesic / Antiphlogistic	Analgesic / Antipyretic

Table 10: Overview on applied model compounds

### 2.1.2 Excipients, buffers and chemicals

A list of utilized excipients, buffers and chemicals is given in Table 11:

Name	Abbreviation	Product specification	Supplier
Dulbecco's phosphate buffered saline	PBS	D1408	Sigma-Aldrich, St. Louis, USA
Kollidon 17PF	Kol	Ph.Eur	BASF, Ludwigshafen, Germany
Lutrol F68	Lut	Ph.Eur	BASF, Ludwigshafen, Germany
Methocel K4M	Met	Ph.Eur	Dow Chemicals, Midland, USA
Tween 20	T20	Ph.Eur	Merck Millipore, Billerica, USA
Tween 80	T80	Ph.Eur	Merck Millipore, Billerica, USA
Bovine serum albumin	BSA	A1933	Sigma-Aldrich, St. Louis, USA
Sodium hyaluronate	SH	Hyasis 850T	Novozymes, Bagsvaerd, Denmark
Bovine synovial fluid	BSF	--	Knee joints of healthy cows
Sodium azide	--	Ph.Eur	Sigma-Aldrich, St. Louis, USA
Ultra-pure water	--	Milli-Q	Merck Millipore, Billerica, USA

Table 11: List of excipients, buffers and chemicals

## 2.2 Methods

### 2.2.1 Preparation of crystal suspensions of MSC1, MSC2 and MSC3

The peptides were weighed in 5 ml vials and vehicle solutions were added to a final concentration of 5, 10, 20 or 40 mg/ml, respectively. The suspension was prepared by slowly increasing power of the Ultra-Turrax<sup>®</sup> device (IKA; Staufen, Germany) and maintaining at maximum power (25,000 rpm) for 1 minute. Subsequently, this procedure was repeated, if agglomerates were detected under cold light. The crystal suspensions were stirred for 24 h for equilibration afterwards. Table 12 gives an overview on the composition of the different suspension vehicles:

Component	Vehicle 1 (PBS)	Vehicle 2 (Methocel/Tween)	Vehicle 3 (Kollidon/Lutrol)	Vehicle 4 <sub>a</sub> (SH)	Vehicle 5 <sub>a</sub> (BSA)	Vehicle 6 <sub>a</sub> (ArtSF)	Vehicle 7 <sub>b</sub> (BSF)
<b>PBS</b>	x	x	x	x	x	x	
<b>Met</b>		0.5 % (w/V)					
<b>T20</b>		0.25 % (w/V)					
<b>Kol</b>			2 % (w/V)				
<b>Lut</b>			1 % (w/V)				
<b>SH</b>				1 % (w/V)		1 % (w/V)	
<b>BSA</b>					2.5 % (w/V)	2.5 % (w/V)	
<b>BSF</b>							x

<sub>a</sub>: due to instability against the high shear rate, SH and/or BSA were added to a suspension in PBS before stirring for 24 hours.

<sub>b</sub>: The suspension of MSC1 in BSF was prepared by weighing the API in a suitable vial and adding BSF to a final concentration of 20 mg/ml.

Table 12: Overview on the applied suspension vehicles

Concerning the vehicle composition, Methocel, Kollidon and Lutrol were added in order to increase the viscosity and to stabilize the suspension. Kollidon, Lutrol and Tween acted as wetting agents.

Sodium-hyaluronate and BSA are essential components of synovial fluid in the joint cavity. Consequently, these components were added in order to investigate their influence on the characteristic of the suspension and the *in vitro* release. The combination of both components was denoted “Artificial Synovial Fluid” (ArtSF).

In order to evaluate the comparability of ArtSF with *in vivo* conditions, a suspension of MSC1 was prepared in bovine synovial fluid as described above.

### 2.2.2 In vitro release methods

In the following section, the applied dissolution, respective *in vitro* release techniques are introduced:

#### Modified USP apparatus IV

Figure 29 illustrates the applied setup, combining a Sotax<sup>®</sup> CE70 flow-through device (Sotax; Allschwil, Switzerland) with a Sotax<sup>®</sup> A4D dialysis adapter system. As mentioned above, this combination of a flow-through cell with a dialysis adapter has the potential to serve as a useful tool for the evaluation of release kinetics of intra-articular applied formulations.

The system was operated in a closed loop setup with an Ismatec<sup>®</sup> IPC peristaltic pump and Tygon<sup>®</sup> MHSL low adsorbing tubings at flow rates from 1-5 ml/min. As illustrated in Figure 30, dialysis adapters were assembled with **50kDa** SpectraPor<sup>®</sup> cellulose ester dialysis membrane tubes, and 1ml of the analyte solution or suspension was added after checking the adapters for potential leakage.

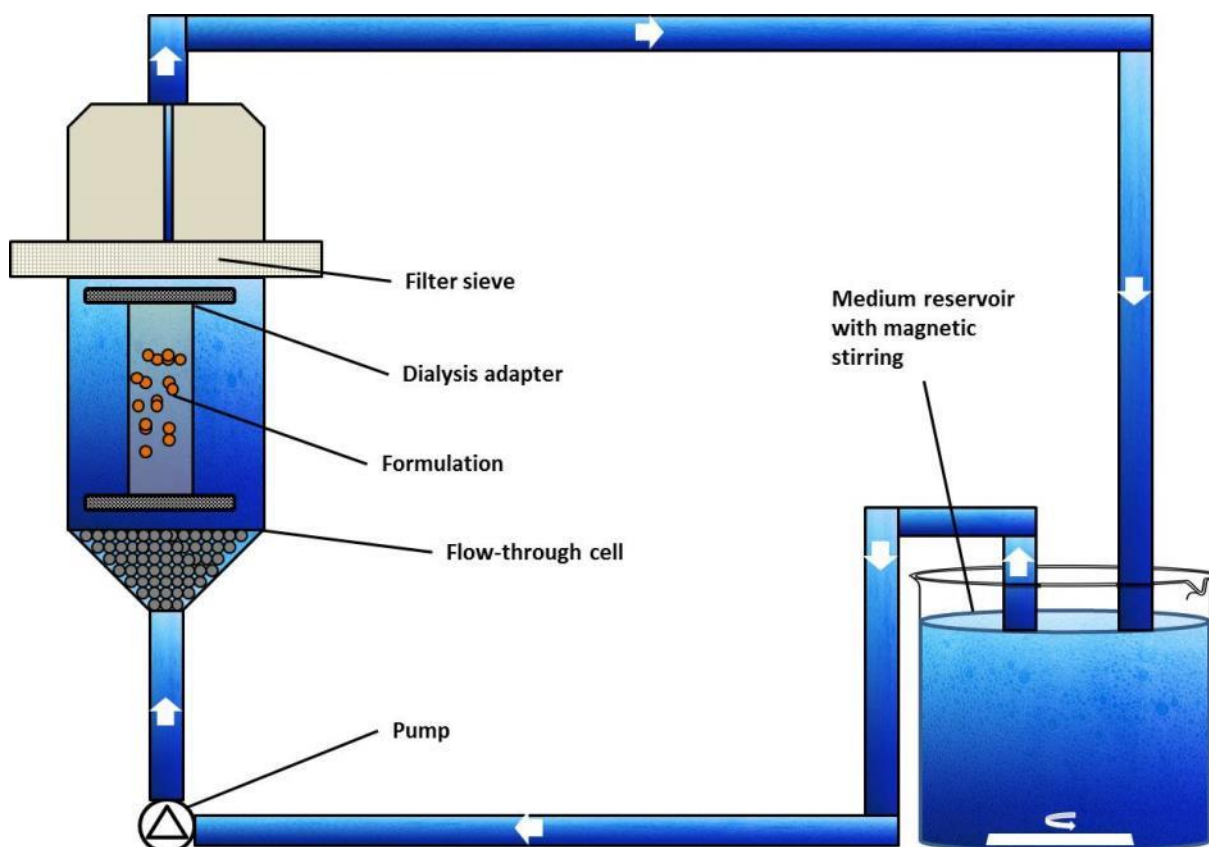


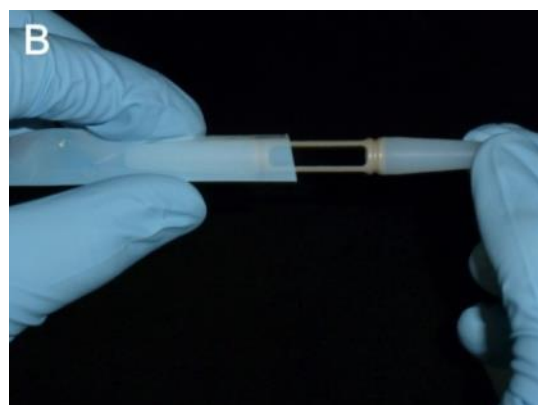
Figure 29: Schematic illustration of the combined flow-through/dialysis system



4 components:

Main body; 2 endcaps

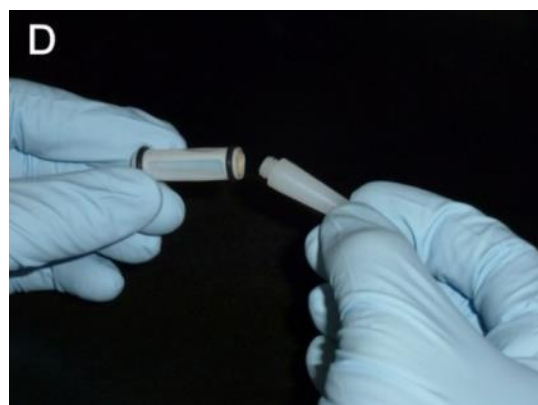
2 O-rings; 2 white auxiliary tools



Insertion of the adapter into the dialysis tubing by  
using the auxiliary tools



Fixation of the dialysis tubing with the O-rings  
and removal of excess tubing



Removal of the auxiliary tools



After sealing one end of the adapter, the adapter  
can be filled with the formulation



After sealing, the adapter is inserted into a 22.6  
mm flow-through-cell

Figure 30: Illustration of the adapter assembly

The prepared dialysis adapters were inserted in 22.6 mm diameter flow-through cells and the device was closed in order to preheat the cells to 37 °C. After 2 minutes, the pump was turned on for circulating preheated release medium.

The applied volume of release medium varied between 25 ml (minimum) and 1 L. It was adjusted considering sink conditions and the limit of detection (LOD) of the respective API.

Samples were withdrawn from medium reservoirs at predetermined time intervals and analyzed by HPLC-UV or UV-spectroscopy. The sample volume varied between 0.5 and 50 ml. It was adapted considering sink conditions and the LOD correspondingly. Samples were stored frozen until analysis.

### **Dialysis method**

Sotax® A4D dialysis adapters were assembled and filled as described above. The adapters were then placed and fixed inside a 1 L glass bottle containing temperature controlled and magnetically stirred release medium.

## **2.2.3 Physico-chemical characterization of the formulations**

### **Stability of Merck Serono compounds**

As MSC1, MSC2 and MSC3 were intended for application in sustained drug delivery from microparticles, *in situ* forming gels or from crystal suspensions, the stability of these compounds in relevant media is an important parameter for IVR testing of respective formulations. Stability tests were performed in solution as well as formulated in a crystal suspension.

For stability in solution, the API (200 µg/ml) was dissolved in PBS and incubated at 37 °C for 7 days under light exclusion. At 2 h, 6 h, 24 h and 7 days, samples were taken and API content was analyzed by HPLC-UV.

The stability of crystal suspensions was tested for suspensions in vehicle 2 at a concentration of 20 mg/ml. The samples were incubated at 8, 25 and 40 °C for 13 weeks. Samples were taken and analyzed for API content by HPLC-UV after 1, 4 and 13 weeks.

**Determination of saturation solubility of MSC1, MSC2 and MSC3**

The solubility of the applied peptides in the suspension media as well as in the release media are crucial parameters for the evaluation of the release behavior of respective crystal suspensions. Consequently, the saturation solubility of MSC1, MSC2 and MSC3 was determined:

For this purpose, an excessive amount of API (~ 2 mg) was weighed in a 2 ml glass vial and 1 ml of medium was added. Under magnetic stirring and at room temperature, samples were withdrawn after 1 h, 2 h and 24 h, in order to ensure equilibrium. Samples were centrifuged and checked for absence of particles. If necessary, an additional filtration step was introduced and quantification of the API was performed by HPLC-UV.

**Particle size measurements**

Besides saturation solubility, also the particle size plays a major role in the interpretation of release data from a crystal suspension formulation.

Thus, particle size distributions were determined by laser diffraction with a Horiba LA-950 (Horiba; Kyoto, Japan). For the measurements, the suspension was re-dispersed and sonicated. About 100 µl of suspension were needed for sufficient scattering signals. Calculation of particle size distribution was performed by applying the Fraunhofer approximation. Values were determined from the volume distribution ( $D_{10}$ ;  $D_{50}$ ;  $D_{90}$ ).

**Light microscopy**

The crystals were investigated by light microscopy with an Olympus BX 60 (Olympus; Tokyo, Japan).

**2.2.4 Quantification of APIs****MSC1, MSC2 and MSC3**

With exception of samples containing SH and/or BSA, all aqueous samples were diluted with methanol (1:1) in order to avoid re-crystallization of the API. As BSA/SH caused interference with HPLC peptide analysis, an additional dilution step with acetonitrile (1:1 v/v) was performed for these components. This enabled precipitation of BSA and SH and their removal by an additional centrifugation step. Afterwards, samples were diluted with Methanol as described above.

For the quantification of the peptides, an Agilent® 1100 HPLC System (Agilent; Santa Clara, USA), coupled to an Agilent® Diode Array Detector was applied. Stability indicating gradient elution was

performed, enabling to monitor API stability. For MSC1, 10 mM ammonium carbonate buffer (pH 10) / acetonitrile (premixed 95%/5% (v/v) for eluent A and 5%/ 95% (v/v) for eluent B) with a Waters XBridge<sup>®</sup> C<sub>18</sub> /5 $\mu$ m column (4.6 x 100mm) (Waters; Milford, USA) at a flow rate of 3 ml/min were used. MSC1 was detected at 214 nm. For MSC2 and MSC3, water / acetonitrile (premixed 95%/5% (v/v) for eluent A and 5%/ 95% (v/v) for eluent B) + 0.01% ammonia (25%) with a Phenomenex Luna<sup>®</sup> C<sub>18</sub> / 3  $\mu$ m column (4.6 x 50mm) (Phenomenex; Torrance, USA) at flow rate of 3 ml/min were utilized. MSC2 and MSC3 were detected at 210 nm. For all analyses Milli-Q<sup>®</sup> ultra-pure water (Merck Millipore; Billerica, USA) was used.

#### **Diclofenac-sodium, sodium-salicylate and paracetamol**

Before HPLC analysis, all samples were diluted with acetonitrile (1:1 v/v). The same instrumental equipment was used as for MSC1, 2 and 3. For all compounds, water/acetonitrile (1:1 v/v), containing 0,015% TFA was used for eluent A. Water, containing 0,015% TFA was used for eluent B. A gradient elution was applied in order to be able to separate a mixture of the APIs on a LiChroCart 55-4-Purospher Star column. Flow was 1.5 ml/min and detection wavelength was 229 nm.

#### **Methylene blue**

The quantification of methylene blue was performed by UV-Vis spectroscopy, applying a Tecan Infinite<sup>®</sup> 200 plate reader.

### 3 Results and discussion

#### 3.1 Physico chemical characteristics

##### 3.1.1 Stability testing

As crystal suspensions of the mentioned hexapeptides are intended to provide prolonged release properties, the stability of these formulations is an important parameter also for the assessment of *in vitro* release data. Thus, stability of the crystal suspensions was investigated:

Conditions	Stability of crystal suspension (20 mg/ml in vehicle 2) after 13 weeks		
	8°C	25°C	40°C
MSC1	100.12 %	100.09 %	100.41 %
MSC2	99.12 %	94.43 %	92.21 %
MSC3	100.23 %	100.43 %	100.46 %

Table 13: Stability of MSC1, MSC2 and MSC3 formulated as crystal suspension

Besides stability of the suspensions, also the stability of dissolved API is of importance for *in vitro* release testing. Thus, also the stability of the hexapeptides in solution was investigated. Table 14 depicts respective results:

Conditions	Stability in solution (37°C)		Comments
	24 hours	7 days	
MSC1	99.65 %	99.83 %	Deviations within analytical uncertainty
MSC2	98.47 %	93.81 %	Instability at physiological conditions → appropriate measures for release testing
MSC3	99.92 %	99.87 %	Deviations within analytical uncertainty

Table 14: Stability of MSC1, MSC2 and MSC3 in solution

MSC1 and MSC3 show very good stability data in solution as well as formulated as a crystal suspension over 7 days and 13 weeks, respectively. The values with negative loss of content can be

explained by the analytical uncertainty in this context ( $\pm 0.5\%$ ). Consequently, suspensions and samples of MSC1 and MSC3 were treated accordingly during the following *in vitro* release and solubility experiments:

- The duration of suspension stability (13 weeks) was not exceeded after preparation of the suspension (including storage at room temperature after preparation as well as the duration of the *in vitro* release at 37°C).
- All samples were analyzed by HPLC-UV within the period of solution stability. Nevertheless, samples were stored frozen until analysis as described above.

In contrast, the poor stability of MSC2 required a slight modification of the respective experiments:

- Prepared crystal suspensions were stored at 8°C and *in vitro* release experiments were started directly after preparation. As suspensions of MSC2 showed release durations of about 2-3 days, the measured loss of content (2.34 % at 40°C after 7 days) is still acceptable.
- Regarding the poor stability of solutions of MSC2, quantification by HPLC-UV was conducted directly after sampling for all experiments with MSC2.

### 3.1.2 Solubility and particle size distribution

For characterization of the applied crystal suspensions, mainly 3 parameters were investigated:

- Solubility of the API in the suspension vehicle
- Particle size distribution of the crystal suspension
- Particle shape

Table 15 gives an overview on size and saturation solubility of the Merck Serono compounds in different media. However, limited availability of substance led to limited data sets for MSC2 and MSC3. As for large parts of this work, MSC1 as most promising representative for this group of APIs was applied, this is not critical.

MSC1 showed solubility values between 216 µg/ml (in PBS) and 403 µg/ml (in 2.5% BSA), while MSC2 (1439 µg/ml) and MSC3 (824 µg/ml) have a clearly higher solubility in the tested media.

Concerning particle size distribution, the median diameter of MSC1 varied between 3.5 and 5.1 µm in all tested vehicles, except for vehicle 2 (7.7 µm). This may be explained by the higher viscosity of

vehicle 2, leading to reduced shear rates during suspension preparation in comparison to PBS and Kollidon/Lutrol.

Comparing the particle sizes of APIs, distinctly larger particles were observed for MSC2.

Medium	MSC1				MSC2				MSC3
	<i>Solub.</i>	<i>D10</i>	<i>D50</i>	<i>D90</i>	<i>Solub.</i>	<i>D10</i>	<i>D50</i>	<i>D90</i>	<i>Solub.</i>
	[ $\mu\text{g/ml}$ ]	[ $\mu\text{m}$ ]	[ $\mu\text{m}$ ]	[ $\mu\text{m}$ ]	[ $\mu\text{g/ml}$ ]	[ $\mu\text{m}$ ]	[ $\mu\text{m}$ ]	[ $\mu\text{m}$ ]	[ $\mu\text{g/ml}$ ]
<b>PBS</b>	216	1.8	4.4	10.4	2110	n/d	n/d		n/d
<b>Vehicle 2</b>	264	4.5	7.7	12.9	1439	0.7	1.0	1.7	824
<b>Vehicle 3</b>	393	1.9	5.1	14.3					
<b>Vehicle 4</b>	373	1.2	3.5	10.0	n/d		n/d		n/d
<b>Vehicle 5</b>	403	1.6	5.0	15.8					
<b>Vehicle 6</b>	303	1.4	4.5	14.6					

Table 15: Solubility and size distribution values for peptides in suspension media (reprinted from <sup>89</sup> with permission)

According to the Noyes-Whitney equation, the dissolution of a substance is determined by the particle surface and its saturation solubility <sup>88</sup>:

$$\frac{dM}{dt} = \frac{D \cdot F}{x} (c_s - c_t) \quad (10)$$

“D” is the diffusion coefficient, “F” the particle surface and “x” the thickness of the unstirred water layer; “c<sub>s</sub>” is the saturation solubility and “c<sub>t</sub>” the concentration of dissolved API.

Considering the retention of particles of a crystal suspension within the joint cavity by the synovial membrane, the dissolution of API is a crucial parameter for duration of API exposure. Consequently, the residence time of a crystal suspension after intra-articular administration is highly dependent on the parameters particle size (as a function of particle surface) and the solubility of API in the vehicle (refer to equation 10). Regarding particle retention, Bonanomi et al. demonstrated that an increase in particle size of a liposomal system from 160 nm up to 750 nm lead to a 2.8 fold increase in synovial retention <sup>25</sup>. In addition, Howie et al. found that polyethylene wear particles below 5  $\mu\text{m}$  diameter trigger a mononuclear macrophage response <sup>27</sup>. In contrast, Horisawa et al. demonstrated PLGA particles with a mean diameter of  $26.5 \pm 0.9 \mu\text{m}$  not to be phagocytosed or transported to the underlying synovial membrane <sup>10</sup>. Instead, they were encapsulated by the formation of multinuclear

giant cells and thus trapped inside the synovial cavity. Accordingly, the particle size of marketed crystal suspension Volon A<sup>®</sup>, for example, is in the range of 10 – 20  $\mu\text{m}$  (73).

From this perspective, the suspension of MSC1 in vehicle 2 (Methocel / Tween) seems to be the most promising candidate for sustained intra-articular drug exposure, as it shows a comparable low saturation solubility in combination with a median particle size of  $>5\mu\text{m}$ .

Concerning particle shape, microscopic pictures of suspensions of MSC1 revealed platelet to needle shaped crystals (Figure 31). The type of vehicle does not seem to have an impact on particle morphology.

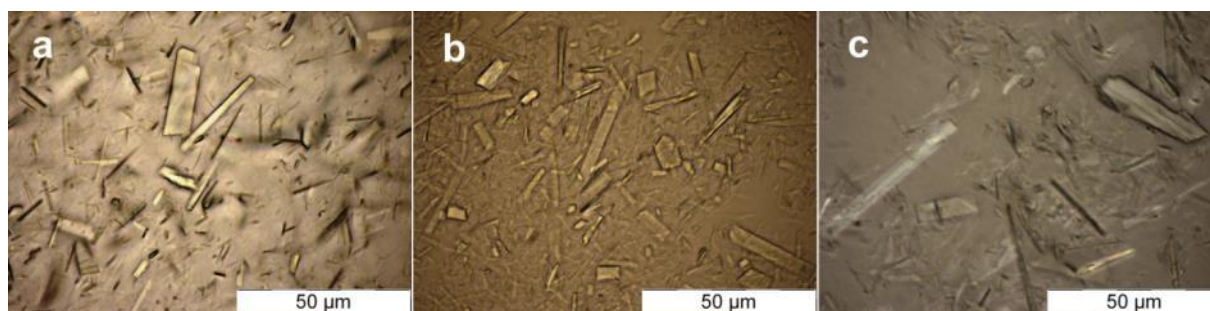


Figure 31: Microscopic pictures of crystal suspensions of MSC1 in (a) PBS, (b) Kollidon/Lutrol and (c) Methocel/Tween vehicle (reprinted from <sup>89</sup> with permission)

Besides solubility and particle size, the shape of the crystals can play a particular important role for the *in vivo* performance as well. It was shown before, that the intensity of inflammatory macrophage response upon intra-articular administration correlates with the shape of the investigated particles <sup>31,32</sup>. It was discovered that spherical particles are to be preferred in this context in comparison to rod or needle shaped particles.

Therefore, the needle-shaped crystals of MSC1 seem to be not optimal for intra-articular administration and an optimization of the particle morphology may be required.

In summary, as mentioned above, it might be concluded that the suspension of MSC1 in vehicle 2 (Methocel / Tween) is the most suitable candidate in terms of solubility and particle size among the vehicles investigated. In turn, a crystal suspensions of MSC2, may undergo rapid clearance by phagocytosis through intra-articular macrophage response. In addition, the lower solubility of MSC1 in comparison to MSC2 and MSC3 presumably leads to slower dissolution of the particles after IA administration and thus enables longer residence times.

However, as all tested suspension vehicles do not differ in terms of the shape of particles, formulated crystal suspension might have to be optimized with regards to particle morphology in order to avoid joint inflammation. Though, the optimization of the formulation was not the focus in this work.

## 3.2 *In vitro* release studies

### 3.2.1 Release of API from solutions

As mentioned above (section 4.1.2.), the physiology of synovial joints comes along with a number of challenges for the establishment of an appropriate *in vitro* release method. The application of a modified USP apparatus IV, combined with a dialysis system to mimic *in vivo* conditions, was chosen as a reasonable approach to fulfill the requirements in this context. In order to investigate the suitability of the described *in vitro* release setup for IA purposes, initial experiments with solutions of different model APIs were performed.

Several investigations on *in vivo* elimination kinetics of dissolved small molecules after intra-articular administration have been performed before <sup>12-15</sup>, showing half-lives of the injected compounds between about one and six hours. Owen et al., for example, reports half-lives for solutions of Diclofenac (5.2 h), Salicylate (2.4 h) and Paracetamol (1.1 h) after intra-articular administration in human rheumatoid patients. Accordingly, release experiments with a mixture of these substances were performed on the combined dialysis / flow-through setup. In parallel, solutions of the peptide MSC1 and methylene blue were investigated as well.

Figure 32 indicates 1<sup>st</sup> order release kinetics for all compounds. This corresponds with previous observations for dialysis experiments with regenerated cellulose membranes: Meyer and Guttman investigated the influence of several parameters on the release behavior of solutions of phenol red and methyl orange. For instance, the application of agitation led to increased release rates from a regenerated cellulose dialysis tube in comparison to an unstirred system. However, in all cases 1<sup>st</sup> order release kinetics were observed <sup>90</sup>.

Furthermore, Pedersen et al. <sup>63</sup> showed that 1<sup>st</sup> order kinetics are correlated with diffusion controlled transport processes following Fick's law of diffusion. This suggests, that the release from a dialysis system is mainly controlled by the diffusion coefficient of the applied analyte.

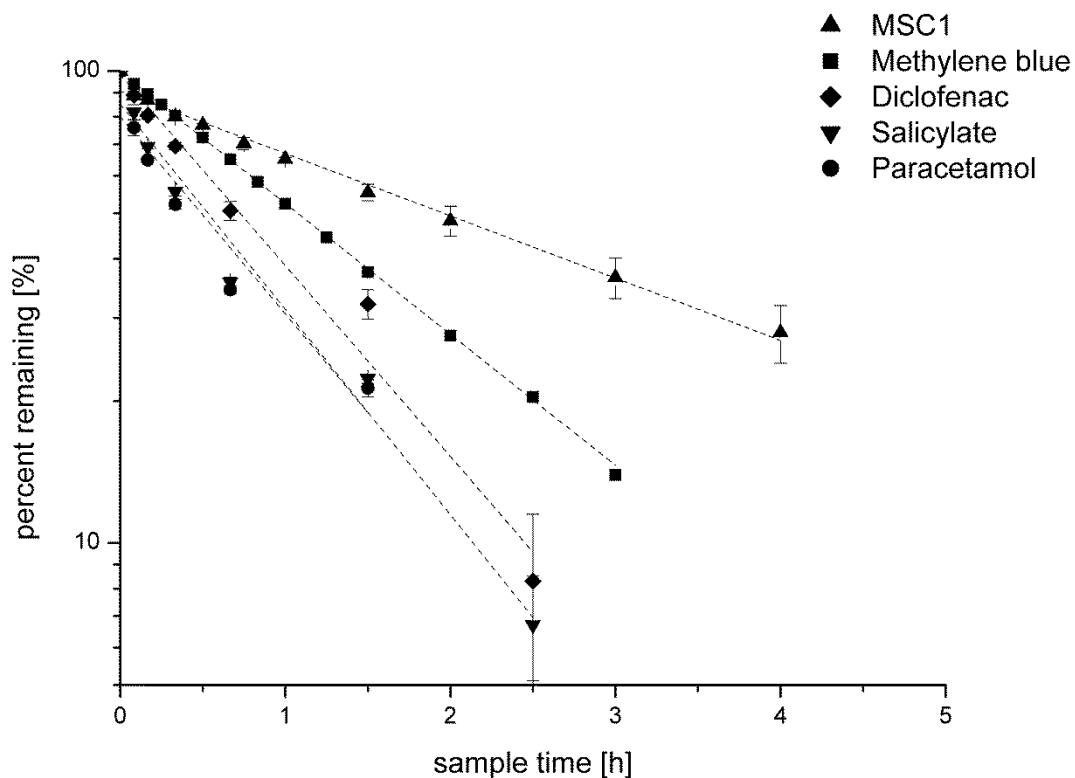


Figure 32: Release profiles of solutions of (□) MSC1, (■) Methylene blue, (◆) Diclofenac, (▼) Salicylate and (●) Paracetamol

Based on the release data, half-lives of the dissolved compounds were determined (see Table 16). With increasing molecular weight, an increase of release duration can be observed. This almost linear relation underlines the suggestion, that the release duration of solutions from the applied dialysis / flow-through system is mainly controlled by the molecular size of the respective compound (see Figure 33).

These results indicate the potential of this setup for *in vivo* relevant *in vitro* testing. In fact, the determined *in vitro* half-lives do not accurately match the values obtained from *in vivo* experiments. However, the release duration of the solutions *in vitro* is in the range of what was reported for several small molecules *in vivo* before (1 – 6 hours)<sup>12-15</sup>. This demonstrates the potential for physiological relevant *in vitro* testing with this combined dialysis / flow-through IVR setup.

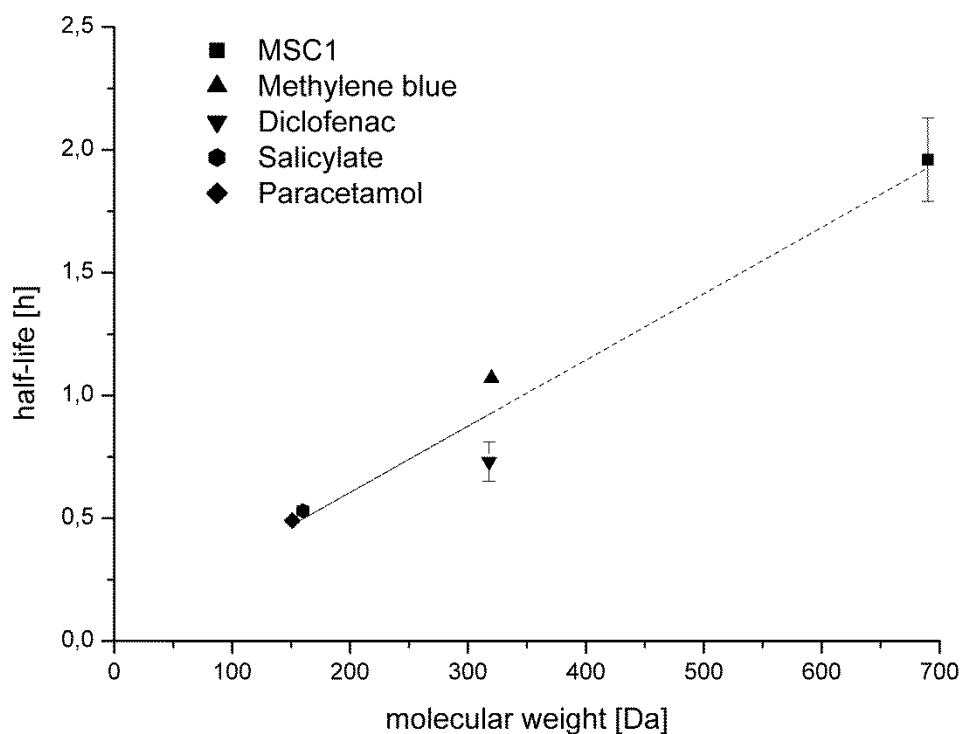


Figure 33: Dependency of the half-life from molecular weight

Compound	Methylene blue	Diclofenac-sodium	Sodium-salicylate	Paracetamol	MSC1
MW [Da]	320	318	160	151	690
$t_{1/2}$ [h]	1.1	$0.7 \pm 0.1$	$0.5 \pm 0.0$	$0.5 \pm 0.01$	$2.0 \pm 0.2$

Table 16: Half-lives of in vitro release kinetics of applied compounds

### 3.2.2 Release of API from crystal suspensions

As demonstrated above, the applied IVR setup showed the potential to serve as a useful tool for bio-relevant IVR testing in the field of intra-articular application of API solutions. However, the goal of this work was the development of a suitable method for sustained release drug products like crystal suspensions, microparticles and *in situ* forming gel systems. In order to further investigate the suitability of the setup for these applications, crystal suspensions of MSC1 were prepared and IVR studies were performed, screening a number of different influence parameters.

#### Kinetic considerations

For the interpretation of *in vitro* release kinetics and the characterization of the setup, it is of great value to understand the kinetic processes during IVR. The following theoretical kinetic considerations are intended to help to understand the kinetic behavior of the tested crystal suspensions.

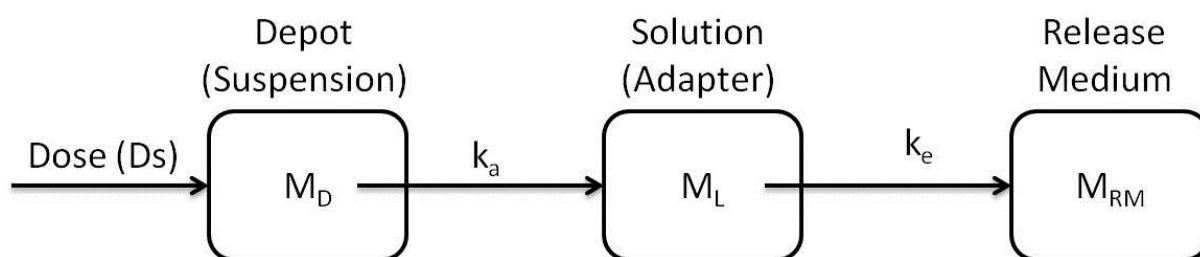


Figure 34: Schematic illustration of release of a crystal suspension in the described setup (reprinted from <sup>89</sup> with permission)

Figure 34 illustrates the kinetic situation in the described IVR setup after administration of a crystal suspension. It can be described as a one-compartment model with a 1<sup>st</sup> order absorption and elimination process. The absorption process describes the dissolution of the crystals, expressed by the constant  $k_a$ , the elimination process describes the disappearance of API from the dialysis adapter into the release medium and is expressed by the elimination constant “ $k_e$ ”. As in all experiments sink conditions in the release medium were existent, the re-distribution into the adapter is negligible. “Ds” is the administered amount of API in the suspension,  $M_D$  is the mass of undissolved API inside the dialysis adapter,  $M_L$  is the amount of API in solution inside the dialysis adapter and  $M_{RM}$  is the amount of drug, eliminated into the release medium.

The absorption, respective the dissolution of API can be described according to a modification of the Noyes-Whitney equation according to Costa et al. <sup>91</sup>:

$$\frac{dM_D}{dt} = -k_a \cdot (V \cdot c_s - M_L(t)) = -k_a \cdot V \cdot (c_s - c_L(t)) \quad (11)$$

V is the volume inside the dialysis adapter,  $c_s$  is the saturation solubility of the API and  $c_L$  the concentration of dissolved API inside the adapter;  $k_a$  can be described as:

$$k_a = \frac{D \cdot A}{h \cdot V} \quad (12)$$

A is the surface area of the particles, D is the diffusion coefficient and h is the thickness of the unstirred diffusion layer.  $M_L$  and  $M_{RM}$  can be described according to:

$$\frac{dM_L}{dt} = \frac{dM_D}{dt} - \frac{dM_{RM}}{dt} \quad (13)$$

$$\frac{dM_{RM}}{dt} = k_e \cdot M_L(t) \quad (14)$$

Equations (11), (12) and (14) depict that the absorption or dissolution rate ( $\frac{dM_D}{dt}$ ), as well as the elimination rate ( $\frac{dM_{RM}}{dt}$ ) are determined by the amount of drug dissolved ( $M_L$ ) and thus from the concentration of API ( $c_L$ ) at a constant volume inside the dialysis adapter.

After an initial distribution phase,  $M_L$ , respective  $c_L$ , will equilibrate at a constant value. This would basically lead to constant concentration gradients and thus to zero order release kinetics from the dialysis adapter. However, as illustrated by equation (13), the dissolution rate is also dependent on  $k_a$  and thus from the surface area of undissolved particles. Considering a declining surface area due to dissolution of the particles, this would lead to decreasing release rates, controlled by a 1<sup>st</sup> order decline of the surface area of the particles. Based on these assumptions, basically two scenarios are imaginable:

- 1) Very high doses of API would lead to a situation, in which the high amount of API underlies very low relative change of the surface area, in comparison to the actual amount of API dissolved. In this case, the decline of surface area can be neglected, resulting in zero order release kinetics.
- 2) Considering lower doses of API, the decrease of the surface area will become relevant and result in decreasing dissolution rates over time. The release would be controlled by a 1<sup>st</sup> order decline, defined by the decline of surface area of the particles.

### Concentration dependence of drug release from suspensions

Crystal suspensions of MSC1 in vehicle 2 (Methocel/Tween) in four different concentrations (5 – 40 mg/ml) were prepared and release experiments were performed in order to investigate the influence of the total dose on drug release in this setup.

As Figure 35a depicts, the suspensions show 1<sup>st</sup> order release kinetics in all concentrations. However, the elucidation of release half-lives reveals a dose-dependency of release durations, with half-lives of 1 day (5 mg/ml) to 7 days (40 mg/ml) (refer to Table 17).

Parameter	5 mg/ml (n=3)	10 mg/ml (n=3)	20 mg/ml (n=3)	40 mg/ml (n=1)
Half-life [d]	1.1 ± 0.1	2.4 ± 0.1	5.0 ± 0.4	8.3 ± 0.0
1 <sup>st</sup> order constant [d <sup>-1</sup> ]	-0.6 ± 0.0	-0.3 ± 0	-0.1 ± 0.0	-0.1 ± 0.0

Table 17: Kinetic parameters of 1<sup>st</sup> order release of suspensions of MSC1

Plotting the determined half-lives against the suspension concentration reveals an almost linear relation between these parameters (Figure 35b). In addition, the second y-axis shows the release rates [ $\mu\text{g}/\text{d}$ ] at three comparable time-points. Only slight deviations of absolute released API amounts can be observed between the differently concentrated suspensions.

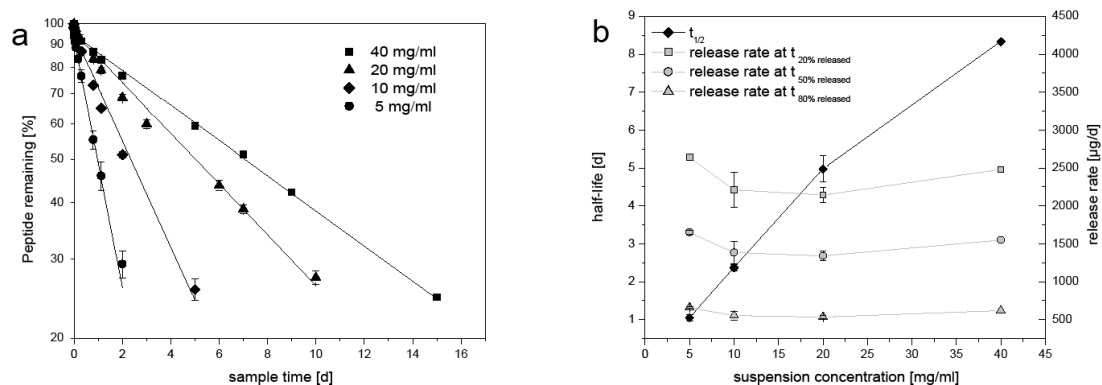


Figure 35: (a) Release profiles (% vs. time in logarithmic scale of y-axis) of crystal suspensions of MSC1 in Methocel/Tween: (●) 5mg/ml (n=3), (◻) 10mg/ml (n=3), (◻) 20mg/ml (n=3), (◻) 40mg/ml (n=1) and (b) half-lives of release kinetics vs. suspension concentrations at different timepoints (20%, 50% and 80% of peptide released) (right y-axis), (reprinted from <sup>89</sup> with permission)

On the one hand, 1<sup>st</sup> order release kinetics indicates the presence of scenario 2, as described above: The release is controlled by the decrease of surface area. On the other hand, the dependency of the half-lives from the concentration of the suspension disagrees with this assumption, as concentration-independent half-lives would have been expected.

This discrepancy can be explained by equations (11) and (12):

A higher initial amount of API (e.g. 40 mg/ml) initially leads to higher absolute dissolution due to a higher initial surface area. This causes equilibration of dissolved API concentration ( $c_L$ ) at a higher level than with lower amounts of administered dose (e.g. 5 mg/ml). Subsequently, lower relative amounts of API are released causing extended half-lives by higher concentrations of total API in suspension.

This kinetic behavior allows the control of the residence time by the amount of substance administered. This would be an ideal release behavior for intra-articular sustained release applications.

### The influence of the suspension vehicle

As demonstrated above, alterations in particle size, particle size distribution and saturation solubility can be caused by variation of the suspension vehicle. Thus, the vehicle can have a distinct impact on the release behavior of the crystal suspension.

In order to test, if the differences between the vehicles can be elucidated by the combined dialysis / flow-through setup, crystal suspensions of MSC1 were prepared for *in vitro* release testing in the three different vehicles (PBS; Methocel/Tween; Kollidon/Lutrol).

Figure 36 illustrates the release kinetics of the three crystal suspensions. Logarithmic scaling of the y-axis (Figure 36b) reveals that the release for all formulations follows 1<sup>st</sup> order kinetics. In comparison to the release experiment with a solution of MSC1, however, significantly prolonged half-lives were observed (see Table 18), which is attributed to the low solubility of MSC1.

Parameter	Solution	Vehicle 1 (PBS)	Vehicle 2 (Meth./Tween)	Vehicle 3 (Kollidon/Lutrol)
Half-life [d]	0.1 ± 0,0	4.0 ± 0.2	5.0 ± 0.4	2.4 ± 0.2
1 <sup>st</sup> order constant [d <sup>-1</sup> ]	- 7.3 ± 0.8	- 0.2± 0.0	- 0.1 ± 0.0	- 0.2± 0.0

Table 18: Overview on release characteristics of MSC1 in solution and formulated as crystal suspension in different vehicles

Furthermore, the half-lives of the suspensions are well in accordance with the results from the physico-chemical characterization:

- The suspension in vehicle 3 (Kollidon/Lutrol) shows a faster release in comparison to the suspension in vehicle 1 (PBS). This is most likely attributed to the higher saturation solubility of MSC1 in this vehicle, caused by solubilizing properties of Lutrol and Kollidon.
- The release of API from vehicle 2 (Methocel/Tween), however, shows decelerated release rates in comparison to vehicle 1. This can be explained by the higher particle size of the crystals in vehicle 2.

These results further confirm the suitability of the applied IVR setup for IVR testing of sustained release dispersed systems. The ability to discriminate and to display relevant changes between different formulations is a very important aspect for IVR methods, especially in early pharmaceutical development.

In addition, the observed half-lives of suspensions of MSC1 between 2.5 and 5 days indicate the potential of poorly soluble compounds to gain prolonged release when formulated as a crystal suspension. Furthermore it was shown that changes in the suspension vehicle may have a significant influence on the duration of API release.

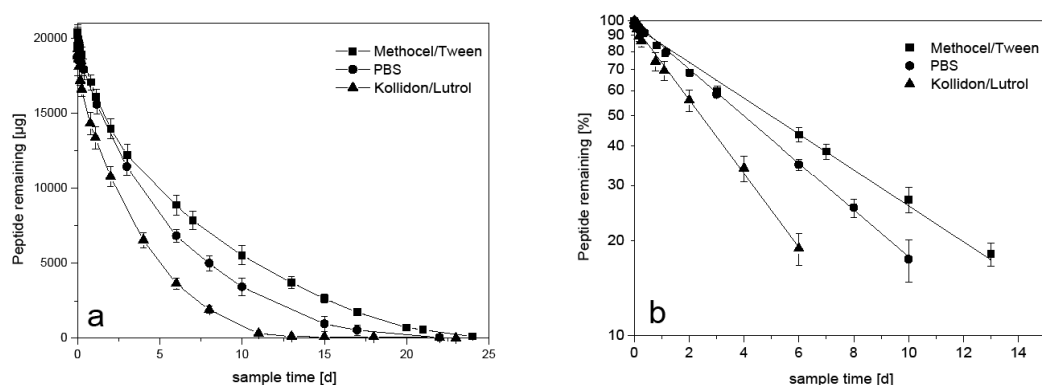


Figure 36: Release profiles of a crystal suspension of 20 mg/ml MSC1 in (●) Methocel/Tween vehicle, (□) PBS and (□) Kollidon/Lutrol vehicle in (mg) vs. time (a) and (%) vs. time (logarithmic scale of y-axis) (b) (reprinted from <sup>89</sup> with permission)

### Influence of synovial fluid on release characteristics

Besides the characterization of release kinetics and the discriminative power of the setup, the *in vivo* relevance is another important aspect for an IVR setup. Thus, it is a reasonable approach to include and investigate the influence of physiological parameters on the release behavior. In the context of intra-articular applications, the synovial fluid plays a particular important role. Thus, two major components of synovial fluid, hyaluronic acid (HA) and albumin were investigated by adding 2.5% bovine serum albumin (BSA) and/or 1% sodium hyaluronate (SH) to the donor compartment of the release setup.

The concentration of 2.5% BSA was applied according to the value for total protein concentration in human synovial fluid. The viscosity of 1% SH in PBS was found to be in accordance with literature data for synovial fluid viscosity ( $\sim 300$  mPa s)<sup>8</sup>.

In addition, release experiments with suspensions in bovine synovial fluid were performed in order to compare the “artificial synovial fluid” with physiological material.

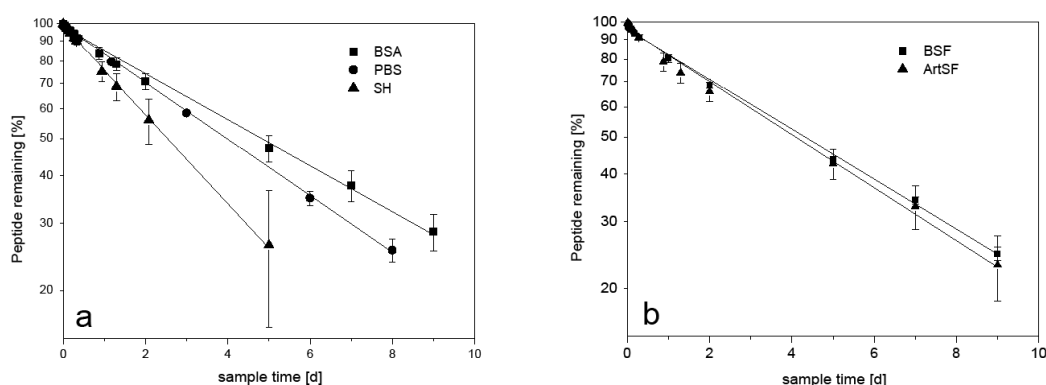


Figure 37: (a) release profiles of suspensions of 20 mg/ml MSC1 in (□) 2,5% BSA, (●) PBS and (▲) 1% SH in (%) vs. time (logarithmic scale of y-axis) and (b) release profiles of crystal suspensions of 20 mg/ml MSC1 in (□) bovine synovial fluid and (●) artificial synovial fluid in (%) vs. time (logarithmic scale of y-axis) (reprinted from<sup>89</sup> with permission)

Figure 37a demonstrates the change of release kinetics after addition of BSA and SH, respectively. While 2.5% BSA slows down the release in comparison to PBS alone, the addition of SH obviously accelerates release rates (refer to Table 19).

Parameter	PBS	2.5% BSA	1% SH	ArtSF	BSF
Half-life [d]	$4.0 \pm 0.2$	$4.8 \pm 0.5$	$2.6 \pm 0.7$	$4.1 \pm 0.5$	$4.3 \pm 0.1$
1 <sup>st</sup> order constant [ $d^{-1}$ ]	$-0.2 \pm 0.0$	$0.1 \pm 0.0$	$-0.3 \pm 0.1$	$-0.2 \pm 0.0$	$0.2 \pm 0.0$

Table 19: Release parameters of suspensions of MSC1 in PBS under addition of BSA and SH and suspensions of MSC1 in BSF

As demonstrated, the addition of BSA leads to distinct decreased release rates of the suspension. Most likely, this is caused by the protein binding properties of MSC1 (fraction unbound  $\sim 25\%$ , unpublished data), as the membrane permeability of bound API is limited due to the size of BSA. As the influence of protein binding on the release duration after IA administration *in vivo* has been shown before<sup>15</sup>, the elucidation of this aspect *in vitro* is of great value, in particular for compounds with higher protein binding properties than MSC1.

In contrast, the addition of SH leads to a shortened half-life of the suspension. This may be explained by the higher saturation solubility of MSC1, resulting in higher concentration gradients and thus faster release rates (refer to equations (11) and (14)).

Beyond the influence of the single components BSA and SH, the actual focus was the development of a suitable “Artificial Synovial Fluid” (ArtSF) for IVR testing of IA administered systems. For this purpose, a combination of PBS, BSA and SH was applied and denoted ArtSF. Release experiments of a suspension of MSC1 in ArtSF seemed to equalize the release accelerating, respective decelerating influence of the single components SH and BSA, resulting in half-lives, similar to those of PBS alone (refer to figure 38).

Furthermore, the release of a suspension of MSC1 in bovine synovial fluid (BSF) showed similar release durations, suggesting the suitability of ArtSF for bio-relevant IVR testing in this context (Figure 37b).

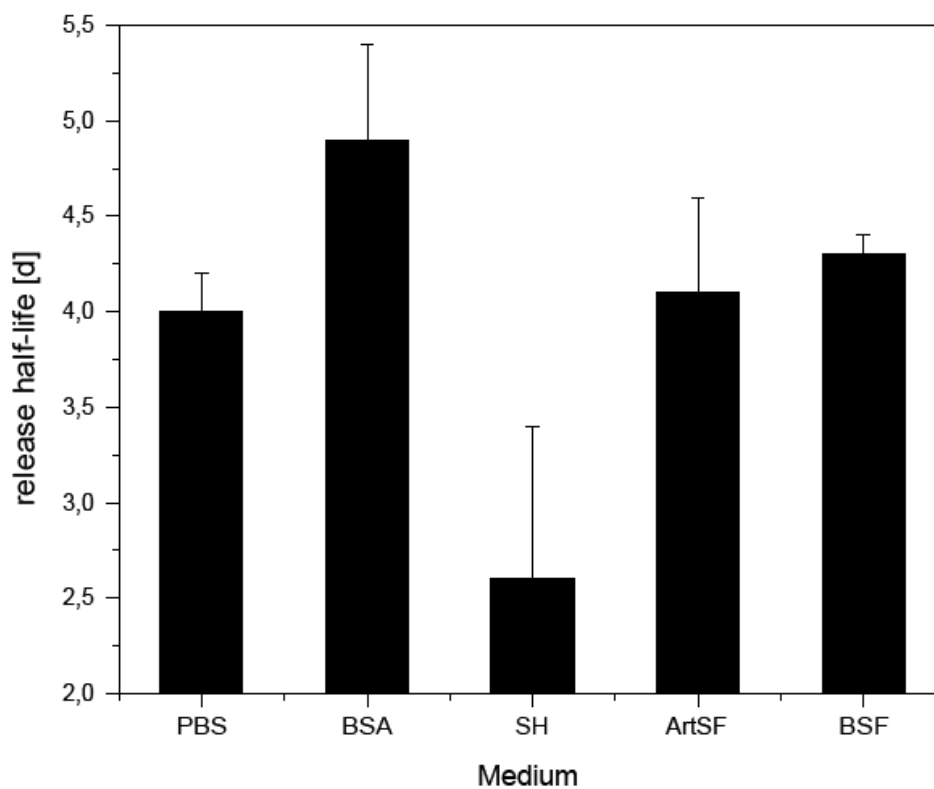


Figure 38: Half-lives of release kinetics of suspensions of MSC1 (20mg/ml) in PBS and under addition of 2,5% BSA and 1%SH as well as in artificial synovial fluid (ArtSF) and bovine synovial fluid (BSF) (reprinted from <sup>89</sup> with permission)

### Suspensions of MSC2 and MSC3

Besides MSC1, crystal suspensions of two further peptides from the Merck Serono pipeline (MSC2 and MSC3) were tested in order to demonstrate the ability of the applied IVR setup to distinguish not only between different formulations, but also between different APIs.

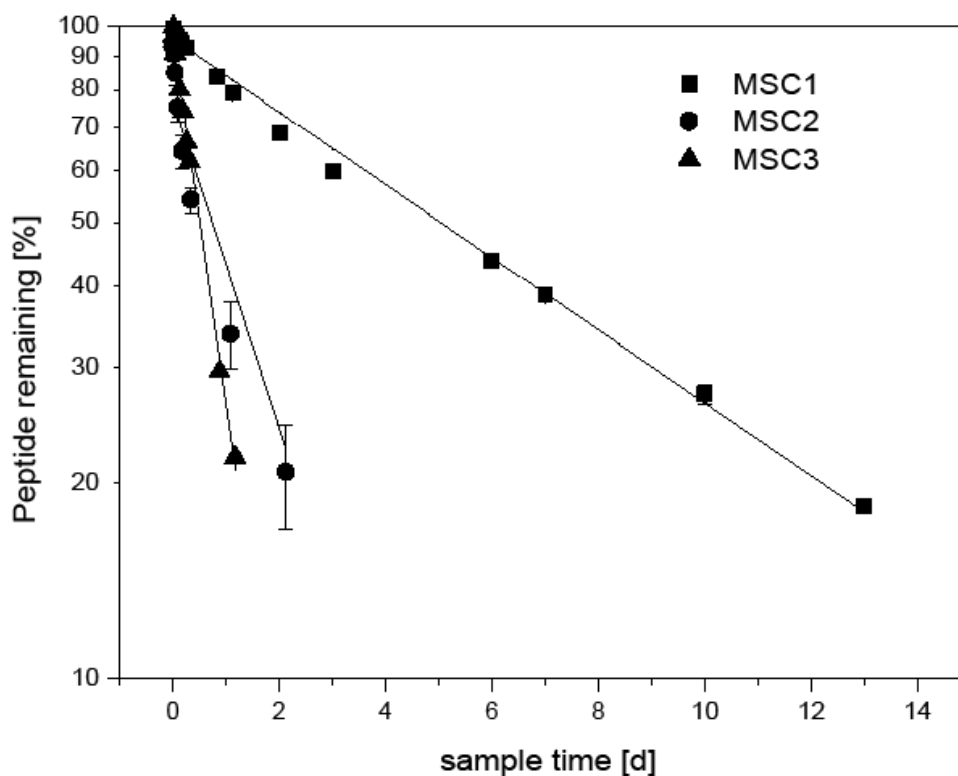


Figure 39: Release profiles of suspensions of (□) MSC1, (●) MSC2 and (▲) MSC3 in Methocel/Tween vehicles in (%) vs. time (logarithmic scale of the y-axis) (reprinted from <sup>89</sup> with permission)

Figure 39 depicts release profiles of MSC2 and MSC3 in comparison to MSC1 in vehicle 2 (Methocel/Tween). Like MSC1, the suspensions apply to 1<sup>st</sup> order kinetics. However, distinctly faster release rates (refer to Table 20) were observed. This can be explained by the higher solubility values (see Table 8) and lower particle diameters in comparison to MSC1. Again this data confirmed the dependency of dissolution rates of a crystal suspension from saturation solubility of the compound in the medium and from particle size.

Parameter	MSC 1	MSC 2	MSC 3
Half-life [d]	5.0 ± 0.4	0.7 ± 0.1	0.5 ± 0.0
1 <sup>st</sup> order constant (k) [d <sup>-1</sup> ]	- 0.1 ± 0.0	0.7 ± 0.1	- 1.3 ± 0.0

Table 20: Release parameters of crystal suspensions of MSC1, MSC2 and MSC3 in vehicle 2 (Methocel/Tween)

However, a differentiation between the two parameters could not be pointed out in these experiments. Nevertheless, these results can make a valuable contribution in the development of new therapeutic options for intra-articular treatment with crystal suspensions of poorly soluble compounds.

#### 4 Conclusion

The need for the development of a suitable IVR method for intra-articular administered sustained release parenterals basically emerged from a combination of two major circumstances:

- A lack of regulatory standards for IVR testing of sustained release parenterals
- A lack of regulatory standards for IVR testing of intra-articular administered drugs

This led to the idea to combine the well-established USP apparatus IV flow-through-cell with a new dialysis adapter system in order to meet the requirements for IVR testing of (i) sustained release parenterals as well as (ii) for IA applications. For the development of the setup, crystal suspensions of poorly soluble peptides from the Merck Serono pipeline were applied. These peptides were intended for IA administration, while their poor solubility enabled sustained drug delivery upon injection into the joint as a crystal suspension.

Initial experiments with solutions of four reference compounds (methylene blue, diclofenac, salicylate and paracetamol) and MSC1 demonstrated the basic suitability of the chosen setup for IA purposes: *In vitro* half-lives of 1<sup>st</sup> order release kinetics from the new IVR setup were shown to vary between 0.5 (paracetamol) and 2 hours (MSC1). These values were in the range of half-lives, reported from *in vivo* experiments of solutions of small molecules upon intra-articular injection. This result illustrated the potential of the new setup to gain *in vivo* relevant *in vitro* data.

Subsequently, the mentioned crystal suspensions were investigated for their IVR behavior, in order to show the suitability of the setup not only for solutions, but for sustained release particular systems. One important issue for IVR methods in general is the ability of the setup to discriminate between relevant formulation parameters. Concerning this matter, release experiments with crystal suspensions

in different suspension vehicles demonstrated the discriminative power of the applied setup. With half-lives of 1<sup>st</sup> order release kinetics of suspensions of 2.5 (vehicle 3), 4 (vehicle 1) and 5 hours (vehicle 2), a distinct differentiation between the formulations was observed. Furthermore, the results were in accordance with physico-chemical parameters (solubility and particle size) of the formulations.

Concerning the kinetic behavior of the crystal suspensions in the new setup, 1<sup>st</sup> order release was observed for all formulations. These characteristics could be described by a one-compartment model, driven by dissolution according to Noyes-Whitney, and elimination across the dialysis membrane following the concentration gradient (equations (11) – (14)). Furthermore, the kinetic model was confirmed by dose-dependent release experiments in which an almost linear correlation between the half-life and the concentration of the applied formulation was shown. The knowledge about kinetic processes within an IVR setup is crucial for the interpretation and comparison of release data. Thus, the kinetic characterization was an important step in the development of this method.

Besides discriminative power and kinetic characterization, the ability of the setup to display physiological characteristics was investigated. For this purpose, release experiments with suspensions of MSC1 were performed under addition of synovial fluid components BSA and SH as well as with a suspension in bovine synovial fluid. It was demonstrated, that these components can have a distinct impact on the release duration. An accelerating influence was observed under addition of SH, while the addition of BSA led to declined release rates. The latter can be explained by protein binding of MSC1 and thus resulting limited membrane permeation. In particular, the ability to imitate the influence of protein binding is a very valuable benefit of this release setup. Furthermore, an “Artificial Synovial Fluid” (ArtSF) was applied. In comparison to the release of a suspension in bovine synovial fluid, the suspension in ArtSF showed a similar release profile, suggesting the suitability of ArtSF to imitate the influence of synovial fluid *in vitro*.

In summary, a reproducible and discriminative new IVR setup for sustained release formulations was developed in this work. Based on release data of crystal suspensions of poorly soluble peptides, the release kinetics were characterized and described by a kinetic model. Furthermore, the suitability of the method for intra-articular purposes and the potential for IVIVC was shown by comparison of *in vitro* data (BSA, SH, ArtSF) and *ex vivo* data (bovine synovial fluid).

**Section E**  
**Summary and outlook**

Experimental sections C and D of this work basically addressed three major aspects regarding prolonged API exposure in synovial joints:

1) Physical retention of particulate systems by the Synovia

As mentioned before, the synovial membrane bears the potential to retain intra-articular injected particulate systems such as micro- and nanoparticles or crystal suspensions within the joint cavity over a longer period of time. For the characterization of the release behavior of such drug delivery systems, a novel testing approach, combining a USP IV flow-through-cell and a dialysis system, was investigated in section D of this work. Upon characterization of the setup, crystal suspensions of 3 poorly soluble peptides (MSC1, MSC2 and MSC3) in various carrier media (vehicle 1, vehicle 2 and vehicle 3) were investigated. It was demonstrated that the system was capable to discriminate between the different vehicles as well as between the different peptides. In addition, the release setup allowed the determination of the kinetic release characteristics, indicating a first order release for all investigated crystal suspension and the release duration being controlled by the initially administered dose. Section D also addressed the question, if the setup is capable to gain predictive release data for the release behavior of crystal suspension *in vivo*. Considering physiological conditions in articular joints, the influence of synovial fluid and synovial fluid components on peptide release was investigated. It was demonstrated that the addition of artificial synovial fluid to the donor compartment of the release setup led to comparable release behavior as under addition of bovine synovial fluid, while the addition of particular synovial fluid components led to accelerated (hyaluronic acid) or decelerated (bovine serum albumin) release.

## 2) Size-selective retention by the synovial membrane

Besides prolonged intra articular drug release with particulate systems, also the size-selectivity of the synovial membrane for dissolved compounds is a possible approach to gain extended drug exposure in synovial joints. Following this approach, the retention of different model polymers (polyethylene glycol, PEG) by the synovial membrane was investigated in Section C of this work. Upon characterization of a customized diffusion chamber, diffusion experiments with PEG 6 kDa, PEG 10 kDa, PEG 35 kDa and PEG 200 kDa through bovine synovial membrane revealed a clear relation between the molecular size of the investigated compounds and the retention by the synovial membrane. It was demonstrated that – related to the small molecule methylene blue – retention factors of 2 (PEG 6 kDa), 3 (PEG 10 kDa), 13 (PEG 35 kDa) and > 20 (PEG 200 kDa) can be achieved. Considering the short intra articular half-life of small molecules (1-6 hours), the evaluated retention values make clear that pure synovial retention will not suffice to gain extended drug exposure in the dimension of weeks or months. However, the results illustrated the size selectivity of the synovial membrane and its potential to retain intra-articular macromolecules inside the joint cavity for several days. This effect may be combined with e.g. particulate retention as described in 1) and retention inside the cartilage matrix as described in 3).

## 3) Retention within the joint by distribution into the cartilage matrix

In addition to retention by the synovial membrane, section C of this work also addressed the potential of retention of intra articular injected compounds via distribution into the cartilage matrix through electrostatic interaction. For this purpose, various model compounds, differing in size and extent of their positive charge were investigated for their potential to accumulate inside cartilage tissue. The experiments revealed a clear relation between the positive charge density (defined as number of positive charges per kDa molecular weight) and the partition coefficient between cartilage tissue and donor medium. This demonstrates the potential of positively charged compounds to be retained inside the joint through interaction with cartilage tissue. Furthermore, experiments with fluorescence labeled derivatives of respective model compounds demonstrated that even high molecular weight and positively charged polymers (up to 233 kDa) penetrate the entire cartilage matrix. In addition, for chitosan molecules, accumulation of analytes inside or around the cartilage cells (chondrocytes) was observed, indicating their potential for cell targeting.

Following the described approaches, the presented work provides an in-depth understanding of potential retention mechanisms in order to gain sustained release upon intra-articular administration of drugs. All three investigated retention mechanisms individually showed their capability to provide retention of compounds within the synovial joint. Furthermore, in particular the combination of two or more retention mechanisms seems to be a promising approach to retain intra-articular injected drugs inside the joint over a longer period of time. Summarizing, the elaborated data provide a sound basis for a rational selection and development of potential drug candidates (NCE or NBE) to be considered for sustained release intra-articular drug delivery. In doing so, the described and investigated *in vitro* release setup was found to be a reasonable approach for the characterization of possible drug formulations with regards to their release behavior.

**List of Abbreviations**

AmphoB	Amphotericin B
API	Active pharmaceutical ingredient
ArtSF	Artificial synovial fluid
BSA	Bovine serum albumin
CD	Charge density
DD	Degree of deacetylation
DDS	Drug delivery system
DMEM	Dulbecco's modified eagle medium
ECM	Extracellular matrix
FITC	Fluorescein Isothiocyanate
GAG	Glycosaminoglycan
GPC	Gel permeation chromatography
HA	Hyaluronic acid
HEMA-Co-TMAP (HCT)	Hydroxyethylmethacrylate-Co-Trimethylammoniumpropylacrylamid
HPLC	High performance liquid chromatography
IA	Intra-articular
IVIVC	<i>In vitro</i> – <i>in vivo</i> correlation
IVR	<i>In vitro</i> release
MW	Molecular weight
NBE	New biological entity
NCE	New chemical entity
OA	Osteoarthritis
PBS	Phosphate buffered saline
$P_{\text{coeff}}$	Partition coefficient

*List of Abbreviations*

---

PDI	Polydispersity index
PEG	Polyethylene glycol
Pen/Strep	Penicillin / Streptomycin
PFA	Paraformaldehyde
PLGA	Poly (lactic-co-glycolic acid)
RA	Rheumatoid arthritis
$R_h$	Hydrodynamic radius
SF	Synovial fluid
SH	Sodium hyaluronate
SM	Synovial membrane
USP	United States Pharmacopeia

## **Bibliography**

- 1 Dijkgraaf, L. C., de Boni, L. G. M., Boering, G. & Liem, R. S. B. Structure of the normal synovial membrane of the temporomandibular joint: A review of the literature. *Journal of Oral and Maxillofacial Surgery* 54, 332-338 (1996).
- 2 Roach, H. & Tilley, S. in *Bone and Osteoarthritis Topics in Bone Biology* (eds Felix Bronner & MaryC Farach-Carson) 1-18 (Springer London, 2008).
- 3 Barbe, M., Driban, J., Barr, A., Popoff, S. & Safadi, F. in *Bone Pathology* (ed Jasvir S. Khurana) 51-60 (Humana Press, 2009).
- 4 Kheir, E. & Shaw, D. Hyaline articular cartilage. *Orthopaedics and Trauma* 23, 450-455 (2009).
- 5 Lipowitz, A. J. in *Textbook of small animal orthopaedics* (ed Charles D Newton) Ch. 86, (1985).
- 6 Mundt, L. A. & Shanahan, K. in *Graff's Handbook of Urinalysis and Body Fluids* Ch. 11, 253-263 (2011).
- 7 Tercic, D. & Bozic, B. The basis of the synovial fluid analysis. *Clinical Chemistry and Laboratory Medicine* 39, 1221-1226 (2001).
- 8 Gerwin, N., Hops, C. & Lucke, A. in *Advanced Drug Delivery Reviews, Drug Delivery in Degenerative Joint Disease Vol. 58* 226-242 (2006).
- 9 Bédouet, L. et al. Intra-articular fate of degradable poly(ethyleneglycol)-hydrogel microspheres as carriers for sustained drug delivery. *International Journal of Pharmaceutics* (2013).
- 10 Horisawa, E. et al. in *Pharm Res, Pharmaceutical Research Vol. 19* 132-139 (Kluwer Academic Publishers-Plenum Publishers, 2002).
- 11 Whitmire, R. E. et al. Self-assembling nanoparticles for intra-articular delivery of anti-inflammatory proteins. *Biomaterials* 33, 7665-7675 (2012).
- 12 Larsen, C. et al. Intra-articular depot formulation principles: Role in the management of postoperative pain and arthritic disorders. *Journal of Pharmaceutical Sciences* 97, 4622-4654 (2008).
- 13 Owen, S. G., Francis, H. W. & Roberts, M. S. Disappearance kinetics of solutes from synovial fluid after intra- articular injection. *British Journal of Clinical Pharmacology* 38, 349-355 (1994).
- 14 Schumacher, H. R. Aspiration and injection therapies for joints. *Arthritis Care & Research* 49, 413-420 (2003).
- 15 Simkin, P., Wu, M. & Foster, D. in *Clin. Pharmacokinet, Clinical Pharmacokinetics Vol. 25* 342-350 (Springer International Publishing, 1993).
- 16 Sabaratnam, S., Arunan, V., Coleman, P. J., Mason, R. M. & Levick, J. R. Size selectivity of hyaluronan molecular sieving by extracellular matrix in rabbit synovial joints. *The Journal of Physiology* 567, 569-581 (2005).
- 17 Scott, D., Coleman, P. J., Mason, R. M. & Levick, J. R. Concentration Dependence of Interstitial Flow Buffering by Hyaluronan in Synovial Joints. *Microvascular Research* 59, 345-353 (2000).
- 18 Michael, J. W.-P., Schlüter-Brust, K. U. & Eysel, P. Epidemiologie, -tiologie, Diagnostik und Therapie der Gonarthrose. *Dtsch Arztebl International* 107, 152-162 (2010).
- 19 Morgen, M. et al. in *Pharm Res, Pharmaceutical Research Vol. 30* 257-268 (Springer US, 2013).

- 20 Schmitt, F. et al. Chitosan-based nanogels for selective delivery of photosensitizers to macrophages and improved retention in and therapy of articular joints. *Journal of Controlled Release* 144, 242-250 (2010).
- 21 Sandker, M. J. et al. In situ forming acyl-capped PCLA-PEG-PCLA triblock copolymer based hydrogels. *Biomaterials* 34, 8002-8011 (2013).
- 22 Betre, H. et al. A thermally responsive biopolymer for intra-articular drug delivery. *Journal of Controlled Release* 115, 175-182 (2006).
- 23 Miao, B., Song, C. & Ma, G. Injectable thermosensitive hydrogels for intra-articular delivery of methotrexate. *Journal of Applied Polymer Science* 122, 2139-2145 (2011).
- 24 Larsen, S. W. et al. In vitro and in vivo characteristics of celecoxib in situ formed suspensions for intra-articular administration. *Journal of Pharmaceutical Sciences* 100, 4330-4337 (2011).
- 25 Bonanomi, M. H. et al. in *Rheumatol Int, Rheumatology International* Vol. 7 203-212 (Springer-Verlag, 1987).
- 26 Bonanomi, M. H., Velvart, M. & Weder, H. G. in *Journal of Microencapsulation* Vol. 4 189-200 (Informa Healthcare, 1987).
- 27 Howie, D. W., Manthey, B., Hay, S. & Vernon-Roberts, B. The synovial response to intraarticular injection in rats of polyethylene wear particles. *Clinical orthopaedics and related research*, 352-357 (1993).
- 28 Edwards, S. H. R. Intra-articular drug delivery: The challenge to extend drug residence time within the joint. *The Veterinary Journal* 190, 15-21 (2011).
- 29 Horisawa, E. et al. in *Pharmaceutical Research* Vol. 19 403-410 (2002).
- 30 Lu, H. D., Zhao, H. Q., Wang, K. & Lv, L. L. Novel hyaluronic acid-chitosan nanoparticles as non-viral gene delivery vectors targeting osteoarthritis. *International Journal of Pharmaceutics* 420, 358-365 (2011).
- 31 Liggins, R. T. et al. in *Inflamm. res, Inflammation Research* Vol. 53 363-372 (Birkhäuser-Verlag, 2004).
- 32 Liu, Y. Z., Jackson, A. P. & Cosgrove, S. D. Contribution of calcium-containing crystals to cartilage degradation and synovial inflammation in osteoarthritis. *Osteoarthritis and Cartilage* 17, 1333-1340 (2009).
- 33 Williams, A. S., Camilleri, J. P., Goodfellow, R. M. & Williams, B. D. A single intra-articular injection of liposomally conjugated methotrexate suppresses joint inflammation in rat antigen-induced arthritis. *Rheumatology* 35, 719-724 (1996).
- 34 Pelletier, J. P., Martel-Pelletier, J. & Abramson, S. B. Osteoarthritis, an inflammatory disease: Potential implication for the selection of new therapeutic targets. *Arthritis & Rheumatism* 44, 1237-1247 (2001).
- 35 Wang, D. & Brömme, D. in *Expert Opinion on Drug Delivery* Vol. 2 1015-1028 (Expert Opinion, 2005).
- 36 D'Souza, S. & DeLuca, P. in *AAPS PharmSciTech* Vol. 6 E323-E328 (Springer-Verlag, 2005).
- 37 Diaz, R. V., Llabrés, M. & Evora, C. One-month sustained release microspheres of 125I-bovine calcitonin: In vitro-in vivo studies. *Journal of Controlled Release* 59, 55-62 (1999).
- 38 Kostanski, J. & DeLuca, P. in *AAPS PharmSciTech* Vol. 1 30-40 (Springer-Verlag, 2000).
- 39 Gaignaux, A. et al. Development and evaluation of sustained-release clonidine-loaded PLGA microparticles. *International Journal of Pharmaceutics* 437, 20-28 (2012).
- 40 Okada, H. in *Advanced Drug Delivery Reviews, Biodegradable Microspheres/Therapeutic Peptide Delivery* Vol. 28 43-70 (1997).
- 41 Evans, C. H., Kraus, V. B. & Setton, L. A. Progress in intra-articular therapy. *Nat Rev Rheumatol* 10, 11-22, doi:Review (2014).
- 42 Kushner, I. & Somerville, J. A. Permeability of human synovial membrane to plasma proteins. Relationship to molecular size and inflammation. *Arthritis & Rheumatism* 14, 560-570 (1971).
- 43 Simkin, P. A. & Pizzorno, J. E. Synovial permeability in rheumatoid arthritis. *Arthritis & Rheumatism* 22, 689-696 (1979).

- 44 Knight, A. D. & Levick, J. R. Morphometry of the ultrastructure of the blood-joint barrier in the rabbit knee. *Quarterly Journal of Experimental Physiology* 69, 271-288 (1984).
- 45 Coleman, P. J., Scott, D., Ray, J., Mason, R. M. & Levick, J. R. Hyaluronan Secretion into the Synovial Cavity of Rabbit Knees and Comparison with Albumin Turnover. *The Journal of Physiology* 503, 645-656 (1997).
- 46 Levick, J. R. Permeability of Rheumatoid and Normal Human Synovium to Specific Plasma Proteins. *Arthritis & Rheumatism* 24, 1550-1560 (1981).
- 47 Levick, J. R. A method for estimating macromolecular reflection by human synovium, using measurements of intra-articular half lives. *Annals of the Rheumatic Diseases* 57, 339-344 (1998).
- 48 Lent, P. L. E. M., Berg, W. B., Putte, L. B. A. & Bersselaar, L. in *Rheumatol Int, Rheumatology International* Vol. 8 145-152 (Springer-Verlag, 1988).
- 49 Maroudas, A. Transport of solutes through cartilage: permeability to large molecules. *J. Anat* 122, 335-347 (1975).
- 50 Sterner, B. et al. The effect of polymer size and charge of molecules on permeation through synovial membrane and accumulation in hyaline articular cartilage. *European Journal of Pharmaceutics and Biopharmaceutics* 101, 126-136, (2016).
- 51 Lewerenz, H. J. S. Pfeifer, P. Pfliegel und H.-H. Borchert: *Grundlagen der Biopharmazie. Pharmakokinetik, Bioverfügbarkeit, Biotransformation.* 352 Seiten, 140 Abb., 63 Tab., 2 Übersichten. VEB Verlag Volk und Gesundheit, Berlin 1984. *Food / Nahrung* 30, 104-104 (1986).
- 52 Park, H., Choi, B., Hu, J. & Lee, M. Injectable chitosan hyaluronic acid hydrogels for cartilage tissue engineering. *Acta Biomaterialia* 9, 4779-4786 (2013).
- 53 Tan, H., Chu, C. R., Payne, K. A. & Marra, K. G. Injectable in situ forming biodegradable chitosan-hyaluronic acid based hydrogels for cartilage tissue engineering. *Biomaterials* 30, 2499-2506 (2009).
- 54 Patchornik, S., Ram, E., Ben Shalom, N., Nevo, Z. & Robinson, D. Chitosan-Hyaluronate Hybrid Gel Intraarticular Injection Delays Osteoarthritis Progression and Reduces Pain in a Rat Meniscectomy Model as Compared to Saline and Hyaluronate Treatment. *Adv Orthop* 2012, 979152 (2012).
- 55 Mao, H. Q. et al. Chitosan-DNA nanoparticles as gene carriers: synthesis, characterization and transfection efficiency. *Journal of Controlled Release* 70, 399-421 (2001).
- 56 Zhao, X., Yu, S. B., Wu, F. L., Mao, Z. B. & Yu, C. L. Transfection of primary chondrocytes using chitosan-pEGFP nanoparticles. *Journal of Controlled Release* 112, 223-228 (2006).
- 57 Zhang, X. et al. Direct chitosan-mediated gene delivery to the rabbit knee joints in vitro and in vivo. *Biochemical and Biophysical Research Communications* 341, 202-208 (2006).
- 58 Pharmacopeia, U. S. *United States Pharmacopeia* 307-313 (2013).
- 59 Pharmacopeia, U. S. *United States Pharmacopeia* (2013).
- 60 Conti, B., Genta, I., Giunchedi, P. & Modena, T. Testing of 'in vitro' dissolution behaviour of microparticulate drug delivery systems. *Drug Development and Industrial Pharmacy* 21, 1223-1233 (1995).
- 61 Douglas, P., Andrews, G., Jones, D. & Walker, G. in *Chemical Engineering Journal, Pharmaceutical Granulation and Processing* Vol. 164 359-370 (2010).
- 62 Gao, Z. & Westenberger, B. in *AAPS PharmSciTech* Vol. 13 944-948 (Springer US, 2012).
- 63 Pedersen, B. T., Østergaard, J., Larsen, S. W. & Larsen, C. Characterization of the rotating dialysis cell as an in vitro model potentially useful for simulation of the pharmacokinetic fate of intra-articularly administered drugs. *European Journal of Pharmaceutical Sciences* 25, 73-79 (2005).
- 64 D'Souza, S. & DeLuca, P. in *Pharm Res, Pharmaceutical Research* Vol. 23 460-474 (Springer-Verlag, 2006).

- 65 Burgess, D. J., Crommelin, D. J. A., Hussain, A. S. & Chen, M. L. Assuring quality and performance of sustained and controlled release parenterals. *European Journal of Pharmaceutical Sciences* 21, 679-690 (2004).
- 66 Martinez, M., Rathbone, M., Burgess, D. & Huynh, M. In vitro and in vivo considerations associated with parenteral sustained release products: A review based upon information presented and points expressed at the 2007 Controlled Release Society Annual Meeting. *Journal of Controlled Release* 129, 79-87 (2008).
- 67 Azarmi, S., Roa, W. & Löbenberg, R. Current perspectives in dissolution testing of conventional and novel dosage forms. *International Journal of Pharmaceutics* 328, 12-21 (2007).
- 68 Larsen, C., Larsen, S. W., Jensen, H., Yaghmur, A. & Østergaard, J. in *Expert Opinion on Drug Delivery* Vol. 6 1283-1295 (Expert Opinion, 2009).
- 69 Tsai, M., Lu, Z., Wientjes, M. G. & Au, J. L.-S. Paclitaxel-loaded polymeric microparticles: Quantitative relationships between in vitro drug release rate and in vivo pharmacodynamics. *Journal of Controlled Release* 172, 737-744 (2013).
- 70 Wöhl-Bruhn, S. et al. Comparison of in vitro and in vivo protein release from hydrogel systems. *Journal of Controlled Release* 162, 127-133 (2012).
- 71 Schaefer, M. J. & Singh, J. Effect of tricaprin on the physical characteristics and in vitro release of etoposide from PLGA microspheres. *Biomaterials* 23, 3465-3471 (2002).
- 72 Negrin, C. M., Delgado, A., Llabres, M. & Evora, C. In vivo–in vitro study of biodegradable methadone delivery systems. *Biomaterials* 22, 563-570 (2001).
- 73 Burgess, D. J., Davis, S. S. & Tomlinson, E. Potential use of albumin microspheres as a drug delivery system. I. Preparation and in vitro release of steroids. *International Journal of Pharmaceutics* 39, 129-136 (1987).
- 74 Aubert-Pouessel, A., Bibby, D., Venier-Julienne, M. C., Hindré, F. & Benoît, J. P. in *Pharm Res, Pharmaceutical Research* Vol. 19 1046-1051 (Kluwer Academic Publishers-Plenum Publishers, 2002).
- 75 Longo, W. E. & Goldberg, E. P. in *Methods in Enzymology, Drug and Enzyme Targeting* (ed J. Widder Kenneth) 18-26 (Academic Press, 1985).
- 76 Wagenaar, B. W. & Müller, B. W. Piroxicam release from spray-dried biodegradable microspheres. *Biomaterials* 15, 49-54 (1994).
- 77 Rawat, A. & Burgess, D. J. USP apparatus 4 method for in vitro release testing of protein loaded microspheres. *International Journal of Pharmaceutics* 409, 178-184 (2011).
- 78 Rawat, A., Stippler, E., Shah, V. P. & Burgess, D. J. Validation of USP apparatus 4 method for microsphere in vitro release testing using Risperdal-« Consta-«. *International Journal of Pharmaceutics* 420, 198-205, (2011).
- 79 Zambito, Y., Pedreschi, E. & Di Colo, G. Is dialysis a reliable method for studying drug release from nanoparticulate systems? A case study. *International Journal of Pharmaceutics* 434, 28-34 (2012).
- 80 Xu, X., Khan, M. A. & Burgess, D. J. A two-stage reverse dialysis in vitro dissolution testing method for passive targeted liposomes. *International Journal of Pharmaceutics* 426, 211-218 (2012).
- 81 Itoh, S. et al. Reciprocating dialysis tube method: Periodic tapping improved in vitro release/dissolution testing of suppositories. *European Journal of Pharmaceutics and Biopharmaceutics* 64, 393-398 (2006).
- 82 Park, T. G., Lu, W. & Crotts, G. Importance of in vitro experimental conditions on protein release kinetics, stability and polymer degradation in protein encapsulated poly (d,l-lactic acid-co-glycolic acid) microspheres. *Journal of Controlled Release* 33, 211-222 (1995).
- 83 Pharmacopeia, U. S. *United States Pharmacopeia* 735-741 (2013).
- 84 Blewis, M. E. et al. Semi-permeable membrane retention of synovial fluid lubricants hyaluronan and proteoglycan 4 for a biomimetic bioreactor. *Biotechnology and Bioengineering* 106, 149-160 (2010).

- 85 Frost, A. B. et al. On the search for in vitro in vivo correlations in the field of intra-articular drug delivery: Administration of sodium diatrizoate to the horse. *European Journal of Pharmaceutical Sciences* 41, 10-15, (2010).
- 86 Larsen, S. W., Østergaard, J., Friberg-Johansen, H., Jessen, M. N. B. & Larsen, C. In vitro assessment of drug release rates from oil depot formulations intended for intra-articular administration. *European Journal of Pharmaceutical Sciences* 29, 348-354, (2006).
- 87 Bhardwaj, U. & Burgess, D. J. A novel USP apparatus 4 based release testing method for dispersed systems. *International Journal of Pharmaceutics* 388, 287-294 (2010).
- 88 Hattori, Y., Haruna, Y. & Otsuka, M. Dissolution process analysis using model-free Noyes–Whitney integral equation. *Colloids and Surfaces B: Biointerfaces* 102, 227-231 (2013).
- 89 Sterner, B., Harms, M., Weigandt, M., Windbergs, M. & Lehr, C. M. Crystal suspensions of poorly soluble peptides for intra-articular application: A novel approach for biorelevant assessment of their in vitro release. *International Journal of Pharmaceutics* 461, 46-53 (2014).
- 90 Meyer, M. C. & Guttman, D. E. Dynamic dialysis as a method for studying protein binding I: Factors affecting the kinetics of dialysis through a cellophane membrane. *Journal of Pharmaceutical Sciences* 59, 33-38 (1970).
- 91 Costa, P. & Sousa Lobo, J. M. Modeling and comparison of dissolution profiles. *European Journal of Pharmaceutical Sciences* 13, 123-133 (2001).

## Scientific output

### Publications

Bernd Sterner, Meike Harms, Markus Weigandt, Maike Windbergs, Claus-Michael Lehr

“Crystal suspensions of poorly soluble peptides for intra-articular application: A novel approach for bio-relevant assessment of their *in vitro* release.”

*International Journal of Pharmaceutics* 461, 46-53 (2014)

---

Bernd Sterner, Steffen Wöll, Meike Harms, Markus Weigandt, Maike Windbergs, Claus-Michael Lehr

“The effect of polymer size and charge of molecules on permeation through synovial membrane and accumulation in hyaline articular cartilage.”

*European Journal of Pharmaceutics and Biopharmaceutics* 101, 126-136 (2016)

### Congress contributions

Bernd Sterner, Meike Harms, Markus Weigandt, Maike Windbergs, Claus-Michael Lehr

„Artificial synovial fluid for *in vitro* release testing of intra-articular applied systems”

Scientific poster on the CRS Local Chapter Meeting 2013 (Ludwigshafen, Germany)

---

Bernd Sterner, Meike Harms, Markus Weigandt, Maike Windbergs, Claus-Michael Lehr

Crystal suspensions of poorly soluble peptides intended for intra-articular administration: *In vitro* release studies on parenteral sustained release dosage forms

Scientific talk on the CRS World Meeting 2013 (Honolulu, Hawaii)

## Curriculum Vitae

### Personal Information

---

Name	Bernd Sterner
Date of birth	October 10 <sup>th</sup> 1982 in Starnberg
Nationality	German
Address	Schweigerstr. 8, 81541 München
E-Mail	berndsterner@gmail.com
Phone	+49 172 2732620

### Professional Career

---

Since 05/2014	<b>Haupt Pharma Amareg GmbH, Regensburg</b> Project Manager for Pharmaceutical Development
11/2010 - 01/2014	<b>Department of Biopharmaceutics and Pharmaceutical Technology, Saarland University, Saarland, Germany (in cooperation with Merck KGaA, Darmstadt)</b> Doctoral thesis Title: Sustained drug delivery for local treatment of joint diseases
08/2009 – 10/2010	<b>Bienen-Apotheke Türkenstrasse, Munich</b>  Pharmacist

### Education and University Studies

---

10/2003 – 05/2009	<b>Ludwig-Maximilians-University, Munich</b>  Studies of Pharmacy, graduated with 3 <sup>rd</sup> state examination in 07/2009
06/2002	<b>„Abitur“ at Gymnasium Puchheim</b>

## **Danksagung**

Ich bedanke mich herzlich bei Prof. Claus-Michael Lehr für die fachliche Betreuung der Arbeit als Doktorvater und insbesondere für kritisches Hinterfragen und die vielen wertvollen Anregungen.

Ganz herzlichen Dank möchte ich auch Dr. Maike Windbergs aussprechen: Maike, Du hast mich als „externen Doktoranden“ am Institut von der ersten Woche an unter Deine Fittiche genommen. Ich bedanke mich für Deine Unterstützung, Deinen Rat und Deinen Zuspruch über all die Jahre, insbesondere bei der Fertigstellung unserer Veröffentlichungen.

Ich bedanke mich bei der Firma Merck, die es mir ermöglicht hat an diesem Thema zu arbeiten. Ein ganz besonderer Dank geht dabei an Dr. Meike Harms: Meike, vielen Dank für Deine Ideen, für Deinen Antrieb, für Deine Kritik und v.a. für Deine Offenheit. Außerdem möchte ich mich ganz herzlich bei Dr. Markus Weigandt und allen Kollegen bei Merck bedanken. Vielen Dank für Eure Unterstützung. Unsere Zusammenarbeit war mir eine Freude!

Ein großes ‚Danke‘ möchte ich auch an meine Mit-Doktoranden aussprechen. Es hat sehr viel Spaß mit Euch gemacht!

Bei meiner Familie möchte ich mich für die immerwährende Unterstützung bedanken. Ohne Euch wäre diese Arbeit nicht möglich gewesen!

Mein wichtigster Dank gilt meiner Frau, Angela: Angie, vielen Dank für Deine Geduld, Deinen Beistand in schwierigen Phasen und insbesondere für das Aushalten von 3 Jahren Fernbeziehung.